Development of a novel and versatile affinity tagging system using an anti-podoplanin antibody NZ-1

（ポドプラニン抗体 NZ-1 を用いた
新規アフィニティータグシステムの確立と応用）

Yuki Fujii

Graduate school of frontier bioscience,
Osaka University

March 2015

Abstract

Peptide-based epitope tagging technology is universally used in nearly all kind of research projects that involve biochemical characterization of a target protein, but not many systems are fully compatible with purification purpose. By utilizing an anti-human podoplanin antibody NZ-1, I constructed a novel epitope tagging system. NZ-1 possesses exceptionally high affinity toward a dodecapeptide (GVAMPGAEDDVV) dubbed “PA tag”, with a characteristic slow dissociation kinetics. Because of its high affinity, PA-tagged proteins in a dilute sample can be captured by immobilized NZ-1 resin in a near complete fashion and eluted by a solution of free PA peptide. This enabled efficient one-step purification of various proteins including soluble (e.g., an ectodomain fragment of neuropilin-1 and a human serum albumin) and membrane proteins expressed in mammalian cells. Mild regeneration condition of the peptide-bound antibody ensures repeated use of the antibody resin, indicating a cost-efficient nature of the system. PA tag/NZ-1 system also exhibits an outstanding performance in the immunodetection experiments (i.e., Western blotting and flow cytometry). An alanine scanning mutagenesis experiment revealed that many amino acid residues within the PA tag sequence contribute to the binding by NZ-1. To understand the molecular details of the PA tag-NZ-1 interaction at atomic resolution, I determined the X-ray crystal structure of the NZ-1 Fab fragment in complex with the PA tag peptide. In the structure, the PA peptide is docked in the antigen-binding cleft of the NZ-1, and there are numerous contacts involving the peptide region encompassing Met4-Asp10. In the NZ-1-bound conformation, the PA peptide assumed a tight 2-residue type II β-turn conformation at the Pro5-Gly6 sequence. This binding mode suggested an interesting possibility that PA tag may be inserted into a loop region of proteins, without losing its high affinity toward NZ-1. Using a cell adhesion receptor integrin $\alpha_{IIb}\beta_3$ as a model protein, I successfully inserted the PA tag into multiple loop regions in the ectodomain of $\alpha_{IIb}\beta_3$ and confirmed that all proteins were reactive with NZ-1. Moreover, by choosing the site of PA tag insertion, it was possible to modulate the function of resultant integrin by inducing conformational change upon the addition of NZ-1. As it is generally difficult to graft linear epitope tag in a structured protein domain, the PA tag system provide unique opportunity to attach purification/labeling handle to a target protein.

Abbreviations

Base abbrevitations

A	Adenine
C	Cytosine
G	Guanine
T	Thymine

Amino acid abbreviations table

1-Letter	3-Letter	Amino acid
A	Ala	Alanine
C	Cys	Cysteine
D	Asp	Aspartic Acid
E	Glu	Glutamic Acid
F	Phe	Phenylalanine
G	Gly	Glycine
H	His	Histidine
I	Ile	Isoleucine
K	Lys	Lysine
L	Leu	Leucine
M	Met	Methionine
N	Asn	Asparagine
P	Pro	Proline
Q	Gln	Glutamine
R	Arg	Arginine
S	Ser	Serine
T	Thr	Threonine
V	Val	Valine
W	Trp	Tryptophan
Y	Tyr	Tyrosine

ASA	Solvent accessible surface area
BLI	Bio-layer interferometry
BPB	Bromophenol blue
BSA	Bovine serum albumin
CBB	Coomassie brilliant blue
CCP4	Collaborative Computational Project, Number 4
CDR	Complementarily determining region
CHO	Chinese hamster ovary
c. sup	Cell culture supernatant
DMEM	Dulbecco's modified Eagle medium
DNA	Deoxyribonucleic acid
DTT	Dithiothreitol
E. coli	*Escherichia coli*
EDTA	Ethylenediamine tetraacetic acid
EGF	Epidermal growth factor
ELISA	Enzymed-Linked ImmunoSorbent Assay
Fab	Fragment antigen-binding
FCS	Fetal calf serum
FITC	Fluorescein isothiocyanate
Fv	Variable fragment
GFP	Green fluorescent protein
HEK	Human embryonic kidney
HEPES	2-[4-(2-hydroxyethyl)-1-piperazin-1-yl]ethanesulfonic acid
HRP	Horse radish peroxdase
HSA	Human serum albuin
IDH	Isocitrate dehydrogenase
IgG	Immunoglobulin G
IPTG	Isopropyl- -D-thiogalactopyranoside
LB	Luria-Bertani's broth
LIBS	Ligand-induced binding sites
MES	2-(*N*-morpholino)ethanesulfonic acid
MFI	Mean fluorescence intensity

MWCO	Molecular weight cut-off
NEAA	Non-Essencial Amino Acids solution
NGF	Nerve growth factor
Nrp	Neuropilin
NSRRC	National Synchrotron Radiation Research Center
OD	Optical density
O/N	Over night
PAGE	Polyacrylamide gel electrophoresis
PBS	Phosphate-buffered saline
PBST	Phosphate-buffered saline and Tween 20
PCR	Polymerase chain reaction
PDB	Protein Data Bank
PE	Phycoerythrin
PEG	Polyethylene glycol
PIPES	1, 4-Piperazinediethanesulfonic acid
PMSF	Phenylmethylsulfonyl fluoride
PVDF	Polyvinylidene difluoride
RMSD	Root mean square deviation
rpm	Rotation per minute
RU	Resonance unit
SA	Streptavidin
SDS	Sodium dodecyl sulfate
SPR	Surface plasmon resonance
TBS	Tris-buffered saline
TBST	Tris-bufferd saline and Tween 20
Tris	Tris (hydroxymethyl) aminoethane
T4L	T4-lysozyme
UV	Ultraviolet
VEGF	Vascular endothelial growth factor
XDS	X-ray Detector Software

Contents

Chapter I

An affinity tag system is a necessary technique for a modern bioscience research and development, because it is almost impossible to detect, visualize, and purify a target protein without this technique. Especially, purification technique using affinity tag is important for the success of the structure-function research on the front line. In the basic biomedical research, there are many cases where we do not understand the exact molecular function of the proteins of interest even if the physiological importance is established. To analyze the functions of such proteins at molecular level, it is often necessary to perform experiments using purified proteins. Generally, a target protein is expressed in *Escherichia coli*, mammalian cells, or insect cells using gene-recombination technique for analysis of protein function. It is difficult to analyze the function of target proteins directly in these cells, because the environment in the host cells is very different from the original location of the target proteins. Therefore, it is often necessary to reconstruct the proper environment with purified protein. Moreover, to determine the three-dimensional structure of functional protein using X-ray crystallography, protein samples with high purify and quality are required. Although many protein samples are commercially available from companies these days, a target protein still must be prepared by oneself for an original research as before. Therefore, development of better affinity tag system is always wanted.

The affinity tag systems are used for the purification and detection of a target protein. A target protein attached with the specific amino acid sequence is captured by molecule that recognizes the sequence specifically. This amino acid sequence is called “tag”, and tag is usually fused to N- or C-terminal with a linker sequence to minimize unwanted effects on the conformation and activity of the target protein. An affinity tag purification system has several advantageous characteristics over conventional purification methods. For example, target proteins can be purified quickly and specifically by taking advantage of the specific molecular interaction of the tag system. The method is generally applicable to many target proteins because the principle of the separation does not depend on the nature of the target protein itself. In contrast, traditional chromatography methods for protein purification (ion-exchange chromatography, hydrophobic interaction chromatography, gel filtration chromatography, and so on) depend on physical-chemical property of each protein. Therefore, affinity tag purification method enables the purification of a target proteins

easily and quickly with fewer steps, without the detailed optimization for each protein. Biologically active proteins are generally unstable in solution, especially when they are isolated from their original environment (e.g., cell cytoplasm). Therefore, it is generally ideal to prepare the sample from the biological specimen within the minimum amount of time. It is unquestionable that shorter time requirement is also highly desirable for other experiments such as Western blotting and immunocytochemistry, to rapidly, examine protein expression and localization.

So far, various affinity tag systems have been developed and become commercially available. The representative affinity tag systems include His tag (Hochuli et al. 1988), GST tag (Benard and Bokoch 2002), FLAG tag (Hopp et al. 1988), HA tag (Field et al. 1988), Myc tag (Evan et al. 1985), Target tag (Tabata et al. 2010). His tag consists of 6-10 histidine residues, and this tag system uses the property that consecutive histidine residues specifically bind to metal ion (e.g., Ni and Co) displayed with chelate agent. GST tag is composed of an enzyme glutathione-S-transferase (approximately 28 kDa), utilizing the enzyme-substrate specific binding to glutathione. The FLAG, HA, Myc, and Target tag consist of oligopeptides with unique amino acids sequence (FLAG tag: DYKDDDDK, HA tag: YPYDVPDYA, Myc tag: EQKLISEEDL, Target tag: YPGQYPGQYPGQYPGQYGQV). These tags can be recognized by proprietary monoclonal antibodies that are highly specific against each peptide sequence. Such tag systems are collectively called “epitope tag” system.

In order to be an excellent affinity tag purification system, it must fulfill many features. For example, very high specificity and affinity between the tag and the binder molecule is indispensable. Also important is the ability to remove the bound target protein from the binder molecule without damaging the target, and to regenerate the immobilized resin for the next round of use. Unfortunately, a perfect system rarely exists. Therefore, we have to choose different tag systems for each case after careful comparison and optimization based on the nature of the target protein. For example, although the purification of His-tagged proteins using metal chelate affinity resin is an excellent choice because of the high capacity and low cost, it usually results in co-purification of metal-binding proteins present in the starting material, necessitating further purification steps (Lichty et al. 2005). GST tag system is superior to many other systems for expression in soluble fraction of *E. coli*, but its large size (~28 kDa) may

affect function of tagged proteins and it is usually required to removed the GST moiety by a protease treatment.

The epitope tag systems such as FLAG, HA, and Myc have several advantages over other tagging technologies. These tags generally do not affect the function and structure of target proteins because they are small, and have high specificity owing to the antigen-antibody interaction. An epitope tag system such as very popular FLAG tag system (Einhauer and Jungbauer 2001) is suitable for the purification of a low-abundance, precious target protein. However, the antibody immobilized resin for purification has relatively low binding capacity, and it is of high cost. Moreover, even the most successful system like FLAG tag/anti-FLAG M2 antibody sometimes suffers from non-specific binding of endogenous proteins in certain cell types (Kato et al. 2003; Sasaki et al. 2012). Another disadvantages of FLAG tag system include the problem of the limited reusability. Although the column regeneration condition recommended by the vendor (treatment with an acidic buffer at pH 3.0) works fine, many users confirmed that this condition gradually deactivate the M2 immobilized resin. Therefore, there is a continuous need for the development of new affinity tag system with high affinity, high specificity, and high reusability. In this research, I aimed at a development of a novel affinity tag system superior to the existing tag systems.

Generally, affinity tag is fused to either the N- or C- terminal of a target protein to facilitate affinity purification and detection, because the tag insertion into the middle of a sequence of a target protein may destroy the local conformation or alter its function. Even when the tag sequence insertion is not expected to affect the function of target protein, such attempts are rare, because the inserted tag does not usually work as a tag any more due to the limited antibody accessibility and/or the altered conformation. However, we sometimes come across cases where protein terminals are important for the function, or buried and not accessible to a binder. In such cases, we have to seek ways to attach tags somewhere else. Therefore, there are unmet needs for the development of general tagging system that is compatible with the “tag insertion”. There are several studies reporting successful insertion of tag sequence in the middle of a protein by targeting at flexible loop region that does not have secondary structure. In these reports, however, either very long loops were chosen as the insertion point (Dinculescu et al. 2002; Smith et al. 2004; Morlacchi et al. 2012) or the inserted tag was flanked by long linker sequences (Facey and Kuhn 2003; Kendall and Senogles 2006).

Even the inserted tag sequence itself is sometimes very long, because of the inclusion of multiple tag sequences in tandem (Kobayashi et al. 2008; Zakrzewska et al. 2009). Although these strategies are necessary to make the tag recognizable by the antibody, they change the local structure of the protein significantly and are rarely compatible with the folded protein domain. As a result, we still lack general and versatile tag-insertion technology and one need to apply sophisticated knowledge of protein engineering to achieve successful epitope grafting (Laird and Desrosiers 2007). Thus it is of great importance to develop simple and general way to insert an epitope tag into the middle of a sequence of a target protein. If successful, such tag may also be used in different application including the site-specific labeling of a receptor. Therefore, I decided to investigate whether a novel affinity tag (PA tag) can be inserted into a tip of turn or in the middle of a loop region of a target protein.

In this thesis, I describe the construction of PA tag system in Chapter II. In Chapter III, I describe the structural characterization of the PA tag system and its application in the development of a unique “epitope grafting” method.

Chapter II

Introduction

An excellent epitope tag system needs the combination of a peptide tag and a monoclonal antibody with high specificity and affinity. However, it is very difficult that we obtain the combination as described above. In fact, the popular epitope tag systems use antibodies that were established to recognize the target protein. HA tag monoclonal antibody was established to recognize human influenza hemagglutinin (Field et al. 1988), and Myc tag monoclonal antibody was established to recognize c-Myc (Evan et al. 1985). Meanwhile, FLAG tag monoclonal antibody is an exception. This antibody was established against the peptide including enterokinase sequence (DDDDK) to use for the epitope tag system (Hopp et al. 1988). Only FLAG tag system was currently developed by design.

Prof. Yukinari Kato *et al*., (Tohoku University) have established a unique rat monoclonal antibody NZ-1 directed against 14-residue peptide segment (EGGVAMPGAEDDVV) in human podoplanin PLAG domain (Kato et al. 2006). Podoplanin is a type I transmembrane protein highly expressed on malignant cancer cells and is implicated in tumor-induced platelet aggregation by binding to CLEC-2 on platelet surface (Kato et al. 2008). NZ-1 inhibits binding of podoplanin to CLEC-2 and is a potential lead for the antibody-based therapy against glioblastoma (Kaneko et al. 2012; Kato et al. 2008). NZ-1 was raised against 14-residue peptide corresponding to residues 38-51 of human podoplanin (Ogasawara et al. 2008). Therefore, I attempted to prove that NZ-1 possesses desirable character as an anti-tag antibody.

Here, I examined that this peptide tag and NZ-1 monoclonal antibody have high affinity and specificity, the peptide-tagged target protein is easy to be eluted by mild condition, and NZ-1 immobilized resin is able to be reused. As a result, the combination of the peptide tag derived from podoplanin and NZ-1 satisfied all the conditions. Moreover, it also exhibited an outstanding performance in the immunodetection experiments (i.e., Western blotting and flow cytometry). Therefore, I report a development of a novel affinity tag system consisting of NZ-1 and its epitope peptide (GVAMPGAEDDVV) dubbed “PA tag”. PA tag system proves to outperform many existing affinity tag systems owing to its high affinity, high selectivity, and extended reusability.

Materials and methods

Construction of expression vectors

Expression constructs for the T4 lysozyme (T4L) attached with various tags shown in the Fig. I-1 (T4L-PA10, T4L-PA12, T4L-PA14, T4L-FLAG, T4L-HA, T4L-Myc, PA10-T4L, PA12-T4L, PA14-T4L, FLAG-T4L, HA-T4L, Myc-T4L) were prepared by extension PCR and cloned into *Nco*I-*Bam*HI site of pET16b vector (Novagen). All constructs contained either C-terminal His × 8 or N-terminal His × 10 tags to facilitate protein purification. These constructs attached with FLAG, HA, or Myc tag were prepared as template that was mutated from 1st Met derived from T4L to Lys using QuikChange strategy (Agilent). Single-residue alanine substitution mutants (G1A, V2A, M4A, P5A, G6A, E8A, D9A, D10A, V11A, V12A) of T4L-PA12 were also produced using QuikChange strategy. The primer list for this research was shown in Table I-1. Construct for GFP_{UV}-PA12 was prepared by replacing T4L segment of T4L-PA12 with the coding sequence of GFP_{UV} (Clontech).

Full-length DNA for human isocitrate dehydrogenase 1 was attached with tandem FLAG and PA12 tags at the C-terminal (IDH1-FLAG-PA12) and cloned into pcDNA3.1 vector (Life Technologies Corp.) as described previously (Kaneko et al. 2013b). For the construction of $mNrp1_{ec}$-PA12, DNA encoding the entire ectodomain of mouse neuropilin-1 (a gift from Prof. A. Kumanogoh, Osaka University) and the linker + PA12 segment from T4L-PA12 were fused by extension PCR and cloned into *Hind*III-*Xba*I site of pcDNA3.1 vector. For the construction of full-length rat neuropilin-2 tagged with PA12 tag, rNrp2-mCherry in pSecTag2A vector (a gift from Prof. Y. Goshima, Yokohama City University) was used to insert PA12 + linker segment (taken from the PA12-T4L) after the signal sequence, and cloned into *Xho*I-*Xho*I site of pcDNA3.1 vector (PA12-rNrp2-mCherry). The cDNA for human serum albumin (HSA) was obtained from Danaform (ID; 100009048). Construct for PA12-HSA was prepared by replacing rNrp2-mCherry of PA12-rNrp2-mCherry with the coding sequence of HSA using *Bam*HI-*Bam*HI site. Construct for HSA-PA12 was used to insert PA12 + linker segment (taken from the T4L-PA12), and cloned into *Eco*RI-*Xba*I site of pcDNA3.1 vector. All constructs were verified by DNA sequencing.

E. coli expression constructs

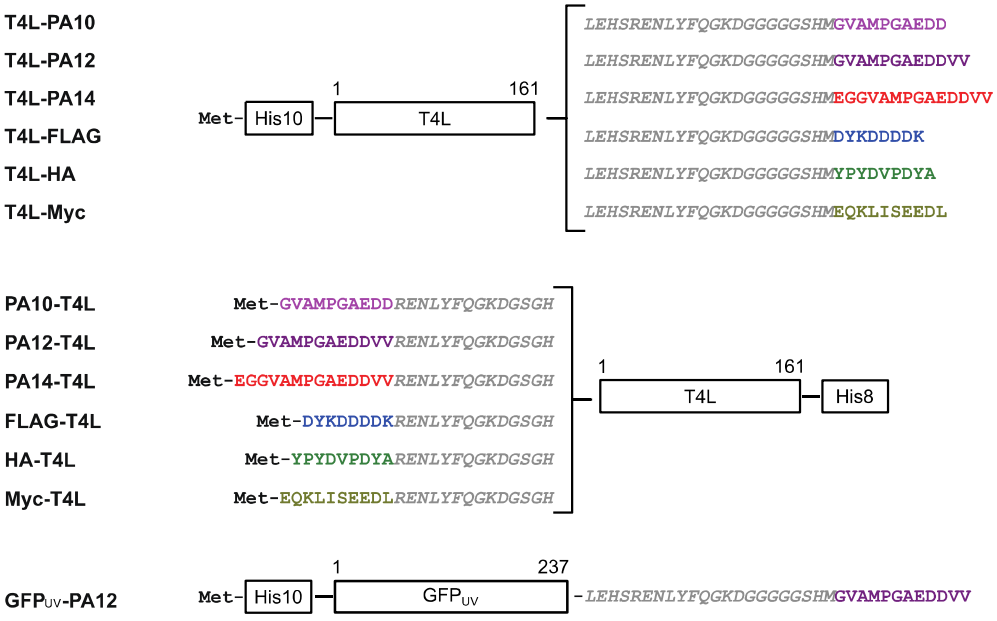

Mammalian expression constructs

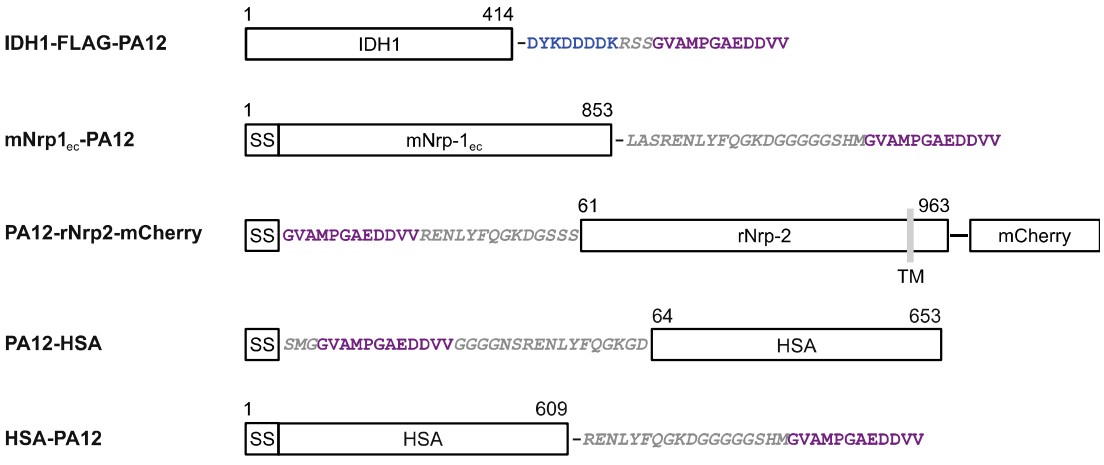

Figure I-1. Expression constructs of recombinant proteins used in Chapter I. Amino acid sequences of the artificially added tag and the linker segments are shown. SS, signal sequence.

Table I-1. Primer list

Construct name	Primer name	Sequence
T4L-PA10	T7 fwd (upper-1, 2)	5'-taatacgactcactataggg-3'
	t4lL11-1 (-) (lower-1)	5'-gcacctggcatggcaacgcccatatgtgaaccgcctccac-3'
	t4lL11-2 (-) (lower-2)	5'-ccggatccttaatcatcttcggcacctggcatggcaacgcc-3'
T4L-PA12	T7 fwd (upper-1, 2, 3)	5'-taatacgactcactataggg-3'
	t4lL11-1 (-) (lower-1)	5'-gcacctggcatggcaacgcccatatgtgaaccgcctccac-3'
	t4lL12-2 (-) (lower-2)	5'-cttacaccacatcatcttcggcacctggcatggcaacgcc-3'
	t4lL12-3 (-) (lower-3)	5'-ccggatccttacaccacatcatcttcg-3'
T4L-PA14	T7 fwd (upper-1, 2, 3)	5'-taatacgactcactataggg-3'
	t4lL13-1 (-) (lower-1)	5'-ggcatggcaacgccgccttccatatgtgaaccgcctccac-3'
	t4lL13-2 (-) (lower-2)	5'-ccacatcatcttcggcacctggcatggcaacgccgccttc-3'
	t4lL13-3 (-) (lower-3)	5'-ccggatccttacaccacatcatcttcggcacct-3'
T4L-FLAG	T7 fwd (upper-1, 2)	5'-taatacgactcactataggg-3'
	t4lmutL58-1 (-) (lower-1)	5'-tcgtcatcgtctttgtagtccatatgtgaaccgcctccac-3'
	t4lmutL58-2 (-) (lower-2)	5'-ccggatccttacttgtcgtcatcgtctttgtagtc-3'
T4L-HA	T7 fwd (upper-1, 2)	5'-taatacgactcactataggg-3'
	t4lmutL56-1 (-) (lower-1)	5'-tctggaacatcgtatgggtacatatgtgaaccgcctccac-3'
	t4lmutL56-2 (-) (lower-2)	5'-ccggatccttaagcgtaatctggaacatcgtatgggta-3'
T4L-Myc	T7 fwd (upper-1, 2)	5'-taatacgactcactataggg-3'
	t4lmutL60-1 (-) (lower-1)	5'-tcagagatcagtttctgttccatatgtgaaccgcctccac-3'
	t4lmutL60-2 (-) (lower-2)	5'-ccggatccttacaggtcttcttcagagatcagtttctgttc-3'
PA10-T4L	t4lL26-1 (upper-1)	5'-tgccaggtgccgaagatgatcgcgagaacctgtacttcca-3'
	t4lL26-2 (upper-2)	5'-tataccatgggcggcgttgccatgccaggtgccgaagatgat-3'
	T7 term (lower-1, 2)	5'-gctagttattgctcagcgg-3'
PA12-T4L	t4lL27-1 (upper-1)	5'-gtgccgaagatgatgtggtgcgcgagaacctgtacttcca-3'
	t4lL27-2 (upper-2)	5'-cgttgccatgccaggtgccgaagatgatgtggtg-3'
	t4lL26-2 (upper-3)	5'-tataccatgggcggcgttgccatgccaggtgccgaagatgat-3'
	T7 term (lower-1, 2, 3)	5'-gctagttattgctcagcgg-3'
PA14-T4L	t4lL27-1 (upper-1)	5'-gtgccgaagatgatgtggtgcgcgagaacctgtacttcca-3'
	t4lL27-2 (upper-2)	5'-cgttgccatgccaggtgccgaagatgatgtggtg-3'
	t4lL28 (upper-3)	5'-tataccatgggcgaaggcggcgttgccatgccaggtgccg-3'
	T7 term (lower-1, 2, 3)	5'-gctagttattgctcagcgg-3'
FLAG-T4L	t4lmutL57-1 (upper-1)	5'-acaaagacgatgacgacaagcgcgagaacctgtacttcca-3'
	t4lmutL57-2 (upper-2)	5'-tataccatgggcgactacaaagacgatgacgacaag-3'
	T7 term (lower-1, 2)	5'-gctagttattgctcagcgg-3'
HA-T4L	t4lmutL55-1 (upper-1)	5'-acgatgttccagattacgctcgcgagaacctgtacttcca-3'
	t4lmutL55-2 (upper-2)	5'-tataccatgggctacccatacgatgttccagattacgct-3'
	T7 term (lower-1, 2)	5'-gctagttattgctcagcgg-3'
Myc-T4L	t4lmutL59-1 (upper-1)	5'-ctgatctctgaagaagacctgcgcgagaacctgtacttcca-3'
	t4lmutL59-2 (upper-2)	5'-tataccatgggcgaacagaaactgatctctgaagaagacct-3'
	T7 term (lower-1, 2)	5'-gctagttattgctcagcgg-3'

Table I-1. Primer list (continued)

Construct name	Primer name	Sequence
T4L (Met→Lys)	t4lL47 (N-terminal tag)	5'-acggtagcggtcataagaatatatttgaaa-3'
	t4lL47 (-) (N-terminal tag)	5'-tttcaaatatattcttatgaccgctaccgt-3'
	t4lL48 (C-terminal tag)	5'-cgaaggtcgtcataagaatatatttgaaat-3'
	t4lL48 (-) (C-terminal tag)	5'-atttcaaatatattcttatgacgaccttcg-3'
G1A	t4lL16	5'-acatatggaaggcgccgttgccatgccagg-3'
V2A	t4lL17	5'-tatggaaggcggcgctgccatgccaggtgc-3'
M4A	t4lL18	5'-aaggcggcgttgccgcgccaggtgccgaag-3'
P5A	t4lL19	5'-gcggcgttgccatggcaggtgccgaagatg-3'
G6A	t4lL20	5'-cgttgccatgccagctgccgaagatgatgt-3'
E8A	t4lL21	5'-catgccaggtgccgcagatgatgtggtgta-3'
D9A	t4lL22	5'-gccaggtgccgaagctgatgtggtgtaagg-3'
D10A	t4lL23	5'-aggtgccgaagatgctgtggtgtaaggatc-3'
V11A	t4lL24	5'-tgccgaagatgatgcggtgtaaggatccgg-3'
V12A	t4lL25	5'-cgaagatgatgtggcgtaaggatccggctg-3'
PA12-rNrp2-mCherry	rNRP2L62 (upper)	5'-atcctcgagccagcaagatccgccctg-3'
	rNRP2L62 (-) (lower)	5'-agactcgagttacttgtacagctcgtcca-3'
PA12-HSA	albU1 (upper)	5'-acggatccgtgtttcgtcgagatgcacac -3'
	albL2 (-) (lower)	5'-tcggatcctataagcctaaggcagcttgac -3'
HSA-PA12	pENTR-U1 (upper)	5'-gggaattcaggctccaccatgaagtggg -3'
	albL1 (-) (lower)	5'-tcactagttaagcctaaggcagcttgac -3'

Antibodies used

The rat anti-PA monoclonal antibody NZ-1 (IgG_{2a}, λ) was provided by Prof. Y. Kato (Kato et al. 2006). The mouse anti-FLAG monoclonal antibody M2, the HRP-conjugated rabbit anti-rat IgG polyclonal antibody, and the HRP-conjugated goat anti-mouse IgG polyclonal antibody were obtained from Sigma-Aldrich. The mouse anti-HA monoclonal antibody 4B2 and the mouse anti-Myc monoclonal antibody 9E10 were obtained from Wako Pure Chemical Industries Ltd. The FITC-conjugated goat anti-rat IgG polyclonal antibody was obtained from Beckman Coulter Inc.

Expression and purification of T4L

The tagged T4L proteins were expressed in transformed *E. coli* BL21 (DE3) cultured at 37 °C in liquid LB medium containing 50 μg/ml ampicillin until OD_{600} (Optical Density at 600 nm) was reached to ~0.6. The T4L expression was induced by the culture for ~3 h at 37 °C in the presence of 1 mM IPTG. The T4L proteins were

purified as described below. Culture medium was centrifuged. The cells were suspended in TBS (pH 7.5) [20 mM Tris-HCl, 150 mM NaCl], and were sonicated. Then the suspension was centrifuged, and the soluble fraction (supernatant) was collected. The soluble fraction was mixed with Ni-NTA Agarose (QIAGEN) and incubated for 0.5~1 h at 4 °C under gentle agitation. The beads were transferred to a small column, washed with wash buffer [20 mM Tris-HCl (pH 8.0), 300 mM NaCl, 20 mM imidazole], and the bound protein was eluted with elution buffer [20 mM Tris-HCl (pH 7.0), 300 mM NaCl, 250 mM imidazole]. The elution samples were dialyzed against PBS (pH 6.0) [100 mM phosphate 100 mM NaCl].

Besides, the constructs for T4L attached with tag at the N-terminal (e.g., PA10-T4L, PA12-T4L, PA14-T4L) were used for the mutated constructs that were mutated from 1st Met derived from T4L to Lys for stopping the translation on the way, because these non-mutated constructs expressed the proteins that the translation started at the downstream Met derived form T4L.

Binding kinetics analysis using bio-layer interferometry (BLI)

Binding kinetics of various antibodies toward T4L protein tagged with their respective antigen peptide was analyzed by BLI using Octet RED system (Pall ForteBio). Binding assays were performed in 96-well microtiter plates at 30 °C with orbital sensor agitation at 1,000 rpm. Amine Reactive (AR2G) sensors were immobilized with each antibody dissolved at 10-20 μg/ml in 10 mM sodium acetate buffer at pH 6.0, followed by quenching with 1 M ethanolamine at pH 8.5. Binding to the serially diluted tagged proteins (1 nM, 3 nM, 10 nM, 30 nM) in PBS containing 0.005% Tween 20 (PBST) with 1% BSA placed in different wells at a volume of 200 μl was monitored for 60 s, followed by dissociation in PBST for 120 s. Binding curves were analyzed by BIAevaluation software (GE Healthcare) with a curve-fitting using a 1:1 binding model.

Binding kinetics analysis using surface plasmon resonance (SPR)

All SPR experiments were performed using BIACORE 2000 instrument (GE Healthcare). CM5 sensor chip were immobilized with NZ-1 dissolved in 10 mM sodium acetate buffer at pH 6.0 till approximately 3,000 RU (Resonance Unit) (1 RU ≈ 1 pg/mm^2), followed by quenching with 1 M ethanolamine at pH 8.5. The PA-tagged T4L

proteins were diluted in PBST (3.125 nM, 6.25 nM, 12.5 nM, 25 nM) and injected at a flow rate of 20 μl/min. Binding was monitored for 60 s, followed by dissociation in PBST for 120 s. This sensor chip was regenerated by incubation with 10 mM Glycin-HCl (pH 3.0), 1 M NaCl for 30 s. Binding curves were analyzed by BIAevaluation software (GE Healthcare) with a curve-fitting using a 1:1 binding model.

All single-residue alanine substitution mutants of T4L-PA12 were similarly measured. However, all mutated T4L-PA12 were injected at the concentration of 20 nM.

Western blot analysis of IDH1-FLAG-PA12

Human osteosarcoma U-2 OS cells (obtained from the American Type Culture Collection (ATCC), Manassas, VA) were transiently transfected with IDH1-FLAG-PA12 and the cell lysate was prepared as described previously (Kaneko et al. 2013b) (a gift form Prof. Y. Kato). The lysate (10 μg per lane) was separated on 10% SDS-PAGE and transferred to a PVDF membrane, followed by blocking with 4% skim milk in PBS (pH 7.4) with 0.05% Tween 20 for 15 min. For the primary antibody step, the membranes were incubated with varying concentrations of NZ-1 (0.01, 0.1, 1, or 3.5 μg/ml) or 3.5 μg/ml anti-FLAG M2 diluted in TBS at pH 8.0, containing 0.05% Tween 20 (TBST), for 1-60 min. For the secondary antibody step, membranes were incubated for 30 min with either HRP-conjugated rabbit anti-rat polyclonal antibody or HRP-conjugated goat anti-mouse polyclonal antibody (both from Sigma-Aldrich) diluted at 1:6,000 in TBST. Four consecutive washes (TBST, 5 min) were conducted between each step. The membranes were developed with ECL™ Prime reagent (GE Healthcare) and analyzed using ImageQuant LAS 4000mini (GE Healthcare).

Flow cytometry analysis of the PA12-rNrp2-mCherry expression cells

CHO-K1 cells (obtained from ATCC) were transiently transfected with PA12-rNrp2-mCherry construct. CHO-K1 cells were incubated by DMEM medium with 10% FCS, 1% Non-Essential Amino Acids solution (NEAA) (Sigma-Aldrich), and 0.5% penicillin-streptomycin (Sigma-Aldrich) (DMEM/10% FCS). The medium of CHO-K1 cells incubated on the 6-well plate were changed to DMEM medium with 5% FCS, 1% NEAA, and 0.5% penicillin-streptomycin (DMEM/5% FCS), and the cells were transfected with PA12-rNrp2-mCherry plasmid DNA (2 μg) using X-tremeGENE HP DNA Transfection Reagent (Roche). After 48 h incubation at 37 °C in 5% CO_2, the

expression of PA12-rNrp2-mCherry was estimated by fluorescence microscope BZ-9000 (KEYENCE) using 540 nm/605 nm filter, and the cells were detached, washed twice, and resuspended in DMEM/5% FCS. The cells were then incubated with DMEM/5% FCS containing NZ-1 at various concentrations (0.01, 0.1, 1, or 10 μg/ml) on ice for 30 min, washed twice with DMEM/5% FCS, and resuspended in DMEM/5% FCS containing FITC-conjugated goat anti-rat IgG antisera (Beckman Coulter Inc.) diluted at 1:100. After 30 min incubation on ice, the cells were washed once and suspended in PBS (pH 7.4), and analyzed on a flow cytometer with 488 nm laser (Guava EasyCyte, Millipore).

Coupling of NZ-1 to resin (NZ-1-Sepharose)

Purified NZ-1 was dialyzed against 0.1 M $NaHCO_3$ (pH 8.3), 0.5 M NaCl. The purpose is final immobilization concentration ~2.0 mg IgG/ml, and CNBr-activated Sepharose 4FF (GE Healthcare) was measured equivalent for it, followed by Sepharose was swollen by adding 1 mM HCl. After swelling, Sepharose was washed three times by 1 mM HCl to remove the impurities. Sepharose was changed buffer to 0.1 M $NaHCO_3$ (pH 8.3), 0.5 M NaCl, and added an antibody solution of the same volume as Sepharose, followed by incubated for ~3 h at room temperature under gentle agitation. After it was confirmed that there was few antibodies in supernatant using absorption spectrometer, the supernatant was removed, followed by Sepharose was incubated with 0.1 M Tris-HCl (pH 8.0) for ~1.5 h at room temperature under gentle agitation for blocking. Next, the supernatant was removed, followed by Sepharose was washed once with 0.1 M $NaHCO_3$ (pH 8.3), 0.5 M NaCl, once with MilliQ, once with 0.1 M NaAcO (pH 5.2), 0.5 M NaCl, and twice with TBS (pH 7.5). Finally, Sepharose was preserved 50% slurry with TBS (pH 7.5).

Expression and purification of mNrp1$_{ec}$-PA12

For the purification of soluble mNrp1$_{ec}$-PA12 secreted from mammalian cells, HEK293T (obtained from ATCC) cells plated in a 15-cm culture dish were transiently transfected with the plasmid using Polyethylenimine (Sigma-Aldrich) and ~25 ml of culture supernatant was harvested ~72 h after the transfection. Cleared supernatant was mixed with NZ-1-Sepharose (250 μl bed volume) and incubated for ~2 h at 4 °C under gentle agitation. The beads were then transferred to a small column (Bio-Rad), washed

with 5 ml (4 column × 5) of TBS (pH 7.5), and the bound protein was eluted with TBS containing 0.1 mg/ml free epitope peptide (EGGVAMPGAEDDVV). The elution was conducted at room temperature in a step-wise manner (1 column × 10), where dissociation time of 5 min was given for each elution step (Fig. I-2). The confirmation of purification quality was performed by all fractions were subjected to 10% SDS-PAGE and stained with CBB (Coomassie Brilliant Blue).

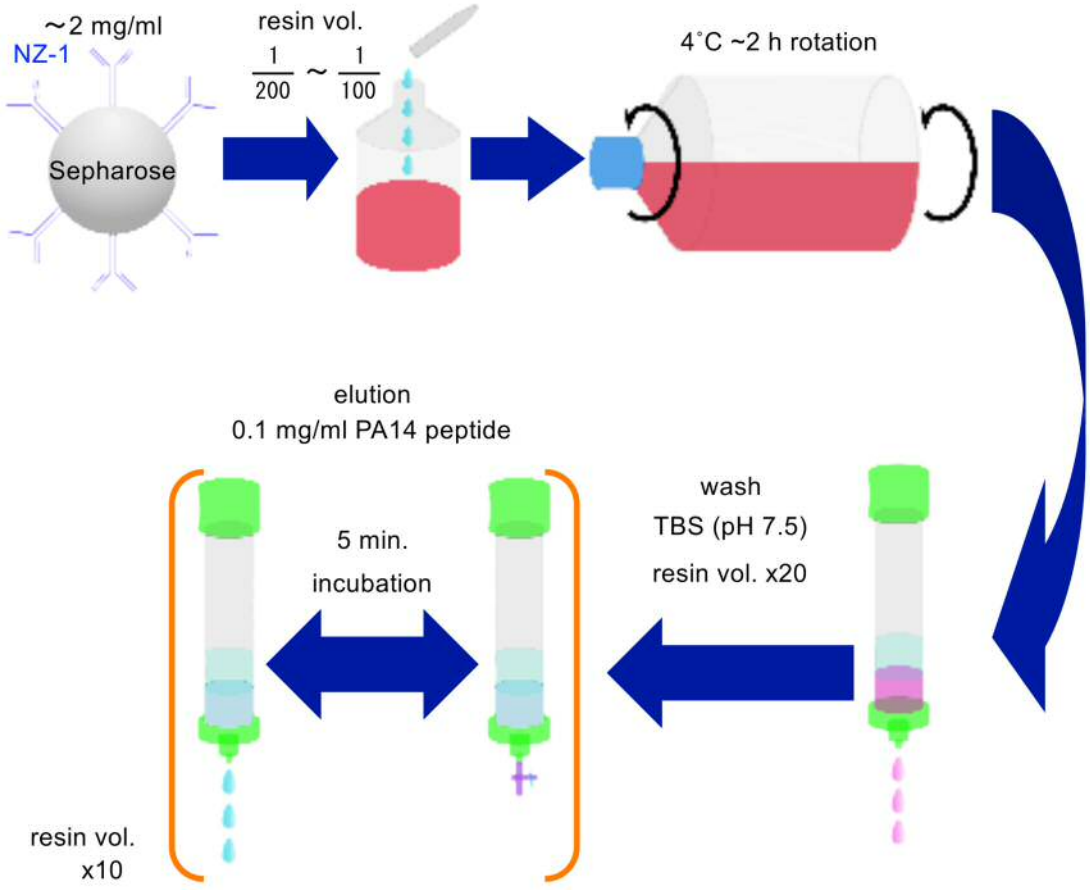

Figure I-2. Outline of protein purification protocol using PA tag system.

The examination of purification condition was carried out using the same

mNrp1$_{ec}$-PA12 culture supernatant. The culture supernatant was mixed with NZ-1-Sepharose at various volumes (1/50, 1/100, 1/200, or 1/400), was incubated for 15-120 min (15 min, 30 min, 60 min, or 120 min), and was eluted by PA peptide at various concentrations (0.05 mg/ml, 0.075 mg/ml, 0.1 mg/ml, or 0.2 mg/ml). In the case of elution by high concentration $MgCl_2$, this experiments was used 10 mM MES (pH 6.0), 3 M $MgCl_2$ or 10 mM MES (pH 6.0), 2 M $MgCl_2$. The evaluations of purified protein quantity were measured by BCA^{TM} Protein Assay (Pierce), after all elution fractions were collected and dialyzed against TBS (pH 7.5).

Western blot analysis of mNrp1$_{ec}$-PA12

The culture supernatant and flowthrough that were obtained in the purification of mNrp1$_{ec}$-PA12 were diluted at 1/2, 1/4, and 1/8 by TBS (pH 7.5). Ten microliters of these samples were separated on 10% SDS-PAGE under reducing condition, and transferred to a PVDF membrane. The membrane was visualized by Western blotting using NZ-1 as described IDH1-FLAG-PA12. Intensity of mNrp1$_{ec}$-PA12 was quantified by densitometric analysis using ImageJ (Schneider et al. 2012).

Expression and purification of HSA

For the purification of soluble PA12-HSA and HSA-PA12 secreted from mammalian cells, HEK293T cells plated in a 15-cm culture dish were transiently transfected with the plasmid using Polyethylenimine (Sigma-Aldrich), and the culture supernatant was harvested ~72 h after the transfection. These purifications were performed as described mNrp1$_{ec}$-PA12.

Screening of NZ-1-Sepharose regeneration condition

These experiments were performed using BIACORE 2000 instrument. CM5 sensor chip were immobilized with NZ-1 as described in binding kinetics analysis. For scouting the condition for the mild dissociation of antigen, the NZ-1 surface was first injected with a 100 nM solution of T4L-PA12 to saturate binding sites, incubated with PBST for 200 s to allow free dissociation, followed by an injection of various buffers for 30 s. Dissociation efficiencies were calculated by the ratio of the binding signal (in RU) before and after the injection of each solution (Fig. I-3).

Figure I-3. SPR screening for the buffer condition suitable for the NZ-1 column

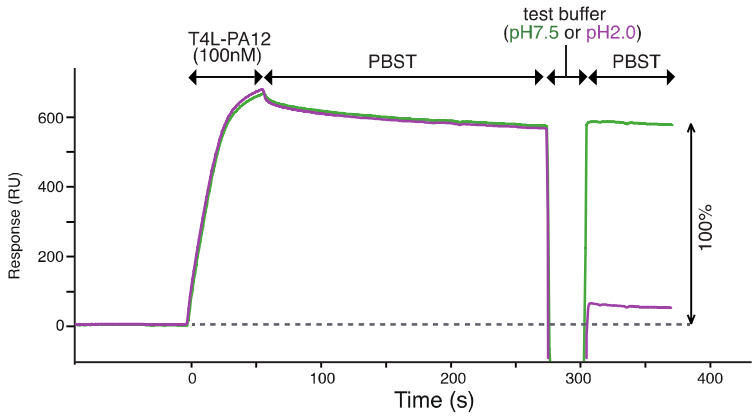

regeneration. Sensorchip surface immobilized with NZ-1 IgG was first infused with 100 nM T4L-PA12 for 60 s, allowed to spontaneously dissociate in PBST (pH 6.0) for 210 s, then treated with various test buffers for 30 s. Amount of T4L-PA12 remaining after the treatment was used to calculate dissociation efficiency shown in the Table I-2. Representative curves for the treatment with TBS, pH 7.5 (green) and Gly-HCl, pH 2.0 (magenta) are shown.

Examination of NZ-1-Sepharose regeneration

GFP_{UV}-PA12 was expressed in transformed *E. coli* BL21 (DE3) cultured at 37 °C in liquid LB medium containing 50 μg/ml ampicillin until OD_{600} (Optical Density at 600 nm) was reached to ~0.6. GFP_{UV}-PA12 expression was induced by the culture for ~24 h at 16 °C in the presence of 1 mM IPTG. Culture medium was centrifuged. The cells were suspended in TBS (pH 7.5) [20 mM Tris-HCl, 150 mM NaCl, 0.25 mM PMSF, 10 μM Leupeptin, 1 μM Pepstatin], and were sonicated. Then the suspension was centrifuged, and the soluble fraction (supernatant) was collected. The lysates were passed through a 0.45 μm filter to remove impurities, and aliquots were stored at -80 °C until later use. Small-scale purification of GFP_{UV}-PA12 was perfomed as follows. A mini column (Bio-Rad) containing 500 μl of NZ-1-Sepharose was equilibrated in TBS. Bacterial lysate (250 μl) was applied onto the column, followed by a washing step (2 ml of TBS) and an elution step (4 ml of 10 mM MES at pH 6.0 containing 3 M $MgCl_2$, 500 μl × 8). No. 2-5 fractions were named as elution fraction, because there were many GFP_{UV} proteins in these fractions. Used NZ-1-Sepharose was washed with TBS (pH 7.5), and this NZ-1-Sepharose was reused the purification for GFP_{UV}-PA12. The evaluation of NZ-1-Sepharose reuse times was performed with the repeat of this purification and regeneration cycle. The GFP_{UV}-PA12 contained in the elution fraction obtained from each purification cycle was quantified with a fluorescence measurement at excitation and emission wavelengths of 390 and 513 nm, respectively, using a Hitachi

F-7000 fluorescence spectrophotometer (Hitachi). All chromatographic procedures were performed at 4 °C (Fig. I-4).

Confirmation of used NZ-1-Sepharose regeneration

NZ-1-Sepharose used for the purification of mNrp1$_{ec}$-PA12 was incubated with × 10 column volume of 3 M $MgCl_2$ in 10 mM MES (pH 6.0) at room temperature under gentle agitation, with varying time and buffer change frequency (10 min × 3, 10 min × 6, 1 h × 1, 1 h × 3, over night × 1). After washing with TBS (pH 7.5) for removing $MgCl_2$, all proteins remaining in the NZ-1-Sepharose were eluted by × 2 SDS Sample buffer [125 mM Tris-HCl (pH 6.8), 4% (w/v) SDS, 20% (w/v) glycerol, 0.01% (w/v) BPB]. These eluted proteins were subjected to 10% SDS-PAGE under reducing condition and stained with fluorescent dye (Oriole, Bio-Rad).

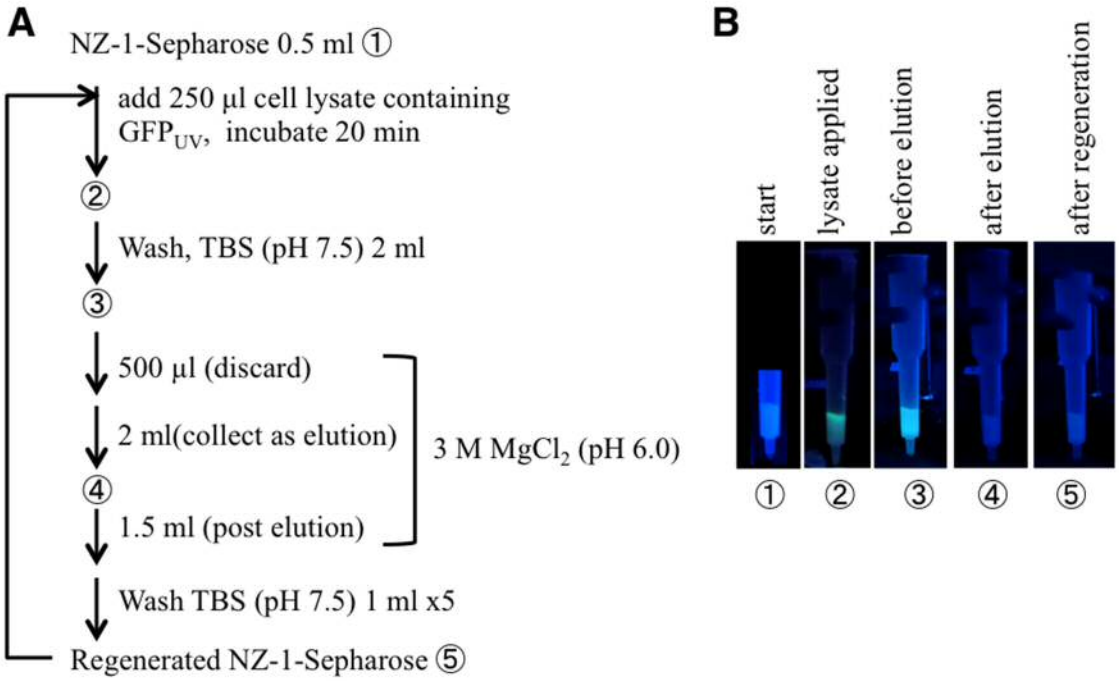

Figure I-4. Repeated purification of GFP_{UV} on NZ-1-Sepharose column for regeneration. (A) Procedure for the regeneration cycle of NZ-1-Sepharose used PA-tagged GFP_{UV} purification. (B) Fluorescent images of the NZ-1 column at each step. The column was illuminated by a hand-held illuminator emitting long wavelength (~365 nm) UV light.

Results

Kinetic analysis of NZ-1/PA tag interaction

Previous investigations by Y. Kato *et al.,* have indicated that NZ-1 had been recognized by linear peptide derived from human podoplanin using ELISA (Enzyme-Linked ImmunoSorbent Assay) (Ogasawara et al. 2008). The construction of an excellent epitope tag system needs a high 1:1 binding affinity between tag and antibody. Although many anti-peptide antibodies bind to multiple peptide tag on a carrier protein with high affinity, the real affinity toward single peptide tag is often low. Such antibodies are not suitable for purification tag system, because they do not effectively capture the tagged proteins in solution, and requires too long capture time and too much the amount of resin. Therefore, I estimated the 1:1 real binding kinetics between NZ-1 and its antigenic peptide in solution.

I evaluated binding kinetics between NZ-1 and its antigenic peptide and compared it with three other tag/mAb pairs that are commercially available as purification systems (FLAG tag system, HA tag system, Myc tag system) using BLI (Bio-Layer Interferometry). BLI is a technology for measuring the biomolecular interactions, observing the optical reflection of sensor surface immobilized the objective molecules. The interactions can be measured in real-time when white light was incident from inside sensor, because the interference pattern is shifted depending on the amount of molecules on the biosensor chip. Antibodies used were M2 (anti-FLAG, available from Sigma-Aldrich) (Brizzard et al. 1994), 4B2 (anti-Myc, available from WAKO Pure Chemical Industries Ltd.), and 9E10 (anti-Myc, available from WAKO Pure Chemical Industries Ltd.) (Chan et al. 1987). In order to make fair comparison, all peptide tags were fused to the same model protein T4 lysozyme (T4L) using identical length of linker (Fig. I-1). Then, the T4L was tagged either N- or C-terminal. Moreover, these T4L attached with various tags were purified by His tag and Ni-NTA agarose. These purified T4L mutants were high purity. The molecular weight of these T4L depended on the attached tag length (Fig. I-5), and it was confirmed that these T4L were monodisperse monomer state in solution using gel filtration chromatography (data not shown). Hereafter, I used these T4L mutants when I calculate the dissociation constant (K_D value).

BLI sensors were immobilized with each antibody using amine coupling method, and the binding affinity of each epitope tag system were estimated using this

sensors and the above T4L mutants. Although all anti-tag mAbs exhibited reasonably appropriate binding behavior toward each antigenic peptide in the biolayer interferography experiments using Octet devise (Fig. I-6), NZ-1/PA tag interaction was exceptional in that it did not show dissociation over the assay time of few minutes (Fig. I-6A, B). In fact, curve fitting tagged C-terminally of each data derived exceptionally slow dissociation rate constant for NZ-1/PA interaction, resulting in much higher overall affinity than other tag systems (Fig. I-6C). Meanwhile, the T4L attached with PA tag at the N-terminal dissociated faster than the T4L attached with PA tag at the C-terminal, and the binding affinity between PA tag and NZ-1 decreased. However, all tagged T4L in this research had similar results, and it was suggested that the reason depended on not only the characteristics of interaction between tag and antibody, but also the characteristics of T4L. The very slow dissociation rate is a property highly desirable for isolation purpose, because it assures that tagged protein are completely captured and does not leak during the washing steps.

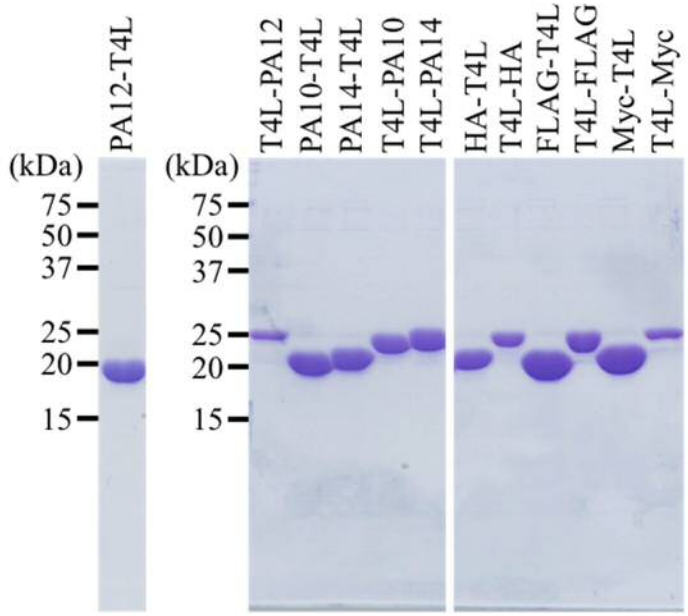

Figure I-5. Purity check of the tagged T4L mutant proteins used for the binding assays. T4L mutant proteins purified by Ni-NTA agarose were subjected to 15% SDS-PAGE under reducing condition and stained with CBB.

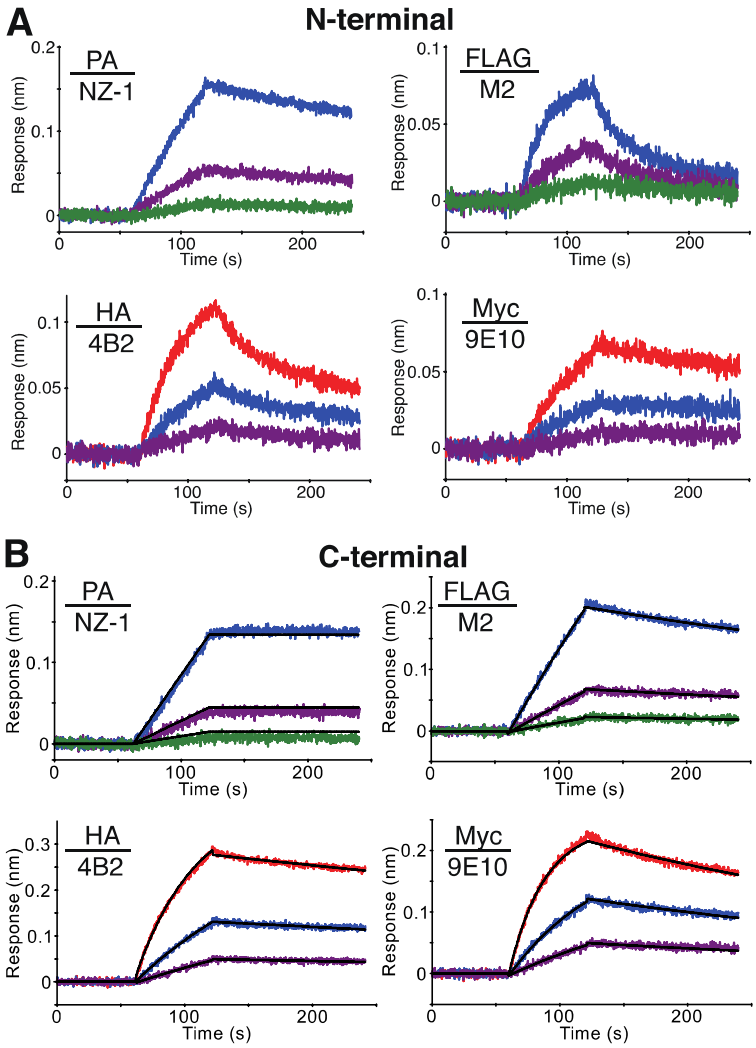

C

Tag (Antibody)	k_a (1/Ms)	k_d (1/s)	K_D (M)
PA (NZ-1)	1.44×10^{4}	5.75×10^{-6}	3.99×10^{-10}
FLAG (M2)	6.08×10^{4}	1.69×10^{-3}	2.78×10^{-8}
HA (4B2)	6.72×10^{5}	1.11×10^{-3}	1.65×10^{-9}
Myc (9E10)	1.13×10^{6}	2.49×10^{-3}	2.19×10^{-9}

Figure I-6. Bio-layer interferometry kinetic analysis of various anti-epitope tag antibodies. (A), (B) Representative BLI binding data for tagged T4L (A, N-terminal; B, C-terminal). Each anti-tag mAb was immobilized on sensor tips. Association (from 60 s to 120 s) and dissociation (from 120 s to 240 s) phases are shown for serial dilution series of the tagged T4L (red, 30 nM; blue, 10 nM; purple, 3 nM; green, 1 nM). Black lines represent a global fit of the data to a 1:1 binding model. (C) Kinetic binding parameters of (B) for each interaction obtained using BIAevaluation.

Minimal sequence requirement for the PA tag

NZ-1 was raised against 14-residue peptide (EGGVAMPGAEDDVV; PA14) corresponding to residues 38-51 of human podoplanin (Kato et al. 2006). Previous study showed that the central 10-residue portion (GVAMPGAEDD; PA10) was indispensable for the recognition (Ogasawara et al. 2008). To decrease the effect on tagged proteins, epitope tag has a preference for a short amino acids sequence. Therefore, in order to determine the minimal peptide region that warrants observed high affinity, I carried out surface plasmon resonance (SPR) binding experiments between NZ-1 and various versions of PA tagged protein.

As shown in Fig. I-7A and B, either PA14 or PA12 (GVAMPGAEDDVV) tags attached C-terminally to T4L bound to NZ-1 with high affinity in an indistinguishable manner, indicating that the N-terminal two residues (Glu-Gly) were dispensable. In contrast, PA10-tagged version showed greatly reduced affinity (~1/10,000) (Fig. I-7C), suggesting that the last two valines were important to ensure the high affinity. I next tested whether PA tag was compatible with N-terminal fusion. As shown in Fig. I-7D, E, and F, both PA14 and PA12 mediated high affinity binding to NZ-1 when appended at N-terminal of T4L, although the dissociation was slightly faster than the C-terminal versions. Interestingly, affinity of PA10-T4L was decreased by only 1.5-fold from PA12 and PA14. It seems likely that the presence of the last two residues is important for the high affinity but they can be substituted by other amino acids (such as Arg-Glu in PA10-T4L). Hereafter, I will use PA12 sequence for all applications.

To determine which amino acid residues within the PA12 are critical for the recognition by NZ-1, ten non-alanine residues were mutated to alanine and each mutant (in the format of T4L-PA12) was evaluated in SPR assay. As clearly shown in the overlaid sensorgrams in Fig. I-8, mutations at M4 and D10 had the most severe effect, indicating the major contribution of these residues in the binding. Effects of four other mutations (P5A, G6A, E8A, and D9A) were less pronounced, and the rest of the mutants exhibited virtually identical binding behavior to the original PA tag. Therefore, NZ-1 seems to achieve the very high affinity toward PA tag using a combination of many interactions to the central core segment (M4-D10), with the contribution of M4 and D10 being dominant.

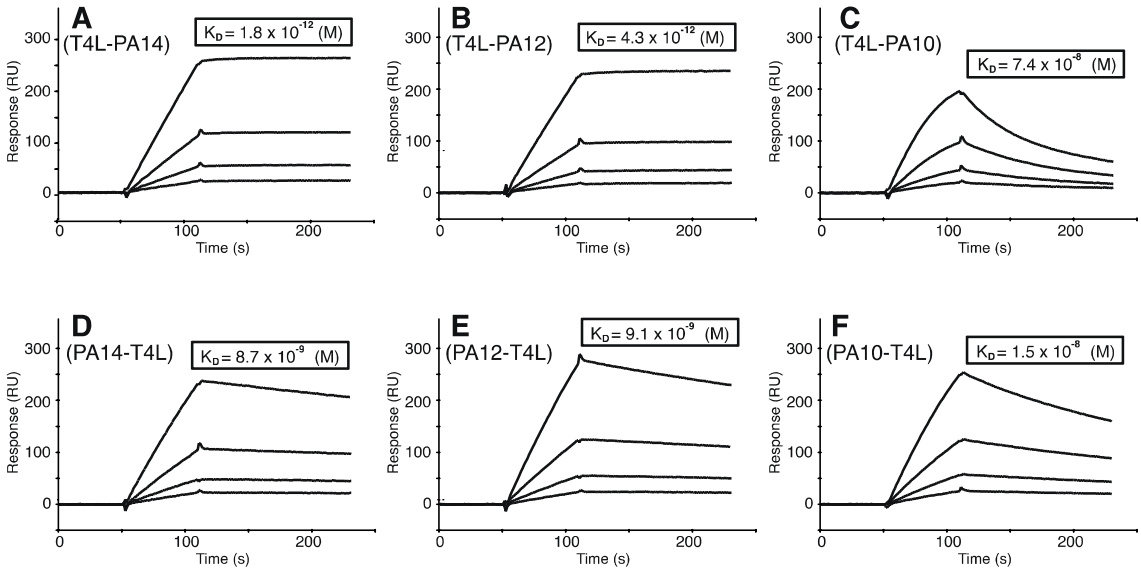

Figure I-7. Surface plasmon resonance kinetic analysis of NZ-1 binding toward various PA tags. Serially diluted PA-tagged T4L proteins (3.125, 6.25, 12.5 and 25 nM) were injected over the CM5 sensor chip immobilized with NZ-1 for 60 s, followed by dissociation in PBST for 120 s at a flow rate of 20 µl/min. PA14 (A, D), PA12 (B, E), or PA10 (C, F) peptides were fused either C-terminally (A-C) or N-terminally (D-F) to T4L protein. Each set of binding curves was globally fitted to 1:1 binding model to derive dissociation equilibrium constant (K_D) values shown in the boxes.

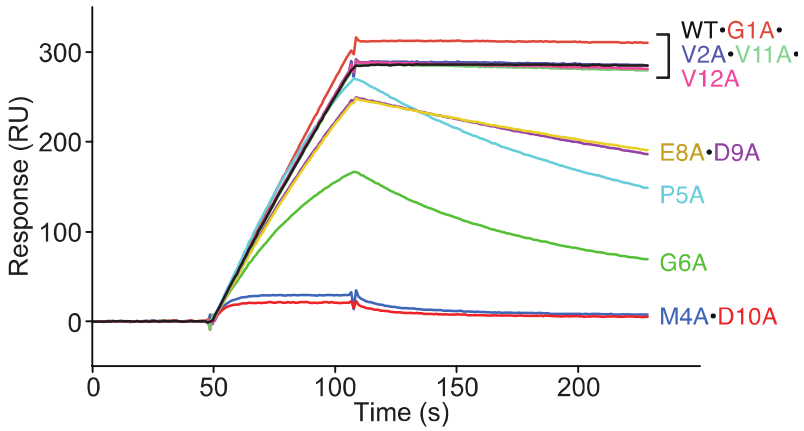

Figure I-8. Effect of alanine substitutions of PA tag sequence on the binding to NZ-1 using SPR. Purified alanine-substituted versions of T4L-PA12 diluted at 20 nM were injected over the surface immobilized with NZ-1 as described in the legend to Fig. I-7 and sensorgrams after subtraction of the buffer control were overlaid.

Utility of NZ-1 as a detection antibody

It is expected that NZ-1 and PA tag can be used as a protein specific detection system, because they had very high affinity and specificity. To test this idea, a cytoplasmic enzyme isocitrate dehydrogenase 1 (IDH1) was doubly tagged with FLAG and PA (IDH1-FLAG-PA12) (Fig. I-1), and expressed in human osteosarcoma cell line U-2 OS that expresses low endogenous podoplanin (obtained from Prof. Y. Kato) (Kato Kaneko et al. 2014). As shown in Fig. I-9A, left lane, Western blotting of the resultant cell lysate with NZ-1 produced a strong band corresponding to the expressed IDH1 (~45 kDa). The same membrane as above stained by CBB visualized many bands, however, IDH1 was not shown in Fig. I-9A, right lane. It is suggested that NZ-1 was able to detect the IDH1 with high sensitivity. NZ-1 immunoblot of the untransfected cells did not show any reactive bands (data not shown), indicating very high specificity of the detection. In contrast, a number of nonspecific bands other than tagged IDH1 were seen in the anti-FLAG M2 antibody immunoblot (Fig. I-9A, middle lane). In addition to the high specificity, detection by NZ-1 was proven highly sensitive, because the signal intensity of the reactive band was saturated after incubating with NZ-1 for as short as 5 min (Fig. I-9B), and at concentration as low as 0.1 μg/ml (Fig. I-9C). Therefore, PA tag/NZ-1 system was proved that this is extremely useful system.

Next, I applied NZ-1/PA tag combination to the flow cytometric analysis of cell surface receptors. An expression construct for a type I transmembrane protein rat neuropilin-2 (rNrp2) was engineered to carry PA tag at its N-terminal (extracellular domain) and mCherry at its C-terminal (cytoplasmic domain) (PA12-rNrp2-mCherry) (Fig. I-1), and was transiently transfected into CHO-K1 cells. Inspection of cells by fluorescence microscopy after transfection indicated that ~20% cells were positive for the Nrp2-mCherry (Fig. I-10A). Similar level of surface expression was confirmed by the flow cytometric analysis of the same cells with NZ-1 (Fig. I-10B, solid line histogram). Furthermore, efficient staining was achieved even when the concentration of the primary antibody was reduced to 0.1 μg/ml NZ-1 (Fig. I-10B, inset), again underscoring the great potential of PA tag as a detection system. Therefore, it was suggested that the flowcytometry using NZ-1 was able to detect and quantify the membrane protein attached with PA tag at the extracellular regions with high sensitively and simply.

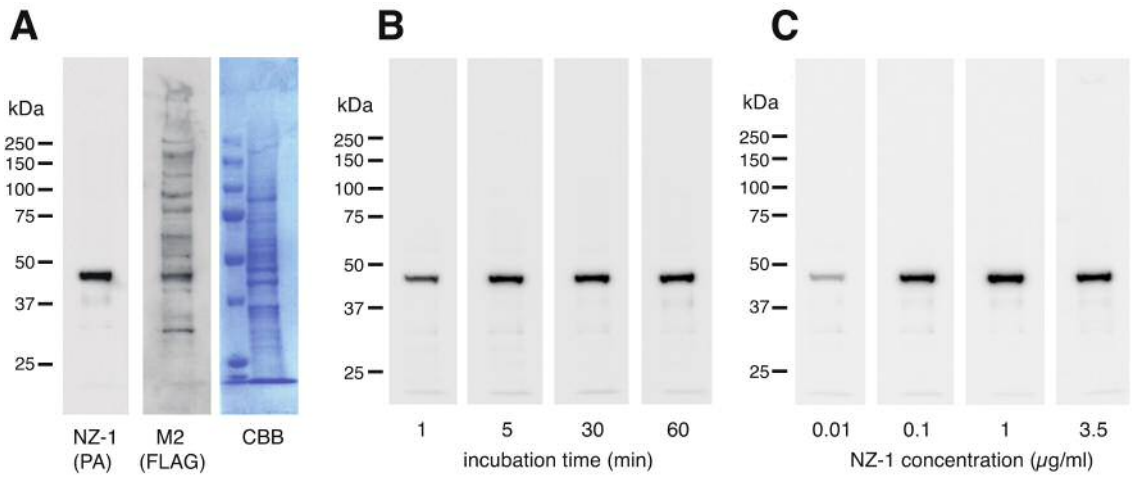

Figure I-9. Western blot analysis of PA tagged IDH1 with NZ-1. (A) Total cell lysates from human osteosarcoma cells expressing the IDH1-FLAG-PA12 were electrophoresed under reducing conditions using 10% SDS-PAGE gel and transferred to a membrane. Three strips of the membrane containing the same amount of lysate were immunoblotted with NZ-1 (left), M2 (center), or directly stained with CBB (right). The same membrane strips were used to assess the time course (B) or dose-dependency (C) of the NZ-1 incubation. In (B), membranes were incubated with 1 μg/ml NZ-1 for the incubated period. In (C), membranes were incubated with varying concentrations of NZ-1 for 30 min. All steps after the NZ-1 incubation, including secondary antibody reaction and chemiluminescence visualization, were conducted under the exactly same condition for all membranes.

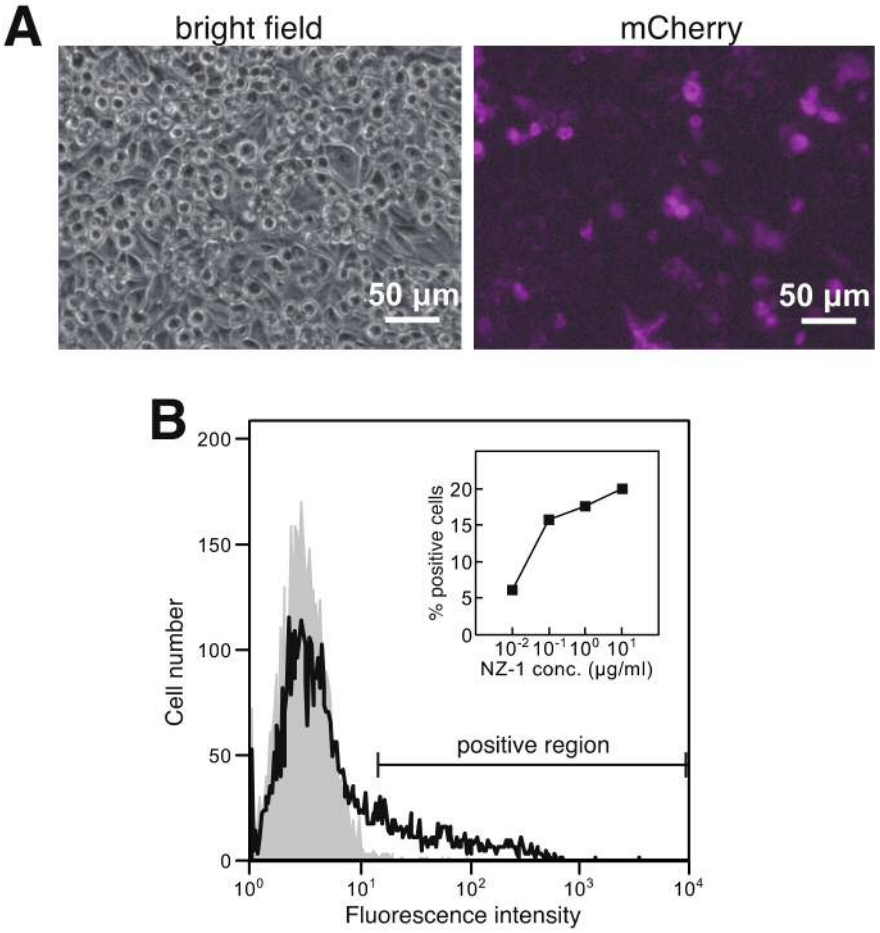

Figure I-10. Flow cytometric analysis of PA-tagged membrane protein. (A) Photographs of CHO-K1 cells transiently transfected with PA12-rNrp2-mCherry. Note that about 20% of the total cells express PA12-rNrp2-mCherry (magenta). (B) Untransfected CHO-K1 cells (gray area) or CHO-K1 cells transiently transfected with PA12-rNrp2-mCherry (solid line) were incubated with 10 μg/ml NZ-1 and stained with FITC-labeled secondary antibody specific for rat IgG. Less than 1% of parental CHO-K1 cell population was positive with NZ-1 (region indicated by a bracket). Staining efficiency was expressed as the % positive cells and plotted against the concentration of primary antibody (inset).

Protein purification using NZ-1 and PA tag

I next explored the possibility to apply NZ-1/PA tag interaction in a protein purification system. The resin immobilized with an antibody is usually used for the epitope tag purification. The flow of protein purification is (1) the tagged target proteins are captured by the resin immobilized with an antibody, (2) the resin is washed for removing the impurities, (3) only the target proteins is eluted from the resin. Many epitope tag systems are compatible with the competitive elution of the tagged protein by free antigen peptide. There are many advantages that it is possible to purify in the neutral condition, the detailed consideration of conditions is unnecessary, and the purification efficiency is high. In fact, various free antigen peptides for elution against various tags have been sold by company. Although the complex of tagged molecules and antibodies seems a stable structure, the interaction is repeated the association and dissociation. The reason why the target proteins can be eluted from an antibody resin by free antigen peptide is that free antigen peptide can inhibit the binding by very fast diffusion rate. Therefore, it was unclear whether PA tag/ NZ-1 system with very slow dissociation rate is possible to elute the target proteins as described above. I focused on the purification of recombinant proteins secreted into culture media from transfected mammalian cells, because such project generally suffers from the lack of robust purification method due to the low abundance of the protein in the starting material (i.e., culture supernatants). First, I used ectodomain fragment of mouse neuropilin-1 (mNrp1) as model protein. Although Nrp1 is membrane protein, I used soluble ectodomain fragment of mouse Nrp1 tagged C-terminally with PA12 ($mNrp1_{ec}$-PA12, Fig. I-1). For the purification of $mNrp1_{ec}$-PA12 from mammalian cells, HEK293T cells were transiently transfected, and the culture supernatant was harvested. Although there were many proteins derived from FCS in the supernatant, the $mNrp1_{ec}$ band was not visualized by SDS-PAGE (Fig. I-11A, c. sup). The electrophoresis image of flowthrough (through the NZ-1-Sepharose) was similar to c. sup (Fig. I-11A, flowthrough). However, the near-perfect capture of tagged protein during the affinity chromatography was confirmed by the presence of less than 5% antigen in the flowthrough fraction (Fig. I-11B). The captured $mNrp1_{ec}$-PA12 did not dissociate in wash with × 20 column volume of wash buffer (4 column × 5) (Fig. I-11A, wash 1-5), and eluted from the resin by a solution containing 0.1 mg/ml PA14 peptide (Fig. I-11A, elution 7-11). The ability of free peptide to competitively elute bound antigen was

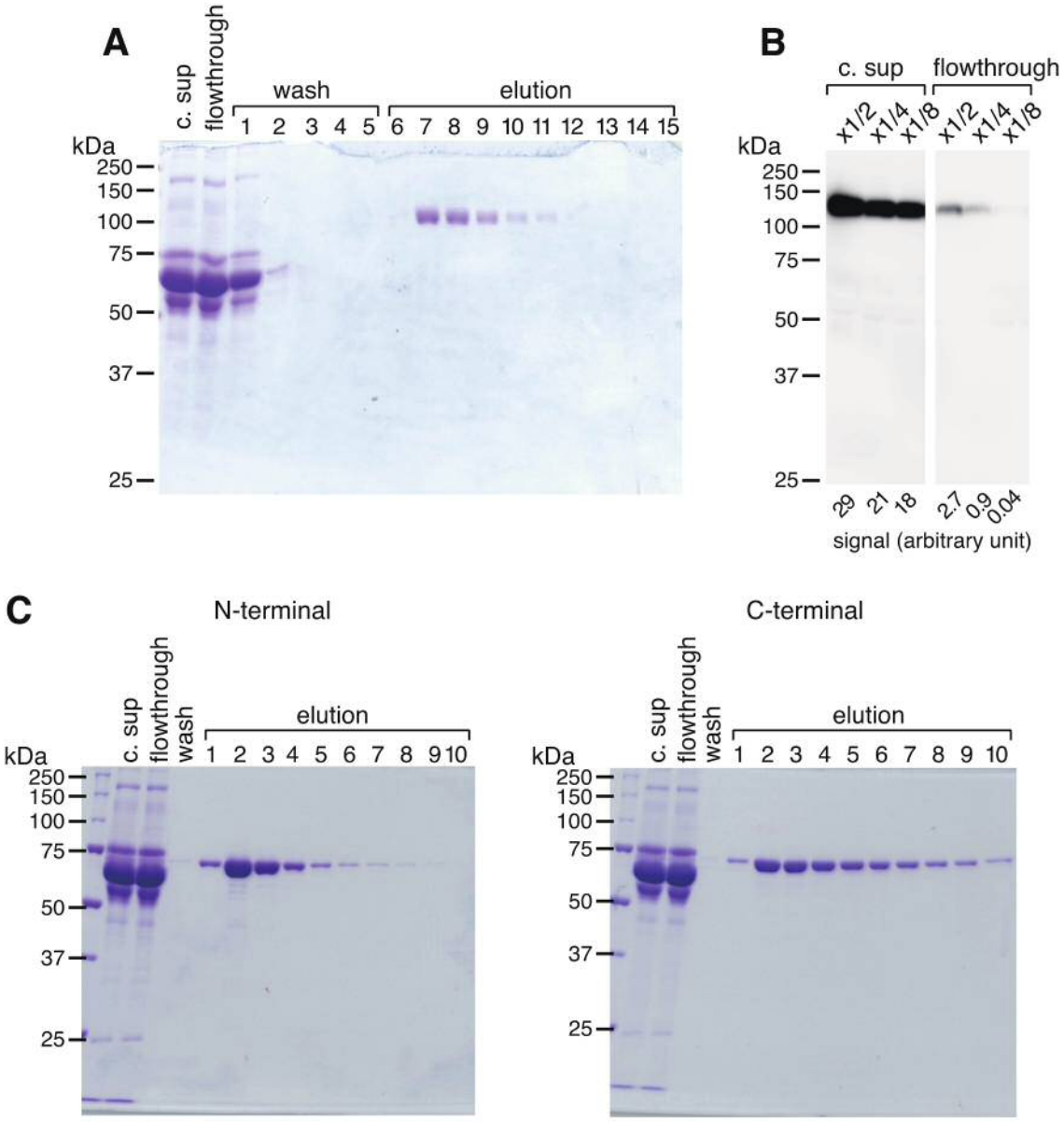

Figure I-11. One-step purification of PA12-tagged proteins. (A) Purification of soluble ectodomain fragment of mouse neuropilin-1. Five microliters of the culture supernatant from the transfected cells before (c. sup) and after (flowthrough) NZ-1-Sepharose capture, as well as 10 µl of the five wash (lane 1-5) and ten peptide-elution fractions (lane 6-15) during the column chromatography were subjected to 10% SDS-PAGE under reducing condition and stained with CBB. (B) The culture supernatant and the flowthrough fractions from the chromatography shown in (A) were diluted with TBS as indicated and subjected to Western blotting using NZ-1. Intensity of the 120-kDa band was quantified by densitometric analysis and, shown below each lane. (C) One step purification of secretory protein human serum albumin (left, PA12-HSA; right, HSA-PA12). Five microliters of c. sup and flowthrough, as well as the 10 µl of the wash and ten peptide-elution fractions during the column chromatography were subjected as described in (A).

rather unexpected, because the interaction seemed to be almost irreversible in the

kinetic binding assays shown in Fig. I-6 and I-7. In fact, I found it essential to perform the elution in a step-wise manner rather than under continuous flow, and allow ~5 min of dissociation time for each fraction. I confirmed that the elution efficiency from NZ-1-Sepharose decreased when I did not incubate for the elution (data not shown). Next, to determine the most suitable affinity purification condition, I evaluated the ratio of sample volume and NZ-1-Sepharose volume, the incubation time for capture, and the concentration of PA14 peptide for elution, respectively. As a result, it was suggested that the most suitable condition is 1/200~1/100 (v/v) (NZ-1-Sepharose volume), 1~2 h (incubation time), over 0.1 mg/ml (PA14 peptide concentration) (Fig. I-2, Table I-2). To confirm the versatility of this method, I constructed human serum albumin (HSA) attached with PA tag at the N- or C- terminal (PA12-HSA, HSA-PA12) (Fig. I-1). HEK293T cells were transiently transfected, and the culture supernatant was purified as described above. As a result, I was able to purify the extremely pure target proteins in both cases (Fig. I-11C). Based on this method, this laboratory have so far applied PA-tag/NZ-1 system to purify the soluble and membrane proteins having widely different molecular weight (from 15 to >300 kDa), where >95% purity was regularly attainable in one step by NZ-1-Sepharose chromatography. Therefore, it was indicated that NZ-1 and PA tag is able to construct the extremely versatile protein purification system.

Table I-2. Purification condition screening

Resin vol.	Incubation time	Elution buffer	Protein yeild
1/100	2 h	0.1 mg/ml PA14 peptide	71.1 μg
1/400	2 h	0.1 mg/ml PA14 peptide	23.8 μg
1/200	2 h	0.1 mg/ml PA14 peptide	36.1 μg
1/50	2 h	0.1 mg/ml PA14 peptide	72.7 μg
1/100	15 min	0.1 mg/ml PA14 peptide	55.0 μg
1/100	30 min	0.1 mg/ml PA14 peptide	60.2 μg
1/100	1 h	0.1 mg/ml PA14 peptide	79.7 μg
1/100	2 h	0.05 mg/ml PA14 peptide	61.2 μg
1/100	2 h	0.075 mg/ml PA14 peptide	78.2 μg
1/100	2 h	0.2 mg/ml PA14 peptide	72.5 μg
1/100	2 h	2 M $MgCl_2$ (pH 6.0)	72.0 μg
1/100	2 h	3 M $MgCl_2$ (pH 6.0)	79.8 μg

Reusability of the NZ-1-Sepharose

In general, antibody-based purification systems tend to be costly compared to other methods that use affinity resins with immobilized chemical compounds (Lichty et al. 2005). Although the major reason for the high cost is the requirement of the use of synthetic peptide for the elution process, it is often noted that the limited reusability of the antibody resin is another cost-elevating factor. This is especially critical in an immunoaffinity system where the antibody binds its antigen tightly, because potentially damaging condition (e.g., high or low pH, denaturing agents, etc.) is required for the regeneration of the column to remove the peptide that was bound during the elution process. In fact, FLAG tag system that is representative of tag system decreases the purification ability for the antibody inactivated by the regeneration cycles, because the regeneration condition of M2 immobilized resin is acidic buffer at pH 3.0. I therefore sought to find conditions that can completely disrupt NZ-1/PA tag interaction while maintaining the functional integrity of the antibody. To this end, NZ-1 was covalently immobilized on a BIACORE sensorchip and allowed to saturate with T4L-PA12, followed by an injection of various buffers (Fig. I-3). Table I-3 shows the effect of brief (30 sec) exposure to a variety of conditions on the dissociation of the bound antigen. Unlike some "polyol-sensitive" antibodies (Burgess and Thompson 2002; Nogi et al. 2008), inclusion of water-miscible organic solvent such as propylene glycol did not have dissociating effects. Strongly acidic condition (pH 2.0) was effective in disrupting the interaction (Table I-3), but it severely damaged the NZ-1 itself, because the surface lost binding ability (data not shown). Lowering the pH of the buffer was generally effective, especially when high concentration of salt was included. I examined the various pH buffer (pH 4~7) with high concentration of various salt (NaCl, NaBr, $MgCl_2$). After testing several combinations, I found that a slightly acidic (i.e., pH 6.0) buffer containing 3M $MgCl_2$ could completely remove bound antigen from the antibody (Table I-3). It was confirmed that brief injection of this buffer onto the NZ-1 surface did not affect the binding capacity (data not shown).

I adopted the above buffer as a column-regeneration condition after each cycle of protein purification using NZ-1-Sepharose. In order to assess potential damaging effect of the regeneration condition, GFP_{UV}-PA12 expressed in bacterial cytosol was used as a test protein (Fig. I-1) and repeated absorption-elution-regeneration cycles were performed on a small column of

NZ-1-Sepharose (Fig. I-4). The quantity of GFP_{UV} was simply estimated by measurement of fluorescence. Surprisingly, the NZ-1 column could withstand 60 times of regeneration cycles, as evidenced by the sustained recovery of the GFP_{UV}-PA12 in each eluted fraction (Fig. I-12). This result indicated that the NZ-1-Sepharose was able to be efficiently regenerated by the treatment with 3M $MgCl_2$ at pH 6.0 without causing any damage on the immobilized antibody. Additionally, the elution of the target proteins from NZ-1-Sepharose was able to be used not only high-cost synthetic peptide but also low-cost buffer, 3 M $MgCl_2$ at pH 6.0 (however, the function of the target proteins must not affect in this condition). In fact, I attempted to purify $mNrp1_{ec}$-PA12 using the elution buffer of 3 M $MgCl_2$ at pH 6.0. As a result, the quantity of the purified protein was similar to one eluted by PA14 peptide (Table I-2). It is therefore clear that the PA-tagged proteins can be eluted from NZ-1-Sepharose by the treatment with PA14 peptide or 3M $MgCl_2$ at pH 6.0.

Table I-3. Effect of various buffers on the interaction between PA tag and NZ-1

Salt, additive	pH (buffer)	Dissociation efficiency (%)
0.15 M NaCl	7.5 (Tris)	0
no	2.0 (Gly-HCl)	91
0.15 M NaCl + 40% propylene glycol	7.5 (Tris)	8
2M NaCl	7.0 (PIPES)	28
	6.0 (MES)	30
	5.0 (Acetate)	40
	4.0(Acetate)	87
2M NaBr	7.0 (PIPES)	52
	6.0 (MES)	59
	5.0 (Acetate)	77
	4.0(Acetate)	97*
2M $MgCl_2$	7.0 (PIPES)	93
	6.0 (MES)	94
	5.0 (Acetate)	96*
	4.0(Acetate)	98*
3M $MgCl_2$	6.0 (MES)	98*

* Conditions suitable for antigen elution

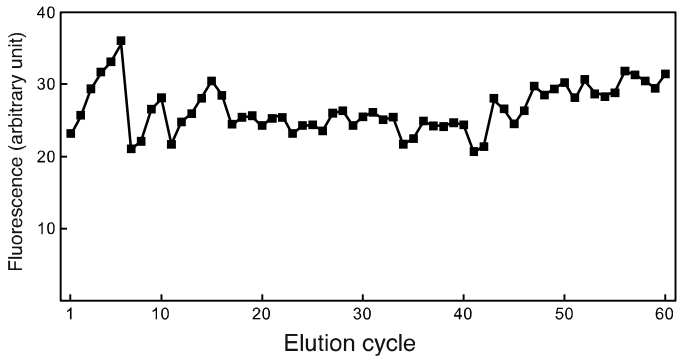

Figure I-12. Effect of the repeated column regeneration treatments on the yield of PA-tagged GFP_{UV} purification by NZ-1-Sepharose. Repeated column purification of GFP_{UV} was performed as described in Fig. I-4. The graph shows the amount of GFP_{UV}-PA12 contained in the pooled eluate fraction from each purification cycle quantified with a fluorescence measurement.

Although NZ-1-Sepharose can be regenerated and reused as described above, there is the danger of cross-contamination when the different target protein is purified by used resin. Finally, I examined the detailed regeneration condition of NZ-1-Sepharose used for protein purification. NZ-1-Sepharose used for the purification of $mNrp1_{ec}$-PA12 was incubated with × 10 column volume of 3 M $MgCl_2$ (pH 6.0) at room temperature under gentle agitation, with varying time and buffer change frequency (10 min × 3, 10 min × 6, 1 h × 1, 1 h × 3, over night × 1). After washing the resin, all proteins remaining in the NZ-1-Sepharose were eluted by SDS. It was confirmed that $mNrp1_{ec}$-PA12 remained very slightly into the resin in any conditions (Fig. I-13). However, the proteins detected in this experiment were soluble by SDS. It was proposed that the proteins were physically captured into resin by the degeneration and aggregation. Therefore, it is suggested that the danger of cross-contamination is not high when the proteins are eluted by mild condition such as free antigen peptide. Finally, it was revealed that the regeneration using 3 M $MgCl_2$ at pH 6.0 is sufficiently the once treatment for 1 h, and it is not impossible to use the same resin for the purification of different proteins, in these experiments.

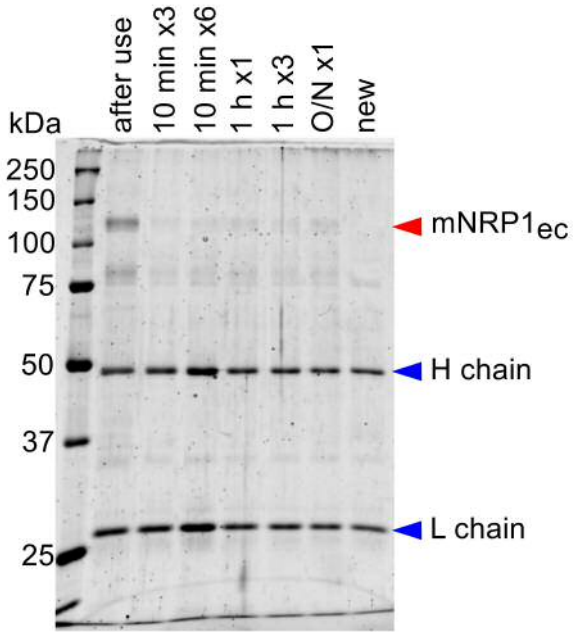

Figure I-13. Residual tagged proteins remaining inside the used NZ-1-Sepharose after the regeneration. NZ-1-Sepharose used in the experiment shown in Fig. I-11 (A) was incubated with x10 column volume of 3 M $MgCl_2$ in 10 mM MES, pH 6.0 at room temperature under gentle agitation, with varying time and buffer change frequency (10 min x3, 10 min x6, 1 h x1, 1 h x3, over night x1). After washing with TBS, all proteins remaining in the NZ-1-Sepharose were eluted by SDS. These eluted proteins were subjected to 10% SDS-PAGE under reducing condition and stained with fluorescent dye. Red arrow, $mNrp1_{ec}$-PA12; blue arrows, NZ-1 subunits.

Discussion

In this research, I have successfully developed a novel affinity tagging system "PA tag system" by applying a unique monoclonal antibody NZ-1 against human podoplanin. Owing to its unusually high affinity toward linear dodecapeptide antigen, NZ-1 can be used to detect, capture, and purify tagged proteins in various assay formats. The most remarkable advantage of this system is the ability to purify low abundant proteins at high yield in one step, along with its extended reusability. Moreover, this system has several advantages. First, the advantage is the characteristics of PA tag amino acid sequence. PA tag consists of 12 amino acid residues of a relatively short length, and does not have large hydrophobic or basic amino acids. Therefore, it is suggested that PA tag has little effect on the tagged protein (e.g., expression level, localization, function). Second, the free antigen peptide (EGGVAMPGAEDDVV) of PA tag is easy to dissolve, and has a high yield in solid-phase peptide synthesis. Third, this peptide does not inhibit the measurement of protein concentration using absorption spectroscopy, because this sequence does not have aromatic amino acid. The fractions eluted by PA peptide can be easily monitored which fractions have the target protein by measurement of absorbance at 280 nm. Finally, it is also a valiant advantage that this system can be used as many protein detection tools (Western blotting (Fig. I-9), flow cytometry (Fig. I-10), immunocytochemistry (Kaneko et al. 2013a)). Particularly, in Western blotting, we have to consider the combination of host cell and tag (and antibody), because the non-specific bands derived from host cell may bear when the low expression level protein was visualized using anti-tag antibody by Western blotting. However, we don't have to consider as above when we use NZ-1 and PA tag. It is possible that this tag system can save the cost and time in all methods, because this system has affinity higher than the existing tag systems.

On the other hand, PA tag system has also disadvantages. Since NZ-1 was established for antibody toward human podoplanin, NZ-1 specifically binds to human podoplanin (and monkey podoplanin that has the same sequence in PLAG domain). Among commonly used cell lines, HEK cells and COS cells have been confirmed the positive reaction for NZ-1 staining. In fact, I confirmed that the signals derived from endogeneous podoplanin in these cell lines were detected in flow cytometry and Western blotting (data not shown). However, it was revealed that PA tag system was able to be used for the purification of soluble proteins in these cell lines (Fig. I-11),

because podoplanin is membrane proteins. Additionally, these cell lines can be used as expression hosts if the purpose is to purify PA-tagged recombinant membrane proteins, because the contamination of endogenous podoplanin is negligible (Fujii et al. 2014). It was tested if PA tag system is compatible with the purification of membrane proteins. HEK293S GnT1$^-$ cells were transfected with N-terminally PA-tagged human EGFR. Next, PA-tagged EGFR was captured by NZ-1-Sepharose and eluted efficiently with 0.1 mg/ml PA14 peptide solution. A great separation power of the PA tag/NZ-1 system is demonstrated by the successful purification of the 145 kDa EGFR protein from the low abundance cell lysate, with virtually no contaminations. Surprisingly, podoplanin (~37 kDa) was not co-purified with the PA-tagged proteins even though the cell line expresses endogenous human podoplanin. It was reported that podoplanin was attached O-linked glycan at 52nd threonine (...EDVVT^{52}PGT...) just behind the sequence of PA tag (Kaneko et al. 2007). It is possible that the effective affinity of NZ-1 for the epitope region (PLAG domain) of native podoplanin is relatively low, probably due to the steric hindrance of the peptide sequence by the nearby glycan chains, resulting in the inefficient capture during the affinity chromatography. After all, we have to be careful of the endogenous podoplanin when we use PA tag/NZ-1 system. On the other hand, as a result of alanine scanning, the side chains of Met4 and Asp10 in PA tag was important for the NZ-1 interaction (Fig. I-8). The NZ-1-reactive sequence is unique to human podoplanin and both Met4 and Asp10 are absent in mouse, rat, hamster, or dog podoplanin (Fig. I-14), indicating that cell lines from these animals are compatible with this system. In fact, NZ-1 does not exhibit any binding toward CHO cells in flow cytometry (Fig. I-10) or in Western blotting (Kato et al. 2006).

This laboratory has already succeeded in the purification of many membrane proteins using PA tag system, and this system was able to be used in the presence of detergents (data not shown). Moreover, it is suggested that PA tag system with high affinity is suitable for a proteomic interactome analyses, because such study requires extremely high affinity (or more accurately, slow dissociation) between the tagged bait and the capture device to withstand extensive washing to eliminate nonspecific binders. In screening research of the specific interaction molecule against target proteins, the beads immobilized with a bait protein *via* anti-tag antibody have to be washed carefully to decrease the false-positive hits derived from non-specific binding. In this case, although tandem affinity purification (TAP) using FLAG tag is the most popular method

(Ogawa et al. 2002; Rigaut et al. 1999), the overwashing facilitates the dissociation of the bait protein and may decrease the ratio of s/n. NZ-1 and PA tag is expected to maximize its ability in this application, because they have the dissociation rate much slower than FLAG/M2.

Overall, it is anticipated that the PA tag system will be a unique and powerful addition to our list of experimental tools in the field of protein expression and purification.

Figure I-14. Sequence alignment of podoplanin PLAG domain from various species. Amino acid sequences are from human (AAM73655.1), mouse (NP_034459.2), rat (NP_062231.1), hamster (XP_005081155.1), and dog (NP_001003220.1) podoplanins.

Chapter III

Introduction

In Chapter II, I constructed a novel affinity tag system "PA tag system" with high affinity and specificity using anti human podoplanin antibody NZ-1, and it was revealed that this tag system proved to outperform many existing affinity tag systems owing to its high affinity, high selectivity, and extended reusability. If this tag system is used only as general affinity tag system, I might as well finish this research at this point. However, it is very useful for the understanding on the physicochemical foundation of the protein-protein interaction that the reasons of the superior interaction between PA tag and NZ-1 are explained. Additionally, to append the desirable advantages and overcome the disadvantages in this system using protein-engineering technology, I have to know the detailed structure. Then, to understand this structural basis, I determined the crystal structures of NZ-1 with bound PA peptide. As a result, it was indicated that NZ-1 recognizes the hairpin turn of the middle of the PA tag sequence. This unique structure suggests that PA tag may be recognized by NZ-1 even if it is inserted into loop of a protein. Therefore, PA tag system may be able to be used as "the system that the tag is able to be easily and generally inserted into the middle of a protein", as described Chapter I.

In the latter half of this chapter, I examined whether it is possible as that PA tag can be inserted into a protein, using integrin $\alpha_{IIb}\beta_3$ as a model protein. Integrin is a heterodimer type I transmembrane protein composed of α subunit and β subunit, and is a main cell adhesion receptor of multicellular animal. It was also known that integrin is dynamically changed the conformation from inactive state (bent conformation) to active state (extend conformation) (Luo et al. 2007; Springer and Dustin 2012; Takagi et al. 2002b). The structure of the entire ectodomain $\alpha_{IIb}\beta_3$ has been determined by X-ray crystallography (Zhu et al. 2008), and $\alpha_{IIb}\beta_3$ has an antibody for evaluating the active conformation (Taub et al. 1989; Ginsberg et al. 1990). Therefore, I used $\alpha_{IIb}\beta_3$ that has much information and many analysis tools, as a model protein. As a result of the examination of the PA tag insertion into various loops of $\alpha_{IIb}\beta_3$ α subunit, it was suggested that PA tag was able to be inserted into the middle of protein with the high affinity toward NZ-1. Moreover, it was revealed that NZ-1 physically induced the conformational change of the PA tag-inserted $\alpha_{IIb}\beta_3$ from inactive form to active form by extending $\alpha_{IIb}\beta_3$ conformation when the site of the PA tag insertion was selected. In this chapter, I

report the development of a novel technology that was impossible in the existing tag systems, using NZ-1 and PA tag.

Materials and methods

Construction of expression vectors

The ectodomain fragments of integrin α_{IIb} were designed as described for $\alpha_V\beta_3$ previously (Takagi et al. 2002b). The complete ectodomains of α_{IIb} and β_3 chains were fused at the C-terminal to leucine zipper peptide that is derived from GCN4. The peptide forms a disulfide-linked α-helical coiled-coil to mimic the closely positioned and interacting the α and β subunit on the cell surface (Fig. II-1). This coiled-coil is called as velcro tag, and it induces the secretion of the stable integrin heterodimer in the culture supernatant (Oshea et al. 1993). The tag insertion into the ectodomain fragments of α_{IIb} chain was designed as shown in Fig. II-2. These mutants were named as follows by the domain name and the elements of secondary structure in the sites of tag insertion, W2_1, W2_2, W2_3, W2_4, W2_5, W1, Cap, W3, W6, Thigh F-G, Calf-1 X-Z, Calf-1 E-F, Calf-2 X-Y, and Calf-2 F-G. For the construction of these mutants, DNA encoding these mutants were constructed by overlap-extension PCR and cloned into the plasmid vector of wildtype α_{IIb} chain. The primer list for this research was shown in Table II-1. W2_1 is described as an example, first the fragments were extended using the combinations of T7fwd and a2bW2PA_L1 (-), and a2bW2PA_U1 and a2bSP3 (-), respectively. Second, these fragments were extended using the combinations of T7fwd and a2bW2PA_L2 (-), and a2bW2PA_U2 and a2bSP3 (-), respectively. Finally, these fragments were overlapped using T7fwd and a2bSP3 (-), and the DNA fragment was cloned into *Spe*I-*Sbf*I site of the template. The others were constructed as above.

For the construction of full-length α_{IIb} and β_3 subunit, the mutated regions of the soluble integrin were cloned into the vector as constructed previously (Luo et al. 2005). After W1, Cap, W2_5, Thigh F-G, Calf-1 X-Z, Calf-1 E-F, Calf-2 X-Y were digested by restriction enzyme, these fragments were cloned into *Spe*I-*Sbf*I site of the template. Only in Calf-2 F-G, the tag was inserted into the template by overlap-extension PCR. These fragments were extended using the combinations of a2bSP6 and a2bCalf2FGGPAL31_1 (-), and a2bCalf2FGPAU31 and Rev21, respectively. The first fragment was extended using the combinations of a2bSP6 and a2bcapPAL27_2 (-). Finally, these fragments were overlapped using a2bSP6 and Rev21, and the DNA fragment was cloned into *Sbf*I-*Xba*I site of the template.

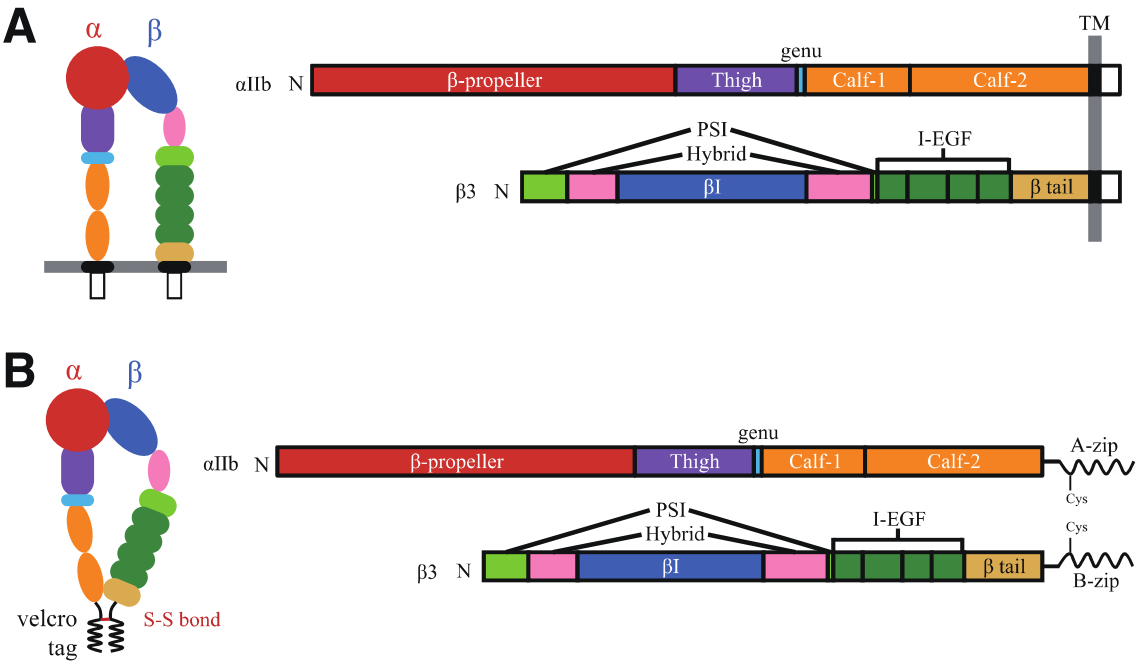

Figure II-1. Schematic representation of the integrin $\alpha_{IIb}\beta_3$ used in Chapter II. Integrins are heterodimers of non-covalently associated α and β subunits. (A) Full length integrin $\alpha_{IIb}\beta_3$. (B) Integrin $\alpha_{IIb}\beta_3$ ectodomain with velcro tag.

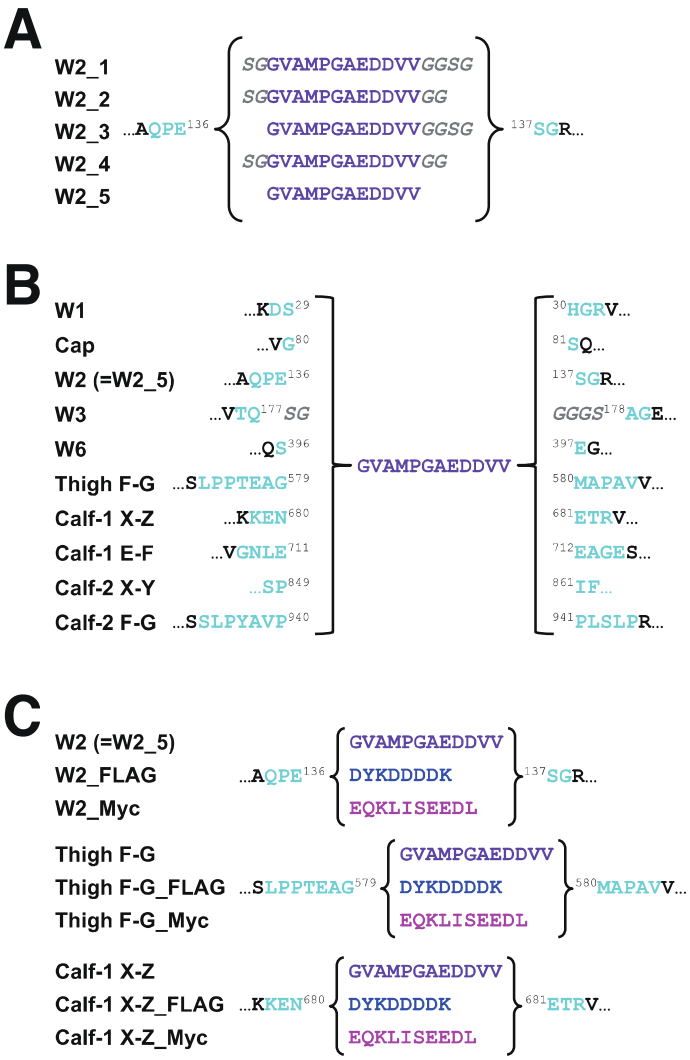

Figure II-2. Amino acids sequences around the regions inserted with each tag used in Chapter II. Amino acid sequences of the artificially added tag and the linker segments are shown. Purple, PA tag sequences; blue, FLAG tag sequences; magenta, Myc tag sequences; cyan, loop sequences; black, secondary structure regions; italic, linker sequences.

Table II-1. Primer list

Construct name	Primer name	Use	Sequence
W2_1 (template: WT)	T7 fwd	fragment1-upper-1, 2	5'-taatacgactcactataggg-3'
	a2bW2PA_L1 (-)	fragment1-lower-1	5'-ggcatggcaacgccgccgctctctggctgagccaaaaagc-3'
	a2bW1PA_L2 (-)	fragment1-lower-2	5'-ccaccacatcatcttcggcacctggcatggcaacgccgcc-3'
	a2bW2PA_U1	fragment2-upper-1	5'-gatgtggtgggtggaagcggaagcggccgc gcgccgag-3'
	a2bW1PA_U2	fragment2-upper-2	5'-gtgccgaagatgatgtggtgggtggaagc-3'
	a2bSP3 (-)	fragment2-lower-1, 2	5'-gatccagaggcctctggtag-3'
W2_2 (template: W2_1)	T7 fwd	fragment1-upper	5'-taatacgactcactataggg-3'
	a2bW2del1L23 (-)	fragment1-lower	5'-ctcggcgcggcggccgcttccacccaccacatcatc-3'
	a2bW2del1L23	fragment2-upper	5'-gatgatgtggtgggtggaagcggccgccgcgccgag-3'
	a2bSP3 (-)	fragment2-lower	5'-gatccagaggcctctggtag-3'
W2_3 (template: W2_2)	T7 fwd	fragment1-upper	5'-taatacgactcactataggg-3'
	a2bW2del2L24_1 (-)	fragment1-lower	5'-catggcaacgccctctggctgagccaaaaagc-3'
	a2bW2del2L24_2	fragment2-upper	5'-ctcagccagagggcgttgccatgccaggtgc-3'
	a2bSP3 (-)	fragment2-lower	5'-gatccagaggcctctggtag-3'
W2_4 (template: W2_2)	T7 fwd	fragment1-upper	5'-taatacgactcactataggg-3'
	a2bW2del3L25_1 (-)	fragment1-lower	5'-ggcggccgctcaccacatcatcttcggcac-3'
	a2bW2del3L25_2	fragment2-upper	5'-gatgatgtggtgagcggccgccgcgccgag-3'
	a2bSP3 (-)	fragment2-lower	5'-gatccagaggcctctggtag-3'
W2_5 (template: W2_3)	T7 fwd	fragment1-upper	5'-taatacgactcactataggg-3'
	a2bW2del3L25_1 (-)	fragment1-lower	5'-ggcggccgctcaccacatcatcttcggcac-3'
	a2bW2del3L25_2	fragment2-upper	5'-gatgatgtggtgagcggccgccgcgccgag-3'
	a2bSP3 (-)	fragment2-lower	5'-gatccagaggcctctggtag-3'
W1	T7 fwd	fragment1-upper-1, 2	5'-taatacgactcactataggg-3'
	a2bW1delL33 (-)	fragment1-lower-1	5'-gcacctggcatggcaacgccgctgtccttgtggaagtcc-3'
	a2bcapPAL27_2 (-)	fragment1-lower-2	5'-caccacatcatcttcggcacctggcatggcaacgcc-3'
	a2bW1delU33	fragment2-upper	5'-gtgccgaagatgatgtggtgcatgggagagtggccatcg-3'
	a2bW2PA-L3PmlI (-)	fragment2-lower	5'-gaggacacgtgccacaaaag-3'
Cap	T7 fwd	fragment1-upper-1, 2	5'-taatacgactcactataggg-3'
	a2bcapPAL27_1 (-)	fragment1-lower-1	5'-gcacctggcatggcaacgccgcctacatttcgggtctc-3'
	a2bcapPAL27_2 (-)	fragment1-lower-2	5'-caccacatcatcttcggcacctggcatggcaacgcc-3'
	a2bcapPAU27	fragment2-upper	5'-gtgccgaagatgatgtggtgtcccaaactttacaaacc-3'
	a2bSP3 (-)	fragment2-lower	5'-gatccagaggcctctggtag-3'
W3	T7 fwd	fragment1-upper-1, 2	5'-taatacgactcactataggg-3'
	a2bW3PA-L1 (-)	fragment1-lower-1	5'-ggcatggcaacgccgccgctctgagtgaccacggagctg-3'
	a2bW1PA-L2 (-)	fragment1-lower-2	5'-ccaccacatcatcttcggcacctggcatggcaacgccgcc-3'
	a2bW3PA-U1	fragment2-upper-1	5'-gatgatgtggtgggtggaagcgccggagagctggtgcttg-3'
	a2bW1PA-U2	fragment2-upper-2	5'-gtgccgaagatgatgtggtgggtggaagc-3'
	a2bSP3 (-)	fragment2-lower-1, 2	5'-gatccagaggcctctggtag-3'

Table II-1. Primer list (continued)

Construct name	Primer name	Use	Sequence
W6	T7 fwd	fragment1-upper-1, 2	5'-taatacgactcactataggg-3'
	a2bW6PAL28_1 (-)	fragment1-lower-1	5'-gcacctggcatggcaacgccactctgacccaggaacacc-3'
	a2bcapPAL27_2 (-)	fragment1-lower-2	5'-caccacatcatcttcggcacctggcatggcaacgcc-3'
	a2bW6PAU28	fragment2-upper	5'-gtgccgaagatgatgtggtggaggggctgaggtcacgtcc-3'
	a2bSP3 (-)	fragment2-lower	5'-gatccagaggcctctggtag-3'
Thigh F-G	a2bSP2	fragment1-upper-1, 2	5'-cttctcccttcgaggtgccg-3'
	a2bFGdelL34 (-)	fragment1-lower-1	5'-gcacctggcatggcaacgcctccagcctccgtgggcgg-3'
	a2bcapPAL27_2 (-)	fragment1-lower-2	5'-caccacatcatcttcggcacctggcatggcaacgcc-3'
	a2bFGdelU34	fragment2-upper	5'-gtgccgaagatgatgtggtgatggcccctgctgtcgtgc-3'
	Rev21	fragment2-lower	5'-aactagaaggcacagtcgagg-3'
Calf-1 X-Z	T7 fwd	fragment1-upper-1, 2	5'-taatacgactcactataggg-3'
	a2bCalf1XZPAL29_1 (-)	fragment1-lower-1	5'-gcacctggcatggcaacgccattctccttcttctgattac-3'
	a2bcapPAL27_2 (-)	fragment1-lower-2	5'-caccacatcatcttcggcacctggcatggcaacgcc-3'
	a2bCalf1XZPAU29	fragment2-upper	5'-gtgccgaagatgatgtggtggagaccagggtggtgctgtg-3'
	a2bSP3 (-)	fragment2-lower	5'-gatccagaggcctctggtag-3'
Calf-1 E-F	T7 fwd	fragment1-upper-1, 2	5'-taatacgactcactataggg-3'
	a2bCalf1EFPAL30_1 (-)	fragment1-lower-1	5'-gcacctggcatggcaacgccttccagattccccacgctc-3'
	a2bcapPAL27_2 (-)	fragment1-lower-2	5'-caccacatcatcttcggcacctggcatggcaacgcc-3'
	a2bCalf1EFPAU30	fragment2-upper	5'-gtgccgaagatgatgtggtggaggctggggagtctgtgtc-3'
	a2bSP3 (-)	fragment2-lower	5'-gatccagaggcctctggtag-3'
Calf-2 X-Y	a2bSP2	fragment1-upper-1, 2	5'-cttctcccttcgaggtgccg-3'
	a2bXYPAL75 (-)	fragment1-lower-1	5'-gcacctggcatggcaacgccgggggaggggctggggatgg-3'
	a2bcapPAL27_2 (-)	fragment1-lower-2	5'-caccacatcatcttcggcacctggcatggcaacgcc-3'
	a2bXYPAU75	fragment2-upper	5'-gtgccgaagatgatgtggtgatcttcctgccagagcccg-3'
	Rev21	fragment2-lower	5'-aactagaaggcacagtcgagg-3'
Calf-2 F-G	abaSP7	fragment1-upper-1, 2	5'-cgtcctagaaaagactgagg-3'
	a2bCalf2FGPAL31_1 (-)	fragment1-lower-1	5'-gcacctggcatggcaacgccgggcaccgcataggggaggg-3'
	a2bcapPAL27_2 (-)	fragment1-lower-2	5'-caccacatcatcttcggcacctggcatggcaacgcc-3'
	a2bCalf2FGPAU31	fragment2-upper	5'-gtgccgaagatgatgtggtgccgctcagcctgccccgagg-3'
	Rev21	fragment2-lower	5'-aactagaaggcacagtcgagg-3'
W2_FLAG	T7 fwd	fragment1-upper	5'-taatacgactcactataggg-3'
	a2bW2FLAGL35 (-)	fragment1-lower	5'-cttgtcgtcatcgtctttgtagtcctctggctgagccaaaaagc-3'
	a2bW2FLAGU35	fragment2-upper	5'-acaaagacgatgacgacaagagcggccgccgcgccgag-3'
	a2bW2PA-L3PmlI (-)	fragment2-lower	5'-gaggacacgtgccacaaaag-3'
W2_Myc	T7 fwd	fragment1-upper-1, 2	5'-taatacgactcactataggg-3'
	a2bW2MycL36_1 (-)	fragment1-lower-1	5'-cagagatcagtttctgttcctctggctgagccaaaaagc-3'
	a2bW2MycL36_2 (-)	fragment1-lower-2	5'-caggtcttcttcagagatcagtttctgttc-3'
	a2bW2MycU36	fragment2-upper	5'-tgatctctgaagaagacctgagcggccgccgcgccgag-3'
	a2bW2PA-L3PmlI (-)	fragment2-lower	5'-gaggacacgtgccacaaaag-3'

Table II-1. Primer list (continued)

Construct name	Primer name	Use	Sequence
Thigh F-G_FLAG	a2bSP2	fragment1-upper	5'-cttctcccttcgaggtgccg-3'
	a2bFGFLAGL37 (-)	fragment1-lower	5'-cttgtcgtcatcgtctttgtagtctccagcctccgtgggcgg-3'
	a2bFGFLAGU37	fragment2-upper	5'-acaaagacgatgacgacaagatggcccctgctgtcgtgc-3'
	Rev21	fragment1-upper-1, 2	5'-aactagaaggcacagtcgagg-3'
Thigh F-G_Myc	a2bSP2	fragment1-lower-1	5'-cttctcccttcgaggtgccg-3'
	a2bFGMycL38 (-)	fragment1-lower-2	5'-cagagatcagtttctgttctccagcctccgtgggcgg-3'
	a2bW2MycL36_2 (-)	fragment2-upper	5'-caggtcttcttcagagatcagtttctgttc-3'
	a2bFGMycU38	fragment2-lower	5'-tgatctctgaagaagacctgatggcccctgctgtcgtgc-3'
	Rev21	fragment1-upper-1, 2	5'-aactagaaggcacagtcgagg-3'
Calf-1 X-Z_FLAG	a2bSP2	fragment1-upper	5'-cttctcccttcgaggtgccg-3'
	a2bXZFLAGL39 (-)	fragment1-lower	5'-cttgtcgtcatcgtctttgtagtcattctccttcttctgattac-3'
	a2bXZFLAGU39	fragment2-upper	5'-acaaagacgatgacgacaaggagaccagggtggtgctgtg-3'
	Rev21	fragment2-lower	5'-aactagaaggcacagtcgagg-3'
Calf-1 X-Z_Myc	a2bSP2	fragment1-upper-1, 2	5'-cttctcccttcgaggtgccg-3'
	a2bXZMycL40 (-)	fragment1-lower-1	5'-cagagatcagtttctgttcattctccttcttctgattac-3'
	a2bW2MycL36_2 (-)	fragment1-lower-2	5'-caggtcttcttcagagatcagtttctgttc-3'
	a2bXZMycU40	fragment2-upper	5'-tgatctctgaagaagacctggagaccagggtggtgctgtg-3'
	Rev21	fragment2-lower	5'-aactagaaggcacagtcgagg-3'
Calf-2 F-G (full length)	a2bSP6	fragment1-upper-1, 2	5'-gtgtgacctgcaggagatgg-3'
	a2bCalf2FGPAL31_1 (-)	fragment1-lower-1	5'-gcacctggcatggcaacgccgggcaccgcataggggaggg-3'
	a2bcapPAL27_2 (-)	fragment1-lower-2	5'-caccacatcatcttcggcacctggcatggcaacgcc-3'
	a2bCalf2FGPAU31	fragment2-upper	5'-gtgccgaagatgatgtggtgccgctcagcctgccccgagg-3'
	Rev21	fragment2-lower	5'-aactagaaggcacagtcgagg-3'

Antibodies used

The rat anti-PA monoclonal antibody NZ-1 (IgG_{2a}, λ) and the FITC-conjugated NZ-1 was provided by Prof. Y. Kato as described in Chapter II. The mouse anti-velcro monoclonal antibody 2H11 was purified from the hybridoma (a gift from E. Reinhart) (Chang et al. 1994). The rabbit anti-velcro polyclonal antibody was conjugated the biotin using EZ-link Sulfo-NHS-LC-Biotin (Thermo Scientific). The mouse anti-β_3 monoclonal antibody AP3 was purified from the hybridoma obtained from ATCC (Newman et al. 1985; Kouns et al. 1990). The AP3 was conjugated the fluorescent dye using DyLight 680 NHS Ester (Thermo Scientific) (DyLight680-AP3). The mouse anti-β_3 monoclonal antibody 7E3 and the mouse anti-α_{IIb} monoclonal antibody 10E5 were purified from the hybridoma (a gift from B. S. Coller) (Coller

1985; Artoni et al. 2004; Coller et al. 1983). The FITC-conjugated mouse anti-$\alpha_{IIb}\beta_3$ monoclonal antibody PAC-1 (FITC-PAC-1) was obtained from Becton, Dickinson and Company (Taub et al. 1989). The Alexa488-conjugated goat anti-mouse IgG polyclonal antibody (rat absorbed) was obtained from Invitrogen. The PE-conjugated goat anti-rat IgG polyclonal antibody (mouse absorbed) was obtained from Southern Biotechnology. The anti-FLAG M2 and the anti-Myc 9E10 were used as described in Chapter II.

Preparation of NZ-1 Fab

Purified NZ-1 was dialyzed against PE buffer (pH 7.0) [20 mM Na/K phosphate, 10 mM EDTA]. The NZ-1 was digested by Immobilized Papain (Thermo Scientific) (2.2 mg IgG/0.2 ml resin) in the presence of 25 mM Cys-HCl (pH 7.0), and incubated for ~4 h at 37 °C under gentle agitation. Immobilized Papain was removed from the solution through the mini column, and the resin was washed twice (1 column × 2) with PE buffer for collection of the antibody solution. The collected antibody solution was dialyzed against TBS (pH 8.0) [50 mM Tris-HCl, 150 mM NaCl], and the solution was slowly added to PA14 peptide-Sepharose (the resin immobilized with PA14 peptide ~5 mg/ml). The PA14 peptide-Separose was washed nine times (1 column × 9) with TBS (pH 8.0), and eluted eight times (1 column × 8) with 10 mM MES (pH 6.0), 3 M $MgCl_2$. After each fraction was monitored which fractions have NZ-1 Fab by measurement of absorbance at 280 nm, all fractions with NZ-1 Fab were collected and dialyzed against TBS (pH 7.5) [20 mM Tris-HCl, 150 mM NaCl]. The Fab solution was concentrated by ultrafiltration using Spin-X UF (MWCO [molecular weight cut-off] :10,000) (Corning), and purified by gel filtration chromatography using AKTAprime (GE Healthcare) on a Superdex 200 16/60 column equilibrated with TBS (pH 7.5), at a flow rate of 0.7 ml/min. Elution fractions were subjected to 12.5% SDS-PAGE and stained with CBB, No. 18-28 fractions with Fab were collected (Fig. II-3). The collected fractions were dialyzed against TBS (pH 7.5) [10 mM Tris-HCl, 50 mM NaCl]. Finally, the Fab solution was concentrated to ~10 mg/ml by ultrafiltration using Spin-X UF (MWCO :10,000).

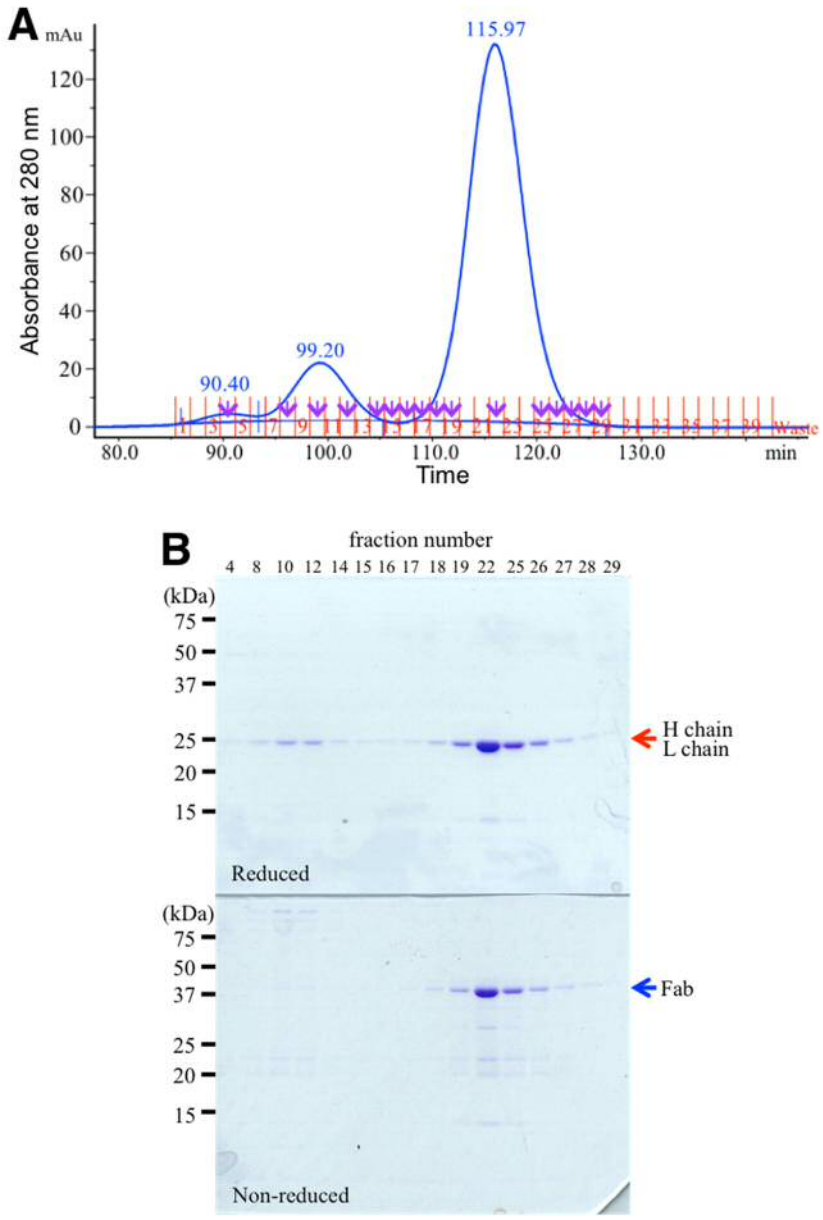

Figure II-3. Purification of NZ-1 Fab using gel filtration chromatography. (A) Gel filtration chart. NZ-1 Fab was purified on a Superdex 200 column equilibrated with TBS, at a flow rate of 0.7 ml/min. (B) Elution fractions of purple arrows in (A) were subjected to 12.5% SDS-PAGE under reducing and non-reducing condition and stained with CBB. Red arrow, NZ-1 heavy and light chains (indistinguishable because they co-migrate); blue arrow, NZ-1 Fab fragment.

Structural analysis of NZ-1 with and without bound PA peptide

To make a co-crystal of NZ-1 Fab and the antigen, PA14 peptide was dissolved in TBS (pH 7.5) [10 mM Tris-HCl, 50 mM NaCl], and added at approximately 3-fold molar excess to the concentrated NZ-1 Fab. Initial screening of crystallization conditions of the NZ-1 Fab/PA14 peptide (complex) and the ligand free NZ-1 Fab (apo) was carried out using Crystal Screen 1 and Crystal Screen 2 (Hampton Research) by the hanging drop vapor-diffusion. As a result, both of the proteins crystallized in many conditions. Initial crystallization condition was further optimized by the change of the precipitant (concentrations and kinds), the buffer (pH and kinds), and the salt (concentrations and kinds). As a result, the apo crystal was grown under the condition of 0.1 M sodium citrate buffer pH 5.6 and 12 or 15% (w/v) PEG4000, and the co-crystal was grown under the condition of 0.1 M sodium citrate buffer pH 5.6 and 24% (w/v) PEG4000. These crystals were moved into the cryoprotectant solution [apo; 0.1 M sodium citrate buffer pH 5.6, 12 or 15% (w/v) PEG4000, 10% (v/v) glycerol, complex; 0.1 M sodium citrate buffer pH 5.6, 24% (w/v) PEG4000, 10% (v/v) ethylene glycol] by the nylon loops (Hampton Research). Then, these crystals were frozen in liquid nitrogen. One of X-ray diffraction data sets of the apo crystal was collected at the beam line BL17A of Photon Factory, and another data set of the apo crystal was collected at the Taiwan beam line BL15A1 of NSRRC. The apo crystal data were processed using HKL2000 program package (Otwinowski and Minor 1997). As a result, the data set collected at NSRRC had high resolution, however, it did not have sufficient number of reflections at low-angle. Since these data sets collected at Photon Factory and NSRRC have the same crystal system (Table II-2), these data was processed using HKL2000 program package together. Initial phase was determined by molecular replacement method using Phaser-MR (McCoy et al. 2007). A rat anti-NGF AD11 antibody Fab (IgG_{2a}) structure (PDB ID; 1ZAN) was used as a search model for the ligand free NZ-1 Fab structure. The co-crystal X-ray diffraction data set was collected at the beam line BL1A of Photon Factory. The co-crystal data were processed using XDS program package (Kabsch 2010). Initial phase was determined by molecular replacement method using Phaser-MR. The apo structure was used as a search model for the NZ-1 Fab/PA14 peptide complex structure. The structure models were built using COOT (Emsley et al. 2010) with model refinement cycle with REFMAC5 (Murshudov et al. 1997). Finally, many rounds of model-correction and refinement

resulted in a *R*-factor of 17.3% and a free *R*-factor of 20.9% in the apo form, and a *R*-factor of 18.3% and a free *R*-factor of 22.1% in the complex form. The structure models were validated using the program MOLPROBITY (Chen et al. 2010). Data collection and refinement statistics were listed in Table II-2. The interaction between PA14 peptide and NZ-1 Fab was calculated using the program LIGPLOT (Wallace et al. 1995). All structure figures were prepared with the program PyMol (Schrödinger, LLC).

Table II-2. Data collection and refinement statistics

Values in parentheses correspond to the highest resolution shell.

	complex	apo (A)	apo (B)
Data collection			
Wavelength [Å]	0.9800	0.9800	1.0000
Space group	$P2_1$	$P1$	$P1$
Unit Cell Parameters	a=42.1 Å, b=79.8 Å, c=132.3 Å β=96.6°	a=42.9 Å, b=57.2 Å, c=101.5 Å α=97.9°, β=101.5°, γ=105.4°	a=42.7 Å, b=57.1 Å, c=101.0 Å α=97.8°, β=101.5 °, γ=105.7°
Resolution [Å]	1.70 (1.75-1.70)	1.65 (1.70-1.65)	
Completeness [%]	98.4 (96.0)	98.5 (95.8)	
R_{sym} [%][a]	5.3 (53.8)	12.9 (50.7)	
$I/\sigma(I)$	22.7 (3.7)	50.8 (3.7)	
Refinement			
Resolution range [Å]	39.92-1.70	97.42-1.65	
No. of atoms			
Proteins	6377	6454	
Ligands	171	0	
Water molecules	611	676	
R_{work}/R_{free} (%)[b]	18.3/22.1	17.3/20.9	
RMSD bond length [Å]	0.011	0.010	
RMSD bond angle [°]	1.46	1.44	

[a] $R_{sym} = 100 \times \Sigma|I_{hkl} - \langle I_{hkl}\rangle|\Sigma I_{hkl}$, $\langle I_{hkl}\rangle$ is the mean value of I_{hkl}.
[b] $R_{work} = 100 \times \Sigma||F_o| - |F_c||/\Sigma|F_o|$. R_{free} was calculated from the test set (5% of the total data).

Immunoprecipitation assay of the soluble $\alpha_{IIb}\beta_3$

HEK293T were transiently transfected with the soluble tag-inserted $\alpha_{IIb}\beta_3$. The medium of HEK293T cells incubated on the 6-well plate were changed to DMEM/5% FCS, and the cells were transfected with the soluble α_{IIb} subunit plasmid DNA (2 μg) and the soluble β_3 subunit plasmid DNA (2 μg) using X-tremeGENE HP DNA Transfection Reagent. The culture supernatant was harvested ~72 h after the transfection, and was centrifuged. Each supernatant was mixed with 20 μl of 2H11-Sepharose (the resin immobilized with 2H11 ~2 mg IgG/ml) or NZ-1-Sepharose and incubated for ~2 h at 4 °C under gentle agitation. After the resin bound the soluble $\alpha_{IIb}\beta_3$ was washed with TBS (pH 7.5) [20 mM Tris-HCl, 150 mM NaCl, 1 mM $CaCl_2$, 1 mM $MgCl_2$] (800 μl × 3), all proteins captured by the Sepharose were eluted by × 2 SDS Sample buffer (25 μl). These eluted proteins were subjected to 7.5% SDS-PAGE under reducing and non-reducing condition and stained with fluorescent dye (Oriole).

The expression level was estimated by Western blotting using the immunoprecipitated proteins. The soluble tag-inserted $\alpha_{IIb}\beta_3$ was expressed as described above. One milliliter of the culture supernatant was mixed with 20 μl of Protein G Sepharose (GE Healthcare) and 2 μg of various antibodies (anti-integrin β_3 7E3, anti-PA NZ-1, anti-FLAG M2, anti-Myc 9E10), and incubated for ~2 h at 4 °C under gentle agitation, to capture $\alpha_{IIb}\beta_3$ *via* an antibody. Next, Protein G Sepharose was washed with TBS (pH 7.5) (800 μl × 3), and all proteins captured by the Sepharose were eluted by × 2 SDS Sample buffer (25 μl). These eluted proteins were separated on 7.5% SDS-PAGE and transferred to a PVDF membrane, followed by blocking with 5% skim milk in TBS (pH 8.0) with 0.05% Tween 20 for 60 min. For the primary antibody step, the membranes were incubated with 5 μg/ml biotinylated anti-velcro polyclonal antibody diluted in TBS at pH 8.0, containing 0.05% Tween 20 and 1% BSA (TBST), for 60 min. For the secondary antibody step, membranes were incubated for 60 min with SA-HRP (VECTOR) diluted at 1:2,000 in TBST. Four consecutive washes (TBST, 5 min) were conducted between each step. The membranes were developed with ECL™ Prime reagent and analyzed using ImageQuant LAS 4000mini.

Assessment of full-length integrin $\alpha_{IIb}\beta_3$

Human podoplanin knockout HEK293T cells (PDIS-2) (a gift from Y. Kato) were transiently transfected with full-length integrin $\alpha_{IIb}\beta_3$. The medium of PDIS-2 cells

incubated on the 6-well plate were changed to DMEM/5% FCS, and the cells were transfected with full-length α_{IIb} plasmid DNA (2 μg) and full-length β_3 plasmid DNA (2 μg) using X-tremeGENE HP DNA Transfection Reagent. After incubation for ~48 h at 37 °C in 5% CO_2, the cells were detached, washed twice with DMEM/10% FCS, and resuspended in 1 ml of Tyrode's buffer (pH 7.4) [137 mM NaCl, 12 mM $NaHCO_3$, 2.6 mM KCl, 5 mM HEPES, 2 mM $CaCl_2$, 2 mM $MgCl_2$, 1 mg/ml BSA, 1 mg/ml dextrose]. In the examination of expression level and recognition toward NZ-1, the cells were incubated with Tyrode's buffer containing 10E5 (1 μg/ml) and NZ-1 (0.5 μg/ml) for 30 min at 20 °C, washed twice with Tyrode's buffer, and resuspended in Tyrode's buffer containing Alexa488-conjugated goat anti-mouse IgG polyclonal antibody (rat absorbed) diluted at 1:400 and PE-conjugated goat anti-rat IgG polyclonal antibody (mouse absorbed) diluted at 1:1,000. After incubation for 30 min at 20 °C, the cells were washed once and resuspended in Tyrode's buffer. In the assay for ligand binding of integrin $\alpha_{IIb}\beta_3$, the cells were incubated for 10 min at 37 °C with or without 15 mM dithiothreitol (DTT). Integrin $\alpha_{IIb}\beta_3$ has been reported that the conformation was changed from inactive state to active state by DTT (Takagi et al. 2002b; Yan and Smith 2001). After washing twice with Tyrode's buffer, the cells were incubated with Tyrode's buffer containing FITC-PAC-1 diluted at 1:20 and DyLight680-AP3 diluted at 1:50 for 30 min at 20 °C, washed once with Tyrode's buffer, and resuspended in Tyrode's buffer. Finally, these cells were analyzed for the measurement of their fluorescent intensity by flow cytometer EC800 system (SONY) (Alexa488 and FITC were measured using 488 nm laser and 525 nm filter, PE was measured using 488 nm laser and 595 nm filter, and DyLight680 was measured using 642 nm laser and 720 nm filter). The evaluation of the recognition toward NZ-1 was analyzed on the 10E5 positive cell population, and the assay for ligand binding was analyzed on the AP3 positive cell population. The 10E5 (anti-α_{IIb} antibody) and 7E3 (anti-β_3 antibody) can be used as the marker of the $\alpha_{IIb}\beta_3$ positive cells, because HEK cell line does not express the endogenous α_{IIb} and β_3, and α chain and β chain of integrin can not be expressed on the cell surface by themselves. All figures and the calculations of Mean. Fluorescent Intensity (MFI) were prepared with the program FlowJo (Digital Biology).

Activation of full-length $\alpha_{IIb}\beta_3$ by NZ-1

The recognition of NZ-1 depending on the site of the PA tag insertion was

examined as described below. The PDIS-2 cells were transiently transfected with full-length integrin $\alpha_{IIb}\beta_3$ inserted PA tag as described above, and the cells were incubated for 30 min at 20 °C in three different conditions (1. DyLight680-AP3 (1/50); 2. DyLight680-AP3 (1/50), FITC-NZ-1 (0.5 μg/ml); 3. DyLight680-AP3 (1/50), FITC-NZ-1 (0.5 μg/ml), 0.5 mM $MnCl_2$, 1 mM RGD peptide (GRGDSPK, Sigma-Aldrich)). The cells were washed twice with Tyrode's buffer, and analyzed by EC800 system. The activation of PA tag-inserted $\alpha_{IIb}\beta_3$ using NZ-1 was estimated as described below. The cells were incubated with Tyrode's buffer containing DyLight680-AP3 diluted at 1:50 and FITC-PAC-1 diluted at 1:20 for 30 min at 20 °C, and with or without 10 μg/ml NZ-1. Finally, these cells were washed twice with Tyrode's buffer, and were analyzed the recognition of PAC-1 by EC800 system.

Results

Structural analysis of NZ-1

In chapter II, it was suggested that the sequence of Met4-Asp10 in PA tag was the central core segment for the recognition toward NZ-1. However, this result was based on alanine scanning, and the detailed information of the binding mechanism between this polypeptide and NZ-1 was not known. To reveal this binding mechanism with the high specificity and affinity, and improve PA tag system, this binding mechanism has to be understood at the atomic resolution level. Therefore, I attempted to determine the crystal structure of NZ-1 with or without bound antigen peptide. As a result of the crystallization of NZ-1 Fab fragment with or without PA14 peptide (EGGVAMPGAEDDVV), each single-crystal was grown under the slightly different conditions. The suitable X-ray diffraction data sets were collected in the Synchrotron Radiation Facility using these crystals, and the complex structure gave 1.70 Å resolution diffraction and the apo structure gave 1.65 Å resolution diffraction (Table II-2).

Next, I describe about these obtained structures. Both of the crystals (complex and apo) contain two copies of molecules in the asymmetric unit (Fig. II-4), and I obtained the two types of structure in each crystal. However, there are differences between these structure, the main difference is the angles between the V_H-V_L region (i.e., F_V region) and C_H1-C_L region (called elbow angle) (Fig. II-5). When the F_V regions (Heavy chain; E20-A137, Light chain; Q20-Q130) that are important for antigen binding were compared, the two molecules of the complex structure are indistinguishable with 0.237 Å RMSD (root mean square deviation), and that of the apo structure are indistinguishable with 0.123 Å RMSD. Therefore, there is no major structural difference between the two molecules. When the complex structure were compared with the apo structure, the conformation of NZ-1 Fv region was similar between the apo and the complex versions, with RMSD of 0.466 Å. Furthermore, these structures are essentially identical at the level of the side chains, even in the CDR (complementarily determining region) (Fig. II-6). I will discuss the minor difference of these structures with or without bound antigen in Discussion. Hereafter, I only discuss about complex structure in this section.

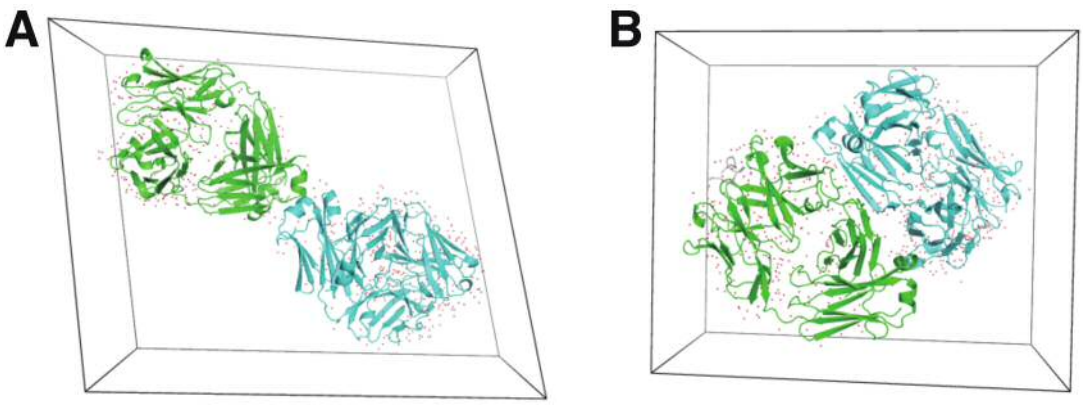

Figure II-4. Crystallographic asymmetric unit for the NZ-1 Fab with or without bound PA14 peptide. Two NZ-1 Fab molecules representing the asymmetric unit are shown in a cartoon model. Crystals of the ligand free NZ-1 Fab (A) and the NZ-1 Fab/PA14 peptide complex (B) had a space group of $P1$ and $P2_1$, respectively. Two molecules are colored differently (green for molecule-1 and cyan for molecule-2). Unit cells are also shown.

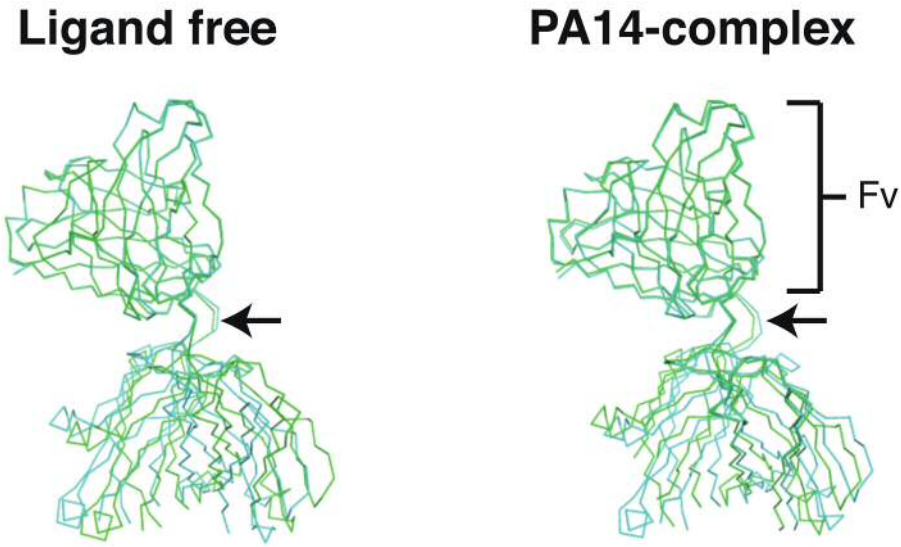

Figure II-5. Structure of the NZ-1 Fab. Ligand free (left) and PA14-bound (right) states of NZ-1 Fab are shown as C_α ribbons, with molecules-1 and 2 colored in green and cyan, respectively. In both cases, two molecules are superposed at the Fv region corresponding to the heavy chain E20-A137 and light chain Q20-Q130, and viewed from the "side" to highlight the bending at the elbow (black arrow).

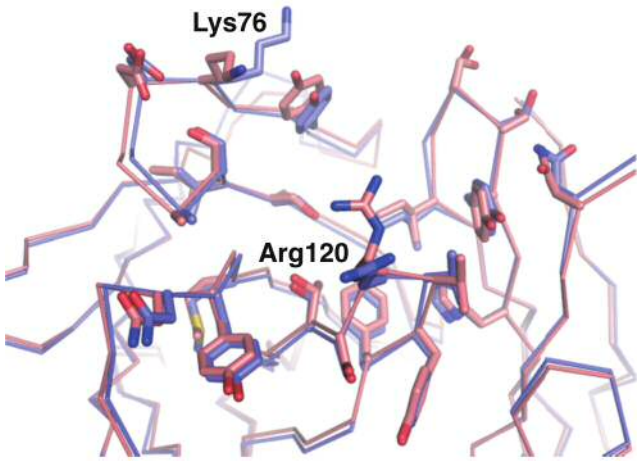

Figure II-6. Structural similarities between NZ-1 Fab with and without bound PA14 peptide. Ligand free NZ-1 Fab molecule-1 (blue) and the NZ-1 Fab/PA14 peptide complex molecule-1 (red) are superposed at the Fv region. Residues that are either near the PA14 peptide (≤4 Å) or involved in water-mediated hydrogen bond interactions to the peptide are shown in stick models. Bound peptide is removed for clarity.

The peptide used for crystallization is PA14 peptide, and this peptide is 2-residue longer in N-terminal than PA12 (GVAMPGAEDDVV) used as PA tag. In the complex structure, all region of PA12 (molecule-2) or 11-residue excepted Gly at the N-terminal (molecule-1) is clearly shown in the electron density of an antigen peptide (Fig. II-7), and the structure from Val2 to Val11 has no major structural difference between the two molecules in asymmetric unit. As shown in Fig. II-8A, the PA peptide is docked in the cleft formed between V_H and V_L of NZ-1, and the buried ASA (solvent accessible surface area) between the PA peptide and NZ-1 is calculated to be ~1,200 $Å^2$. Within the binding pocket of NZ-1, the PA peptide assums a tight 2-residue type II β-turn conformation, with Pro7 and Gly8 being the tip of the hairpin, and NZ-1 recognizes the entire peptide with horseshoe shape centering on the hairpin (Fig. II-8A, B). This binding mode is different from the general binding mode that the extended peptide is recognized by anti-peptide antibody. There are a number of contacts between the peptide and the Fab, particularly at the region encompassing Met4-Asp10 (Fig. II-8C). The side chain of Met6 is deeply inserted into the cleft and makes many van der Waals interactions. The side chain of Asp12 is also inserted into the cleft and makes

multiple hydrogen bonds, with Gly52, Thr118, Ser119, and Arg120 within the Fab heavy chain *via* direct hydrogen bonds. In Chapter II, many amino acid residues (Met4-Asp10) were confirmed to be essential for the binding through a series of SPR binding assays in which ten non-alanine residues in PA peptide were mutated to alanine (Fig. I-8). Moreover, M4A and D10A mutations in the tag sequence nearly eliminated the binding toward NZ-1, indicating that these are the most important residues. Additionally, the main chain of Val2, Ala3, and Val11 interact with the Fab *via* direct hydrogen bond. It is suggested from these observations that at least 10-residue portion of the PA peptide (Val2-Val11) is required for the high affinity.

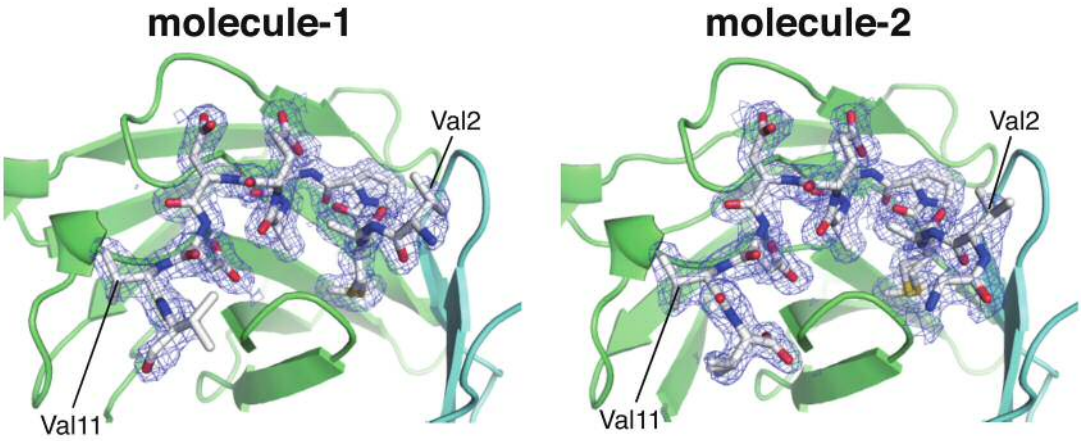

Figure II-7. Electron density map of PA14 peptide. The weighted $2F_o$-F_c electron density map (blue wireframe) is contoured at 1.0 σ. The NZ-1 Fab heavy chain, light chain and PA14 peptide are shown in green, cyan and white, respectively.

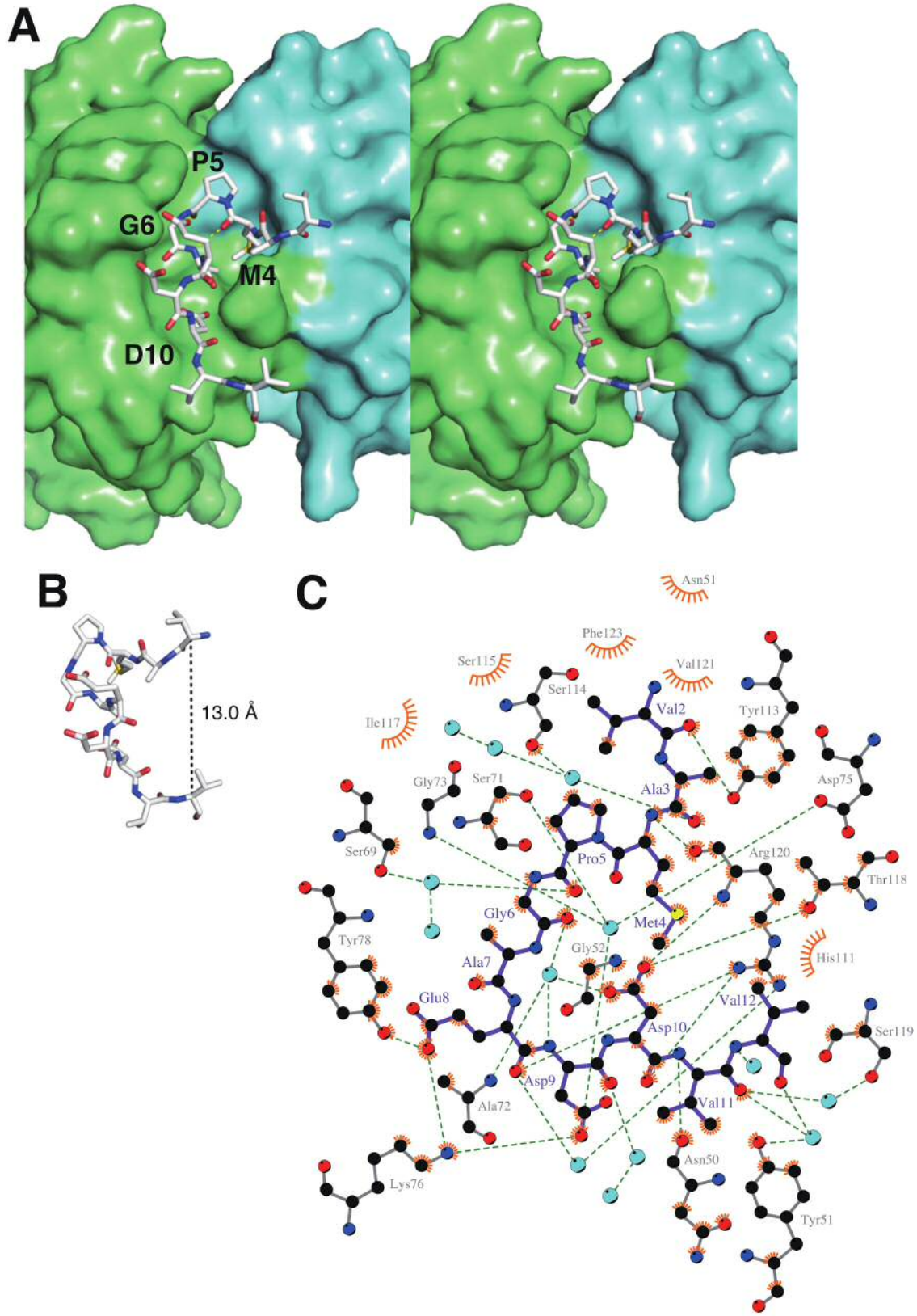
A
P5
G6
M4
D10
B
13.0 Å
C
Asn51
Phe123
Ser115
Val121
Ser114
Val2
Tyr113
Ile117
Gly73
Ser71
Ala3
Asp75
Ser69
Pro5
Arg120
Thr118
Gly6
Met4
Tyr78
Gly52
His111
Ala7
Glu8
Val12
Asp10
Ser119
Asp9
Ala72
Val11
Asn50
Lys76
Tyr51

As described in Chapter II, PA tag sequence is derived from human podoplanin PLAG domain. Human podoplanin is one of platelet aggregation factors on malignant cancer cells, and is implicated in tumor-induced platelet aggregation by binding to CLEC-2 on platelet surface. NZ-1 inhibits the binding of podoplanin to CLEC-2, and the platelet aggregation (Kato et al. 2008; Kato et al. 2006). Recently, M. Nagae *et al.,* reported the complex structure of CLEC-2 and glycopeptide derived from human podoplanin (Nagae et al. 2014). In the report, the part of PA tag sequence is included in the peptide sequence recognized by CLEC-2, and amino acids equivalent to Glu8 and Asp9 are important for the binding (Fig. II-9A). Human podoplanin with bound NZ-1 does not bind to CLEC-2, because Glu8 and Asp9 are inside the binding pocket of NZ-1 when human podoplanin binds to NZ-1 (Fig. II-9B). Therefore, the reason why NZ-1 can inhibit the platelet aggregation was revealed.

Figure II-8. Recognition mode of PA peptide by NZ-1 Fab. (A) Stereo view of the PA14 peptide docked onto the binding site of the NZ-1 Fab. NZ-1 Fab structure is shown in a surface model, and PA14 peptide structure is shown in a stick model. The NZ-1 Fab heavy chain, light chain and PA14 peptide are shown in green, cyan and white, respectively. Main chain hydrogen bond maintaining the type II β-turn is shown in yellow dotted line. (B) Structure of PA14 in (A). The length between Val2 C_α and Val12 C_α is measured using PyMol. (C) Residue-wise contacts between NZ-1 Fab (gray bonds) and PA14 peptide (purple bonds) analyzed by LIGPLOT program. Bond length cutoff is set to 3.35 Å for hydrogen bonds (denoted by green dotted line) and inter-atomic distance range of 2.9-3.9 Å is used for van der Waals contacts (orange eyelash). Oxygen, nitrogen, carbon, and water molecules were shown in red, blue, black, and cyan spheres.

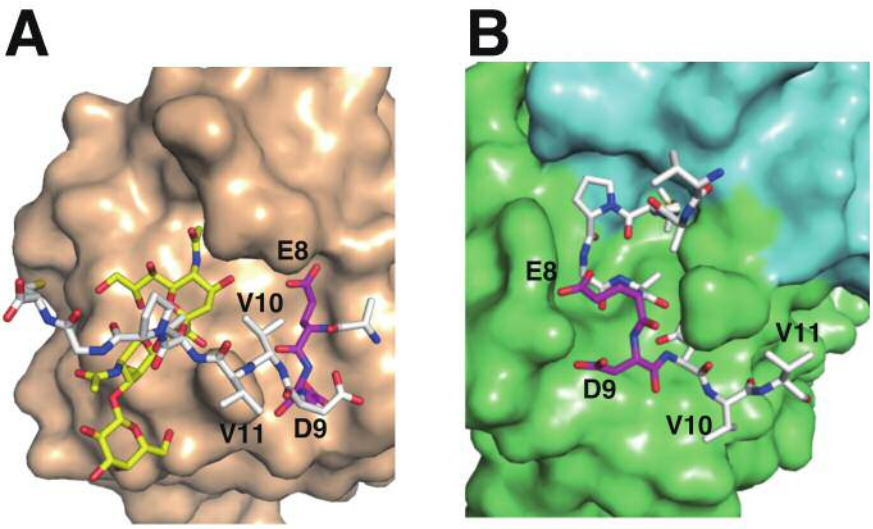

Figure II-9. Crystal structure of CLEC-2/glycopeptide complex and NZ-1 Fab/PA14 peptide complex. (A) Structure of CLEC-2/glycopeptide complex (PDB ID: 3WSR), with the CLEC-2 and glycopeptide is shown in surface and stick models, respectively. The carbohydrate moieties within the podoplanin glycopeptide are colored in yellow. Glu8 and Asp9 are highlighted in magenta. (B) Crystal structure of NZ-1 Fab/PA14 peptide complex as in Fig. II-8A but viewed from an orientation to highlight the position of the Glu8-Asp9 segment (magenta).

Binding assay of NZ-1 and PA tag inserted into loop region

As a result of structural analysis of the NZ-1/PA peptide complex, NZ-1 recognizes the central part of PA tag with β-turn, and both of N- and C-terminal in PA tag have projected outward from antibody (Fig. II-8A, B). This corresponds to the reslt that the amino acids of PA tag at the N- and C-terminal are not important for the binding, and it was suggested that PA tag can be recognized by NZ-1 even if it was inserted into the site of the restricted structure as a hairpin turn of a protein. To prove this hypothesis, I used α_{IIb} subunit of integrin $\alpha_{IIb}\beta_3$ that consists of four β-rich domains and has many β-turns, as a model protein (Fig. II-10A). Integrin is a heterodimer transmembrane protein with α subunit and β subunit. To enable the exhaustive analysis for expression level of mutants, I used the soluble $\alpha_{IIb}\beta_3$ that was removed a transmembrane domain of both subunits, and was attached with a disulfide-linked α-helical coiled-coil (velcro tag) at the C-terminal. The mutated α_{IIb} subunit and β_3 subunit were secreted in the culture

supernatant as a stable heterodimer, when the α_{IIb} and β_3 chains were co-expressed. The expression level of the mutants was evaluated by anti-velcro antibody or anti-β_3 antibody (Fig. II-1).

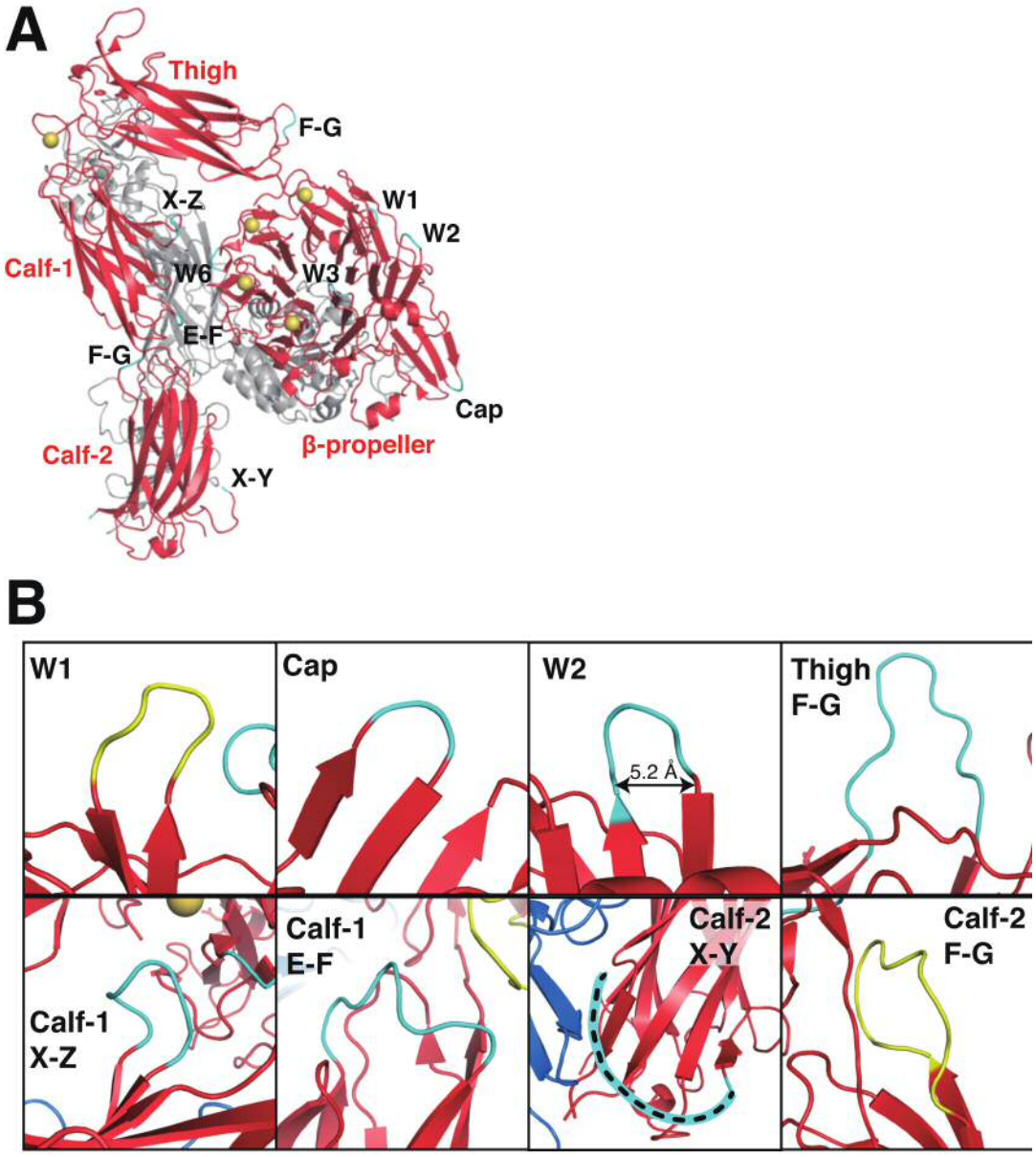

Figure II-10. Surface exposed loops in integrin $\alpha_{IIb}\beta_3$ ectodomain selected for the tag insertion. (A) Crystal structure of $\alpha_{IIb}\beta_3$ ectodomain (PDB ID: 3FCS) is shown in a cartoon model, with each β-rich α_{IIb} structural domains (β-propeller, Thigh, Calf-1, and Calf-2) labeled in red. The ten loop regions used for the tag insertion are shown in cyan and labeled with black letters. (B) Close-up view of the loop regions that were compatible with PA-tag insertion. Loops with good expression upon the tag insertion are colored in cyan, while that with low expression level are in yellow.

PA tag was inserted into the site of 3-4 loop region in W2 that belongs to seven blades of β-propeller domain in α subunit (blade; it is described as W1-W7 because it consists of 4-stranded β-sheet). This region forms the turn of 5-residue (QPESG) including proline (Fig. II-10B). The end-to-end length of PA peptide in the complex structure (Cα length between Val2 and Val12) is 13.0 Å (Fig. II-8B), and the length at the base of the hairpin loop in W2 is 5.2 Å (Fig. II-10B). If PA tag was inserted into the site without linker sequence, the structure of PA tag might be destroyed. Therefore, to be made to have flexibility at the terminals of PA tag, I prepared several constructs with linker sequence of 2-4 residue (Fig. II-2A). Integrin is known as the extremely complex multidomain protein, and the expression of the heterodimer is inhibited by small structural imperfections (Takagi et al. 2002a). The structural imperfections of mutants were able to be estimated by the examination of expression and secretion in heterodimer. The resultant $\alpha_{IIb}\beta_3$ ectodomain mutants were subjected to the immunoprecipitation with anti-velcro antibody, and the bands of integrin heterodimer in all mutants were similar to wildtype (Fig. II-11, lane 7-12). Moreover, it was revealed that PA tag was able to be not only inserted into a hairpin loop in W2 but also recognized by NZ-1 without optimization, because all mutants were able to be immunoprecipitated by NZ-1 (Fig. II-11, lane 2-6). It was suggested that PA tag was able to be inserted into the site near to both terminals without considering the steric hinderance and conformational change, because the mutant without linker sequence (W2_5) was able to bind to NZ-1.

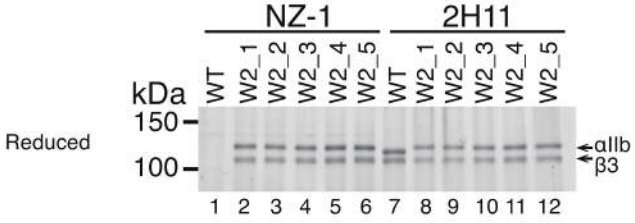

Figure II-11. PA tag can be inserted at W2 site without addition of any linker segment. PA tag was inserted into the site W2 with various lengths of linker (see Fig. II-2A) and the resultant $\alpha_{IIb}\beta_3$ ectodomain mutants were subjected to the immunoprecipitation with 2H11 and NZ-1. Bound proteins were subjected to 7.5% SDS-PAGE under reducing condition and stained for protein with fluorescent dye.

Binding assay of NZ-1 and PA tag inserted into various loop regions

PA tag was able to be inserted into very tight hairpin turn in W2 (Fig. II-10B) without linker sequence. To examine that the above result is versatile, I inserted PA tag into other various loop regions. I selected the nine regions, (1) a hairpin turns similar to W2 (W1, Cap, W3, W6, Calf-1 X-Z), (2) a long loop regions over 8-residue (Thigh F-G, Calf-1 E-F, Calf-2 F-G) and a long disordered loop including furin cleavage site (Calf-2 X-Y) (Fig. II-2B, Fig. II-10). The expression of many mutants excepting W3 and W6 were confirmed by the examination of the expression and secretion of each mutant heterodimer as described in W2 (Fig. II-12). It was suggested that the tag insertion was not structurally permitted in W3 and W6, because these integrin heterodimer were not detected. Since these two mutation sites exist near the calcium binding sites important for the stabilization of α subunit structure, these mutations may affect the calcium coordination (Jennings and Phillips 1982). In W1 and Calf-2 F-G, there was the possibility that the tag insertion affected the structural stability because they had low expression level. In other five mutants, it was suggested that the tag insertion did not affect the structure stability because these expression level was similar to wildtype. To examine that these mutations did not affect the integrin functions, full-length integrin mutants were expressed on the cell surface. As a result of examination using anti-human α_{IIb} monoclonal antibody 10E5, all seven mutants including W1 and Thigh F-G (excepting Cap that is not recognized by 10E5) had high expression level on the cell

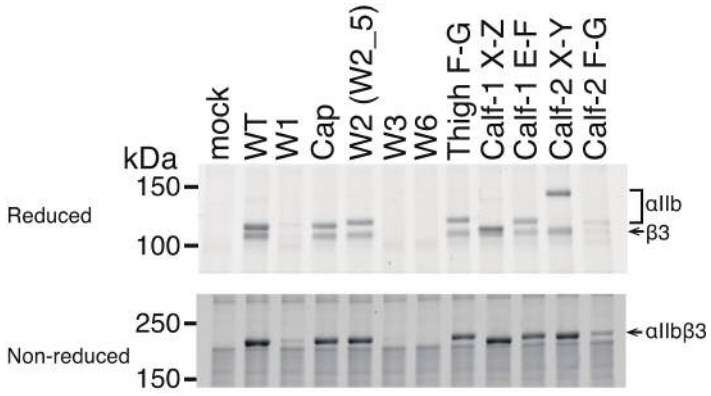

Figure II-12. Effect of the PA tag insertion into the α_{IIb} loop regions on the expression level. Various α_{IIb} mutants were co-transfected with wildtype β_3 and subjected to the immunoprecipitation with anti-velcro antibody 2H11. Bound integrins were subjected to 7.5% SDS-PAGE under reducing and non-reducing condition and stained with fluorescent dye. Note that the mobility of the Calf-1 X-Z and Calf-2 X-Y mutant α_{IIb} chains are different from the wildtype, due to the elimination of an N-linked glycosylation site at N680 (for Calf-1 X-Z) and a furin-cleavage site at $KRDRR^{859}$ (for Calf-2 X-Y).

surface (Fig. II-13A). Moreover, these $\alpha_{IIb}\beta_3$ mutants were recognized by ligand mimetic antibody PAC-1 that was able to bind to only the active $\alpha_{IIb}\beta_3$ (Fig. II-13B). PAC-1 is a mimetic of fibrinogen that is original ligand of $\alpha_{IIb}\beta_3$ (Taub et al. 1989; Ginsberg et al. 1990). Therefore, all mutated integrin had normal function, and it was suggested that the PA tag insertion did not affect not only the structure of $\alpha_{IIb}\beta_3$ but also the function.

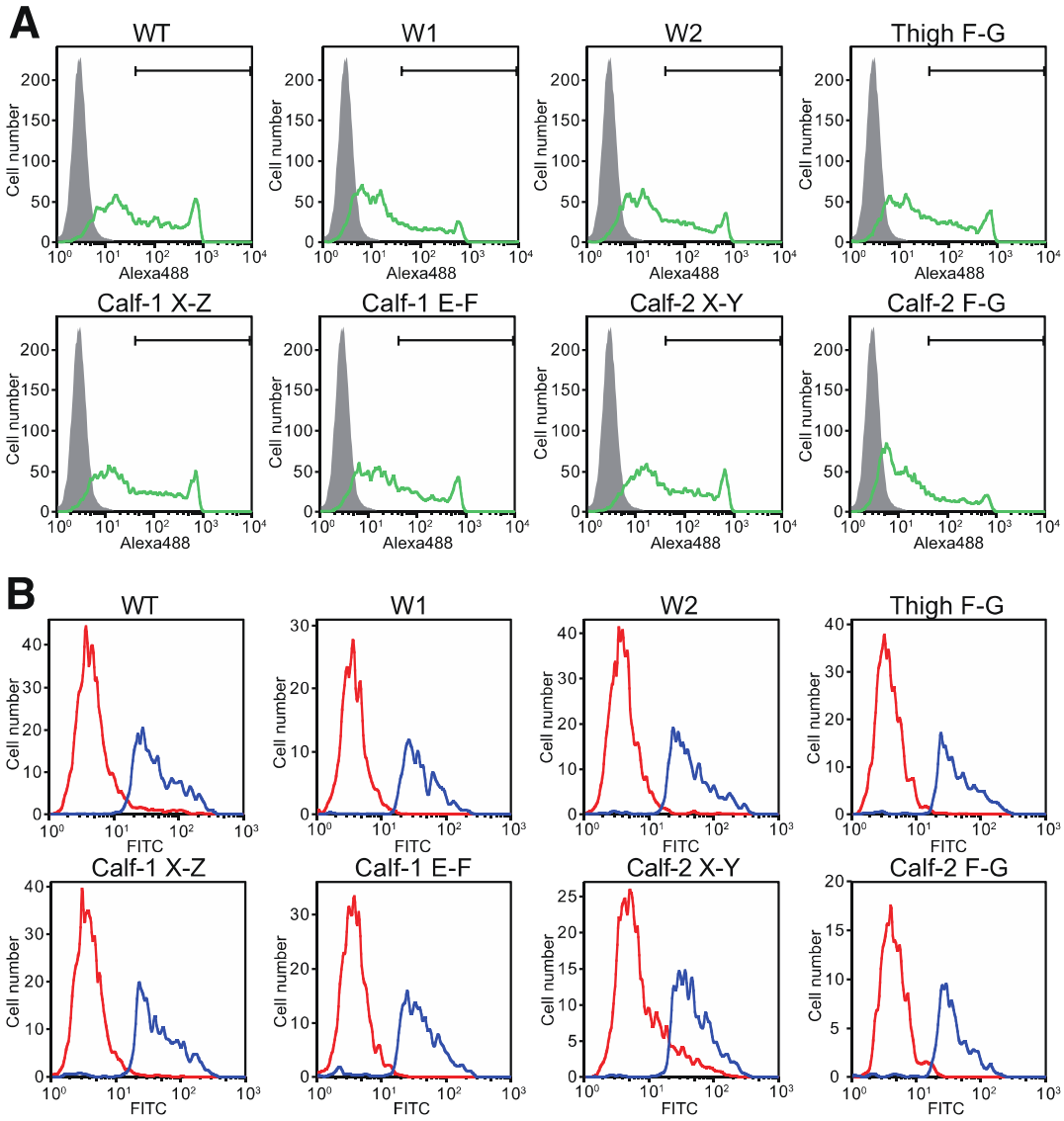

Figure II-13. Assessment of cell surface expression and ligand binding activity of PA tag-inserted $\alpha_{IIb}\beta_3$ mutants. (A) PDIS-2 cells (human podoplanin knockout in HEK293T cells) (gray area) or PDIS-2 cells transiently transfected with PA tag-inserted $\alpha_{IIb}\beta_3$ (green solid line) were incubated with 1 μg/ml 10E5 and stained with Alexa488-labeled secondary antibody specific for mouse IgG. (B) Ligand binding activity of PA tag-inserted $\alpha_{IIb}\beta_3$. PDIS-2 cells transiently transfected with PA tag-inserted $\alpha_{IIb}\beta_3$ were left untreated (red solid line) or incubated with DTT (blue solid line) and stained with Dylight680-AP3 and FITC-PAC-1. The histograms show the FITC fluorescence (i.e., PAC-1 binding) from the cell populations that are positive for AP3 staining.

In the mutants with normal expression and function, it was examined that the inserted PA tag was able to be recognized by NZ-1. The mutant $\alpha_{IIb}\beta_3$ ectodomain fragments were subjected to the immunoprecipitation with NZ-1, and immunoblotted with anti-velcro antibody. As a result, all mutants were able to be immunopreciated by NZ-1, and only wildtype without PA tag did not react (Fig. II-14, upper panel). When this result was compared with the immunoprecipitation results using anti-β_3 antibody 7E3 (Fig. II-14, lower panel) to evaluate the total expression level of heterodimer, NZ-1 was able to immunoprecipitate all integrin heterodimer excepting Cap mutant, and did not lose the recognition ability toward the inserted PA tag. In Cap mutant, PA tag was inserted into very short length type I' β-hairpin turn of 2-residue (Fig. II-10B), and it was suggested that PA tag could not form the suitable conformation for the recognition of NZ-1, because both terminals of PA tag were made to near. However, surprisingly, NZ-1 was able to bind to PA tag inserted into a very tight turn with some binding affinity. Therefore, it was expected that PA tag was able to be inserted into the middle of loop region of various proteins without considering the choice of insertion site and the addition of linker sequence, and the inserted PA tag was able to be recognized by NZ-1 in native conformation (i.e., it was able to use as affinity tag).

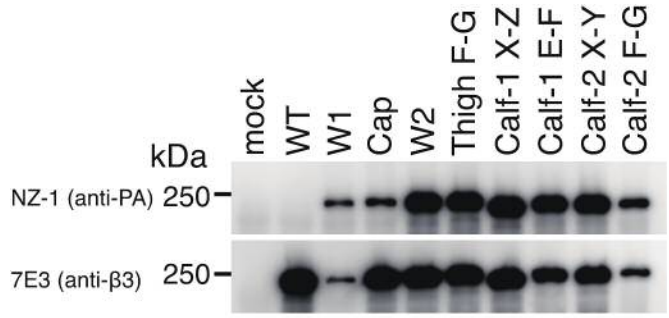

Figure II-14. Recognition of the inserted PA tag by NZ-1. The mutant $\alpha_{IIb}\beta_3$ ectodomain fragments were expressed as in Fig. II-12 and subjected to the immunoprecipitation with NZ-1 (upper panel) or anti-β_3 antibody 7E3 (lower panel). Bound proteins are separated on 7.5% SDS-PAGE gel under nonreducing condition, transferred to PVDF membranes, and immunoblotted with anti-velcro polyclonal antibody.

Meanwhile, are these characteristics of PA tag system the unique one? Previously, there were no examples that the possibility of the tag insertion into loop was systematically examined in the popular epitope tag. Thus, I performed the examination using FLAG tag and Myc tag as described for PA tag. FLAG tag and Myc tag were inserted into three sites of integrin $\alpha_{IIb}\beta_3$ (W2, Thigh F-G, Calf-1 X-Z) where the inserted PA tag had high affinity toward NZ-1 (Fig. II-2C). It was revealed that all mutations did not involve the expression and secretion of integrin heterodimer by immunoprecipitation with anti-β_3 antibody 7E3 as shown in PA tag (Fig. II-15, lane 5, 6). It was confirmed that these tag insertion did not affect the integrin conformation. I was able to acknowledge this result because FLAG tag (8-residue) and Myc tag (10-residue) were shorter than PA tag. However, it was revealed that these all mutants completely lost the recognition ability toward each antibody, when I attempted to immunoprecipitate these mutants using each anti-tag antibody (FLAG tag; M2, Myc tag; 9E10) (Fig. II-15, lane 2, 3). It was suggested that the conformations of FLAG tag and Myc tag inserted into loop region were fixed, and the FLAG tag and the Myc tag were not able to be recognized by each monoclonal antibody. The structure of the M2/FLAG peptide complex has not been determined, on the other hand, the structure of the 9E10/Myc peptide complex has been determined already (Krauss et al. 2008). The result indicated that Myc peptide with the extended β-structure is recognized by 9E10, and suggested that Myc tag inserted into loop region lost the affinity toward 9E10. As a result, it was concluded that the characteristics of PA tag that the tag inserted into loop region was able to function as tag with high affinity is extremely unique.

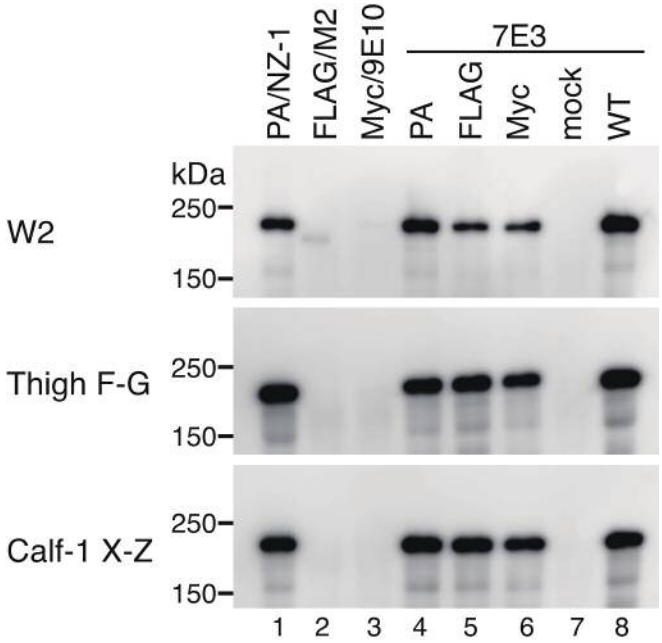

Figure II-15. Comparison among various epitope tags in the "loop insertion" application. $\alpha_{IIb}\beta_3$ ectodomain fragments with PA (lanes 1 and 4), FLAG (lanes 2 and 5), and Myc (lanes 3 and 6) tags inserted at three different sites (W2, Thigh F-G, and Calf-1 X-Z) were immunoprecipitated with 7E3 (lanes 4-6) or corresponding anti-tag antivodies (lanes 1-3), and visualized by anti-velcro immunoblotting as in the legend to Fig. II-14. Culture supernatants from the mock (lane 7) and wildtype $\alpha_{IIb}\beta_3$ integrin-expressing (lane 8) cells were used as negative and positive controls, respectively.

Usability of PA tag as research tool for integrin conformational change

The features of PA tag that the can be inserted into a middle of a protein have various possibilities for research. For example, it is expected that PA tag system is able to detect the exposure level and accessibility of a particular region in a target protein. It was reported that integrin used as a model protein was dynamically changed the conformation (Rosano and Rocco 2010; Luo et al. 2007; Springer and Dustin 2012; Takagi et al. 2002b). Integrin has the bent conformation in inactive state, and has the extend conformation when it is activated by the ligand binding. Therefore, there are the epitope regions that the exposure level is different before or after the conformational change, and the monoclonal antibodies that recognize the regions were used as the reporting tool for integrin active state. These were called LIBS (ligand-induced binding sites) antibody (Fig. II-16) (Kouns et al. 1990; Bazzoni et al. 1995). Usually, LIBS

antibody was accidentally obtained from a number of antibodies. However, it is possible that versatile tool for the detection and induction of integrin conformational change is able to be constructed by using PA tag and NZ-1.

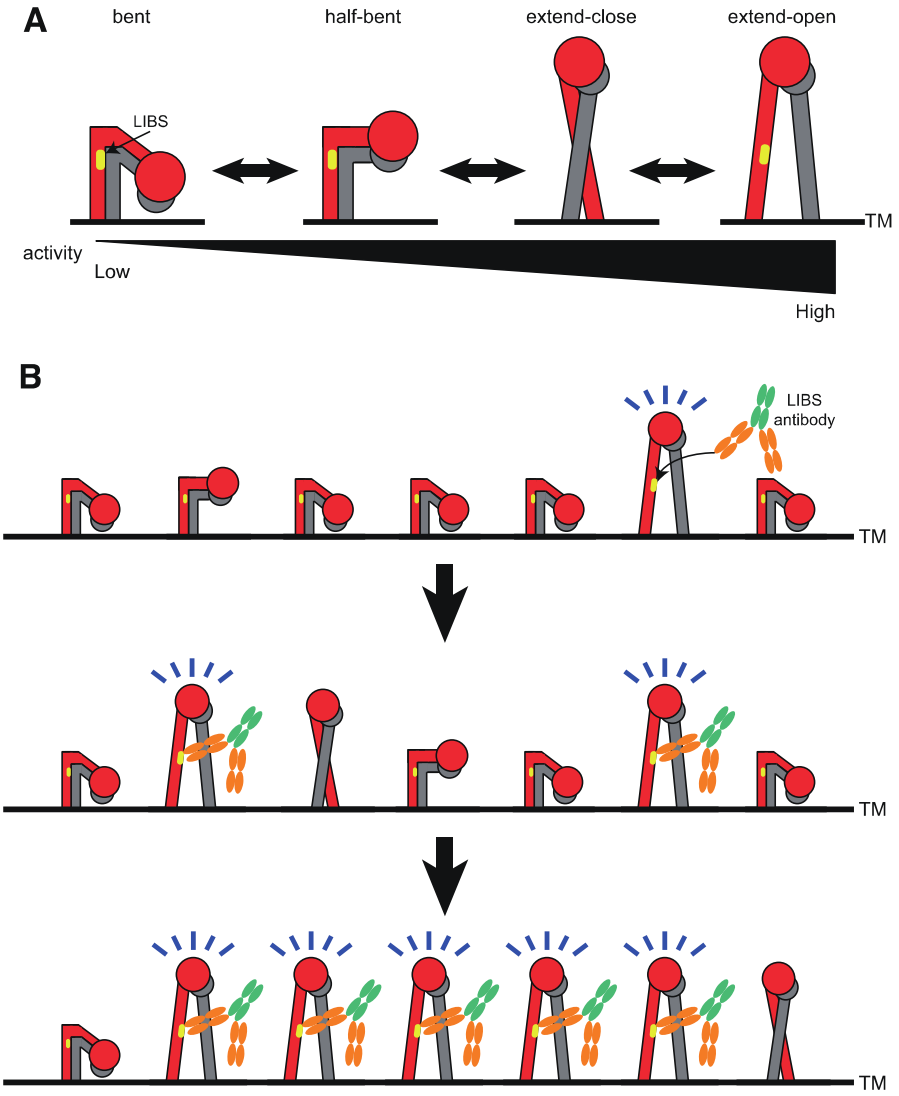

Figure II-16. Scheme of integrin activation with LIBS antibody. (A) Conformational equilibrium of cell surface integrin. Four putative conformers (bent, half-bent, extend-close, and extend-open) are postulated to be present on cell surface, with each abundance among the population determined by the particular cell condition (Luo et al. 2007). The wedge below the cartoon represents the relative ligand-binding activity. (B) Mechanism of integrin activation by LIBS antibodies. In the resting state (above), most cell-surface integrins are in the bent conformation (i.e., low activity) but spontaneously extend and are bound by LIBS antibody. As the LIBS antibody-bound integrins do not bend back, the population of the extended integrins (highly active as denoted by eyelash) increases, leading to the overall upregulation of integrin activity on the cell.

Interestingly, as shown in Fig. II-17, the reactivity of full-length Calf-1 E-F on cell surface toward NZ-1 was lower than other mutants. This result corresponded to the fact that this inserted site was hidden inside the bent conformation in original conformation of integrin $\alpha_{IIb}\beta_3$ on cell surface (Fig. II-18A). It was confirmed that the binding ability was enhanced (Fig. II-18B, left panel), when this mutant was examined the reactivity toward NZ-1 in the condition that integrin was activated and induced the ligand binding (i.e., the condition of integrin extend conformation). This change was not shown in other mutation sites (W2, Thigh F-G) (Fig. II-18B, middle and right panel), and this was the unique phenomenon for Calf-1 E-F site with increasing the exposure level by conformational change (extension). As a result, it was revealed that NZ-1 was able to be used as LIBS antibody for the conformational change reporter by the choice of PA tag insertion sites.

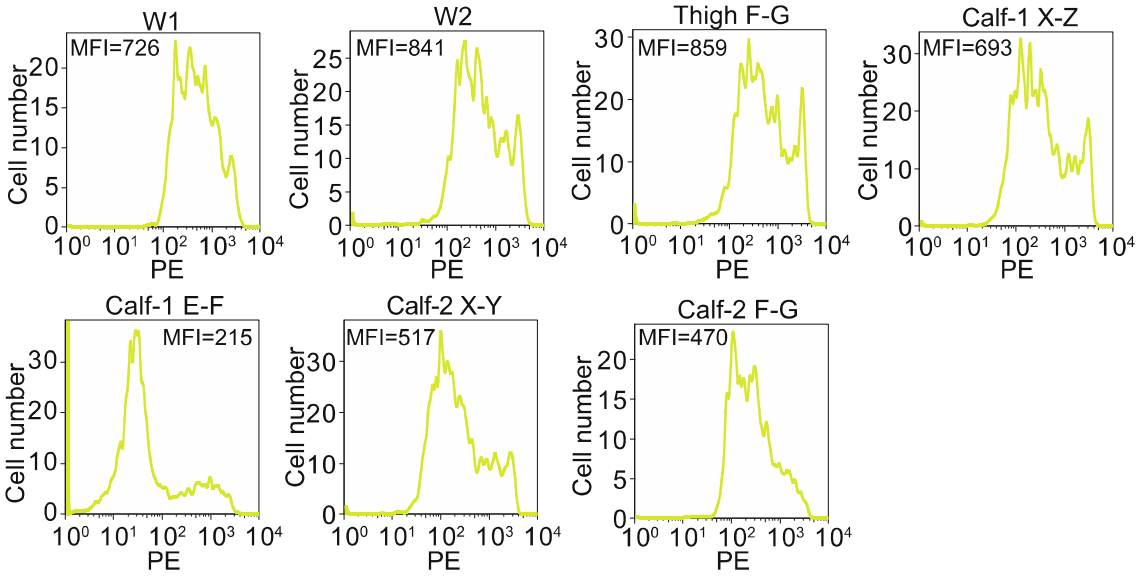

Figure II-17. Comparison of NZ-1 staining efficiency among various PA tag-inserted $\alpha_{IIb}\beta_3$ mutants. Cells expressing various mutant $\alpha_{IIb}\beta_3$ were simultaneously stained with 0.5 μg/ml NZ-1 and 1 μg/ml 10E5, followed by incubation with PE-labeled anti-rat IgG and Alexa488-labeled anti-mouse IgG. The histogram show PE fluorescence (i.e., NZ-1 staining) for the 10E5-positive cell population (corresponding to the region indicated by brackets in Fig. II-13A). MFI (mean fluorescence intensity) value for the PE fluorescence is shown above each histogram.

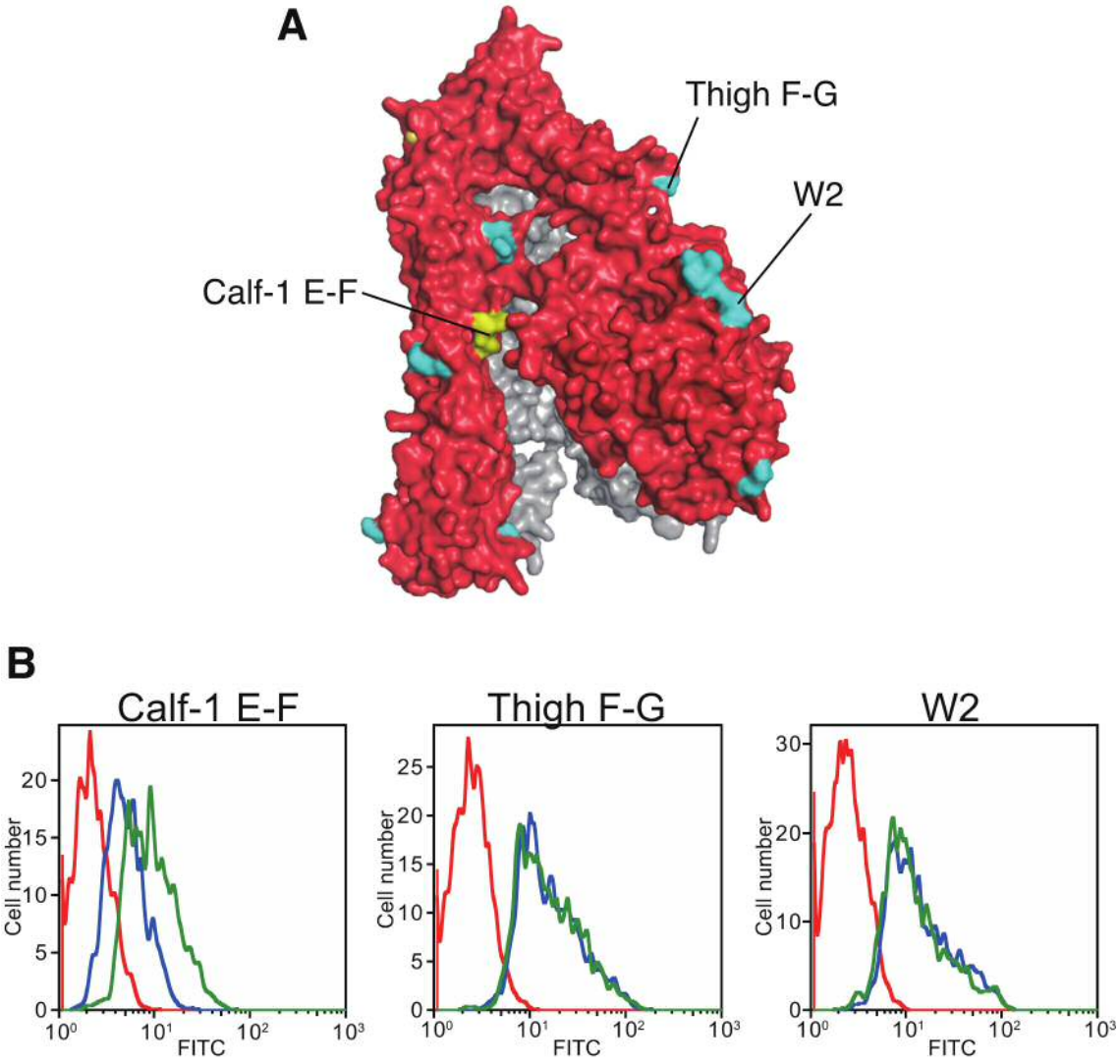

Figure II-18. The "LIBS" nature of the PA tag inserted at Calf-1 E-F site. (A) Location of the loop-insertion. The entire $\alpha_{IIb}\beta_3$ ectodomain in the bent form is shown as surface presentation with α_{IIb} and β_3 chains colored in red and gray, respectively. Locations of the loop insertion used in Fig. II-14 are highlighted in cyan, except for the Calf-1 E-F shown in gold. Note that Calf-1 E-F site is located inside the bend, partially occluded by the β-propeller domain. (B) Conformation dependent epitope exposure. PDIS-2 cells transiently expressing $\alpha_{IIb}\beta_3$ with three different PA-tag insertions were incubated with (1) Dylight680-AP3 alone (red solid line), (2) Dylight680-AP3 and FITC-NZ-1 (blue solid line), or (3) Dylight680-AP3, FITC-NZ-1, 0.5 mM $MnCl_2$, and 1 mM RGD peptide (green solid line). Shown are FITC fluorescence histogram obtained with AP3-positive cell populations.

As many proteins with conformational change, integrin has a state of equilibrium between four putative conformers (bent, half-bent, extend-close, extend-open) (Fig. II-16A). Therefore, it was known that LIBS antibody induces the integrin activation on cell surface, because the integrin of extend conformation is stabilized when LIBS antibody binds to integrin, and the equilibrium as described above is shifted to the extend conformation (Fig. II-16B) (Bazzoni et al. 1995; Dormond et al. 2004; Luo et al. 2003). Therefore, I examined the ligand binding ability in all PA tag inserted mutants with or without NZ-1. As a result, the ability for integrin ligand binding were not changed by NZ-1 in many mutants, and only Calf-1 E-F was grown the PAC-1 binding ability by NZ-1 (Fig. II-19). These results suggested that NZ-1 has the characteristics of integrin LIBS antibody in Calf-1 E-F, and the rarely obtained integrin LIBS antibody (conformational change reporter and artificial activation tool) was able to be developed in every integrin.

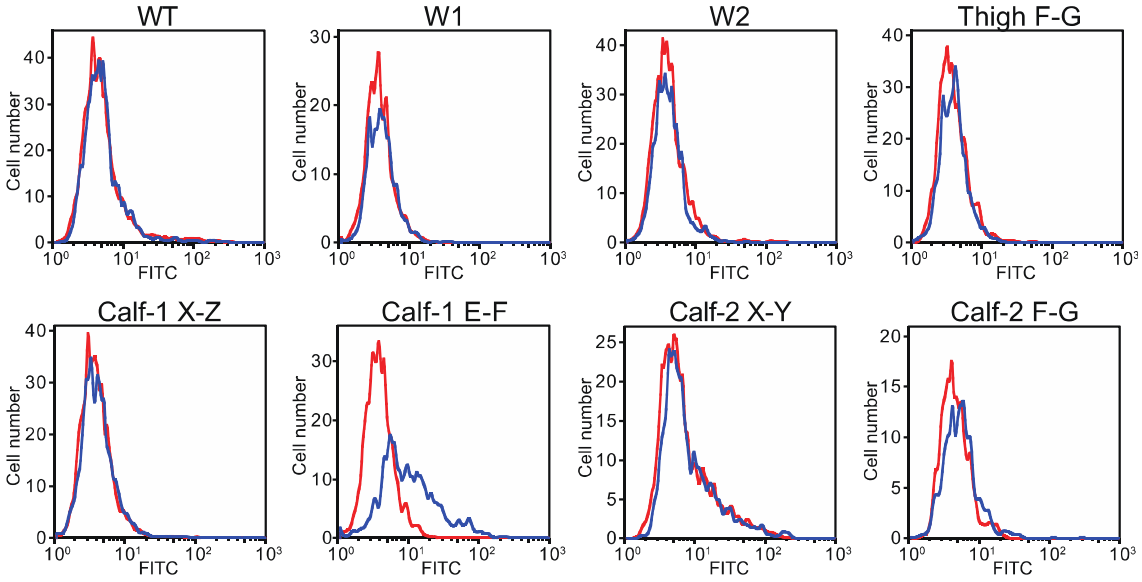

Figure II-19. Ligand binding activity of $\alpha_{IIb}\beta_3$ with cryptic epitope can be activated by NZ-1. PDIS-2 cells transiently transfected with PA tag-inserted $\alpha_{IIb}\beta_3$ were stained with Dylight680-AP3 and FITC-PAC-1 in the absence (red solid line), or presence (blue solid line) of 10 μg/ml NZ-1. FITC fluorescence histograms from the cell populations that are positive for AP3 staining are shown.

Discussion

As a result of the structural analysis of the NZ-1/PA peptide complex, it was revealed that the complex has many contacts between the peptide and the Fab (Fig. II-8B). However, it is difficult to explain the reason why the binding affinity between PA tag and NZ-1 is high (10^{-9}~10^{-12} M), because the binding surface area is as large as the general interface area between protein and peptide. Therefore, I discuss the reason why PA tag has high affinity toward NZ-1. When the apo structure was compared with the complex structure, these structures are essentially identical at the level of the side chains in the CDR, and only Lys76 and Arg120 have obvious difference in the side chain conformation (Fig. II-6). There are many hydrogen bonds between NZ-1 and PA peptide *via* water molecules (Fig. II-20A), and these hydrogen bonds remain in the apo structure by the additional water molecules in place of PA peptide (Fig. II-20B). The result suggested the reason why PA tag system has high affinity. The reason is that PA peptide can bind to NZ-1 without loss of energy, because structure of NZ-1 including water molecules has no major difference with or without bound PA peptide. Additionally, another important point is that within the binding pocket of NZ-1, the PA peptide assumes a tight 2-residue type II β-turn conformation, with Pro7 and Gly8 being the tip of the hairpin (Fig. II-8A, B). It is known that Pro-Gly sequence easily structures a β-turn (Guruprasad and Rajkumar 2000; Hutchinson and Thornton 1994). Therefore,

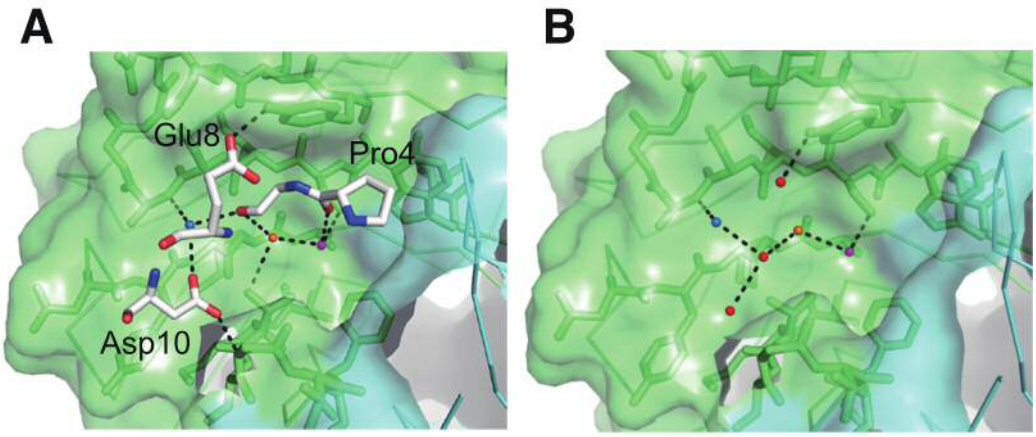

Figure II-20. Surface water molecules observed at the peptide binding site of NZ-1. Close-up view of the binding pocket of NZ-1 Fab in the peptide-bound (A) and peptide-free (B) states, with the interface residues shown in stick models and colored as in Fig. II-8. In (A), interfacial water molecules involved in hydrogen bonding network (black dotted lines) are shown as blue, orange, and magenta spheres, along with selected PA14 residues. In (B), three surface-bound waters occupying nearly identical positions are colored similarly. In addition, three other water molecules are present and shown as red spheres.

this region in PA tag is easy to form a β-turn in solution without bound NZ-1. Generally, the linear epitope peptide does not have a fixed conformation in solution, and such conformation is formed when it binds to an antibody. This means that the loss of entropic force upon the NZ-1/PA tag interaction is relatively small, which may be the reason for the high affinity. In fact, it was reported that P5A and G6A mutants for the destruction of β-turn had the severe effect in Chapter II (Fig. I-8).

Next, it was suggested that PA tag was able to be inserted into loop regions of a protein, on the basis of the discovery that PA tag with turn was recognized by NZ-1. There were the several reports that the existing tags inserted into loop region were recognized by anti-tag antibody (Dinculescu et al. 2002; Smith et al. 2004; Morlacchi et al. 2012; Facey and Kuhn 2003; Kendall and Senogles 2006). However, these reports were described that linker sequence was inserted between loop and tag, and the tag sequence was inserted into very long loop region. As shown in Fig. II-14, NZ-1 had high affinity toward PA tag inserted into 5-residue loop. Furthermore, PA tag was able to be easily inserted into loop without linker sequence (Fig. II-11). It was suggested that PA tag was able to be inserted into turn/loop region without try and error for optimization, and this system was able to be applied various proteins, by the exhaustive examination using integrin α_{IIb}. Additionally, I propose that the difficult application for the existing tags was able to be permitted by this system of tag insertion. First, this system gives the third choice for protein purification, when a target protein can not be attached with peptide tag to N- or C-terminal because those regions are important for the protein function and conformation. For example, this system can prepare an antibody that is accessible from extracellular area to multi-pass membrane protein with both terminals buried intracellular area (Deng et al. 2014). Second, this system enables the site-specific fluorescent labeling of a protein using the high affinity (extremely slow dissociation rate) between PA tag and NZ-1, because PA tag can be inserted into various sites of protein without affecting on the protein conformation and function. Particularly, it is possible that FRET (fluorescence resonance energy transfer) probe for monitoring the conformational change and molecular assembly of protein can be introduced with high accuracy, and the specific labeling of domain and subunit can be accomplished in electron microscope. Third, NZ-1 can be used as a protein conformational change reporter and inducer by the choice of PA tag insertion sites (Fig. II-18, 19). Integrin $\alpha_{IIb}\beta_3$ has many LIBS antibodies (Luo et al. 2003), and use of these antibodies facilitates

the research. However, LIBS antibodies were not obtained in all integrin, and especially the reporter antibody for integrin excepting human species was rarely given. Additionally, it was difficult for comparison between the examination results using different reporter/activate antibodies, because the affinity and isotype was different with each antibody. In contrast, it is possible that PA tag system can examine the conformational change of integrin without LIBS antibodies, and compare the kinetics of various LIBS epitope exposure level in an integrin. This application may be used for the conformational change research of various receptors. Finally, this system may be used as a crystallization accelerator. Recently, the co-crystallization with antibody fragment for the fixing structure and the providing various packing surface is general method in the crystallization of membrane and low crystallizability proteins (Hino et al. 2012; Manolaridis et al. 2013). However, the exiting tag system is not suitable for this purpose, because usually the antibody that recognizes the tag artificially fused to flexible region moves considerably with tag sequence. When PA tag is inserted into hairpin loop, it is possible that NZ-1 is usable crystallization accelerator (crystallization chaperon), as an antibody recognizing the three dimensional structure of a target protein.

In conclusion, NZ-1 recognizes PA tag with unique conformation. Moreover, it was indicated that PA tag inserted into loop could be recognized by NZ-1, because PA tag has the unique structure. These facts suggested that PA tag system can be used not only as protein detection and purification system, but also as various tools for analysis of protein function that is impossible in the existing tag systems.

References

Artoni A, Li J, Mitchell B, Ruan J, Takagi J, Springer TA, French DL, Coller BS (2004) Integrin beta3 regions controlling binding of murine mAb 7E3: implications for the mechanism of integrin alphaIIbbeta3 activation. Proceedings of the National Academy of Sciences of the United States of America 101 (36):13114-13120. doi:10.1073/pnas.0404201101

Bazzoni G, Shih DT, Buck CA, Hemler ME (1995) Monoclonal Antibody 9EG7 Defines a Novel 1 Integrin Epitope Induced by Soluble Ligand and Manganese, but Inhibited by Calcium. Journal of Biological Chemistry 270 (43):25570-25577. doi:10.1074/jbc.270.43.25570

Benard V, Bokoch GM (2002) Assay of Cdc42, Rac, and Rho GTPase activation by affinity methods. Methods Enzymol 345:349-359

Brizzard BL, Chubet RG, Vizard DL (1994) Immunoaffinity purification of FLAG epitope-tagged bacterial alkaline phosphatase using a novel monoclonal antibody and peptide elution. BioTechniques 16 (4):730-735

Burgess RR, Thompson NE (2002) Advances in gentle immunoaffinity chromatography. Current Opinion in Biotechnology 13 (4):304-308. doi:10.1016/s0958-1669(02)00340-3

Chan S, Gabra H, Hill F, Evan G, Sikora K (1987) A novel tumour marker related to the c-myc oncogene product. Mol Cell Probes 1 (1):73-82

Chang HC, Bao ZZ, Yao Y, Tse AGD, Goyarts EC, Madsen M, Kawasaki E, Brauer PP, Sacchettini JC, Nathenson SG, Reinherz EL (1994) A General-Method for Facilitating Heterodimeric Pairing between 2 Proteins - Application to Expression of Alpha-T-Cell and Beta-T-Cell Receptor Extracellular Segments. Proceedings of the National Academy of Sciences of the United States of America 91 (24):11408-11412. doi:Doi 10.1073/Pnas.91.24.11408

Chen VB, Arendall WB, 3rd, Headd JJ, Keedy DA, Immormino RM, Kapral GJ, Murray LW, Richardson JS, Richardson DC (2010) MolProbity: all-atom structure validation for macromolecular crystallography. Acta crystallographica Section D, Biological crystallography 66 (Pt 1):12-21. doi:10.1107/S0907444909042073

Coller BS (1985) A new murine monoclonal antibody reports an activation-dependent

change in the conformation and/or microenvironment of the platelet glycoprotein IIb/IIIa complex. The Journal of clinical investigation 76 (1):101-108. doi:10.1172/JCI111931

Coller BS, Peerschke EI, Scudder LE, Sullivan CA (1983) A murine monoclonal antibody that completely blocks the binding of fibrinogen to platelets produces a thrombasthenic-like state in normal platelets and binds to glycoproteins IIb and/or IIIa. The Journal of clinical investigation 72 (1):325-338

Deng D, Xu C, Sun P, Wu J, Yan C, Hu M, Yan N (2014) Crystal structure of the human glucose transporter GLUT1. Nature 510 (7503):121-125. doi:10.1038/nature13306

Dinculescu A, McDowell JH, Amici SA, Dugger DR, Richards N, Hargrave PA, Smith WC (2002) Insertional mutagenesis and immunochemical analysis of visual arrestin interaction with rhodopsin. The Journal of biological chemistry 277 (14):11703-11708. doi:10.1074/jbc.M111833200

Dormond O, Ponsonnet L, Hasmim M, Foletti A, Rüegg C (2004) Manganese-induced integrin affinity maturation promotes recruitment of αVβ3 integrin to focal adhesions in endothelial cells: evidence for a role of phosphatidylinositol 3-kinase and Src. Thrombosis and Haemostasis. doi:10.1160/th03-11-0728

Einhauer A, Jungbauer A (2001) The FLAG peptide, a versatile fusion tag for the purification of recombinant proteins. J Biochem Biophys Methods 49 (1-3):455-465

Emsley P, Lohkamp B, Scott WG, Cowtan K (2010) Features and development of Coot. Acta crystallographica Section D, Biological crystallography 66 (Pt 4):486-501. doi:10.1107/S0907444910007493

Evan GI, Lewis GK, Ramsay G, Bishop JM (1985) Isolation of Monoclonal Antibodies Specific for Human c-myc Proto-OncogeneProduct. Mol Cell Biol 5 (12):3610-3616

Facey SJ, Kuhn A (2003) The sensor protein KdpD inserts into the Escherichia coli membrane independent of the Sec translocase and YidC. European Journal of Biochemistry 270 (8):1724-1734. doi:Doi 10.1046/J.1432-1033.2003.03531.X

Field J, Nikawa J, Broek D, Macdonald B, Rodgers L, Wilson IA, Lerner RA, Wigler M (1988) Purification of a Ras-Responsive Adenylyl Cyclase Complex from Saccharomyces-Cerevisiae by Use of an Epitope Addition Method. Molecular

and Cellular Biology 8 (5):2159-2165

Fujii Y, Kaneko M, Neyazaki M, Nogi T, Kato Y, Takagi J (2014) PA tag: a versatile protein tagging system using a super high affinity antibody against a dodecapeptide derived from human podoplanin. Protein expression and purification 95:240-247. doi:10.1016/j.pep.2014.01.009

Ginsberg MH, Frelinger AL, Lam SC, Forsyth J, McMillan R, Plow EF, Shattil SJ (1990) Analysis of platelet aggregation disorders based on flow cytometric analysis of membrane glycoprotein IIb-IIIa with conformation-specific monoclonal antibodies. Blood 76 (10):2017-2023

Guruprasad K, Rajkumar S (2000) Beta-and gamma-turns in proteins revisited: a new set of amino acid turn-type dependent positional preferences and potentials. J Biosci 25 (2):143-156

Hino T, Arakawa T, Iwanari H, Yurugi-Kobayashi T, Ikeda-Suno C, Nakada-Nakura Y, Kusano-Arai O, Weyand S, Shimamura T, Nomura N, Cameron AD, Kobayashi T, Hamakubo T, Iwata S, Murata T (2012) G-protein-coupled receptor inactivation by an allosteric inverse-agonist antibody. Nature 482 (7384):237-240. doi:10.1038/nature10750

Hochuli E, Bannwarth W, Dobeli H, Gentz R, Stuber D (1988) Genetic Approach to Facilitate Purification of Recombinant Proteins with a Novel Metal Chelate Adsorbent. Bio-Technology 6 (11):1321-1325. doi:Doi 10.1038/Nbt1188-1321

Hopp TP, Prickett KS, Price VL, Libby RT, March CJ, Cerretti DP, Urdal DL, Conlon PJ (1988) A Short Polypeptide Marker Sequence Useful for Recombinant Protein Identification and Purification. Bio-Technology 6 (10):1204-1210. doi:Doi 10.1038/Nbt1088-1204

Hutchinson EG, Thornton JM (1994) A revised set of potentials for beta-turn formation in proteins. Protein science : a publication of the Protein Society 3 (12):2207-2216. doi:10.1002/pro.5560031206

Jennings LK, Phillips DR (1982) Purification of glycoproteins IIb and III from human platelet plasma membranes and characterization of a calcium-dependent glycoprotein IIb-III complex. The Journal of biological chemistry 257 (17):10458-10466

Kabsch W (2010) Xds. Acta crystallographica Section D, Biological crystallography 66 (Pt 2):125-132. doi:10.1107/S0907444909047337

Kaneko MK, Kato Y, Kameyama A, Ito H, Kuno A, Hirabayashi J, Kubota T, Amano K, Chiba Y, Hasegawa Y, Sasagawa I, Mishima K, Narimatsu H (2007) Functional glycosylation of human podoplanin: glycan structure of platelet aggregation-inducing factor. FEBS letters 581 (2):331-336. doi:10.1016/j.febslet.2006.12.044

Kaneko MK, Kunita A, Abe S, Tsujimoto Y, Fukayama M, Goto K, Sawa Y, Nishioka Y, Kato Y (2012) Chimeric anti-podoplanin antibody suppresses tumor metastasis through neutralization and antibody-dependent cellular cytotoxicity. Cancer science 103 (11):1913-1919. doi:10.1111/j.1349-7006.2012.02385.x

Kaneko MK, Morita S, Tsujimoto Y, Yanagiya R, Nasu K, Sasaki H, Hozumi Y, Goto K, Natsume A, Watanabe M, Kumabe T, Takano S, Kato Y (2013a) Establishment of novel monoclonal antibodies KMab-1 and MMab-1 specific for IDH2 mutations. Biochemical and biophysical research communications 432 (1):40-45. doi:10.1016/j.bbrc.2013.01.088

Kaneko MK, Ogasawara S, Kato Y (2013b) Establishment of a Multi-Specific Monoclonal Antibody MsMab-1 Recognizing Both IDH1 and IDH2 Mutations. Tohoku Journal of Experimental Medicine 230 (2):103-109. doi:Doi 10.1620/Tjem.230.103

Kato Kaneko M, Liu X, Oki H, Ogasawara S, Nakamura T, Saidoh N, Tsujimoto Y, Matsuyama Y, Uruno A, Sugawara M, Tsuchiya T, Yamakawa M, Yamamoto M, Takagi M, Kato Y (2014) Isocitrate dehydrogenase mutation is frequently observed in giant cell tumor of bone. Cancer science 105 (6):744-748. doi:10.1111/cas.12413

Kato Y, Fujita N, Kunita A, Sato S, Kaneko M, Osawa M, Tsuruo T (2003) Molecular identification of Aggrus/T1alpha as a platelet aggregation-inducing factor expressed in colorectal tumors. The Journal of biological chemistry 278 (51):51599-51605. doi:10.1074/jbc.M309935200

Kato Y, Kaneko MK, Kunita A, Ito H, Kameyama A, Ogasawara S, Matsuura N, Hasegawa Y, Suzuki-Inoue K, Inoue O, Ozaki Y, Narimatsu H (2008) Molecular analysis of the pathophysiological binding of the platelet aggregation-inducing factor podoplanin to the C-type lectin-like receptor CLEC-2. Cancer science 99 (1):54-61. doi:10.1111/j.1349-7006.2007.00634.x

Kato Y, Kaneko MK, Kuno A, Uchiyama N, Amano K, Chiba Y, Hasegawa Y,

Hirabayashi J, Narimatsu H, Mishima K, Osawa M (2006) Inhibition of tumor cell-induced platelet aggregation using a novel anti-podoplanin antibody reacting with its platelet-aggregation-stimulating domain. Biochemical and biophysical research communications 349 (4):1301-1307. doi:10.1016/j.bbrc.2006.08.171

Kendall RT, Senogles SE (2006) Investigation of the alternatively spliced insert region of the D2L dopamine receptor by epitope substitution. Neuroscience letters 393 (2-3):155-159. doi:10.1016/j.neulet.2005.09.057

Kobayashi T, Morone N, Kashiyama T, Oyamada H, Kurebayashi N, Murayama T (2008) Engineering a novel multifunctional green fluorescent protein tag for a wide variety of protein research. PLoS One 3 (12):e3822. doi:10.1371/journal.pone.0003822

Kouns WC, Wall CD, White MM, Fox CF, Jennings LK (1990) A conformation-dependent epitope of human platelet glycoprotein IIIa. The Journal of biological chemistry 265 (33):20594-20601

Krauss N, Wessner H, Welfle K, Welfle H, Scholz C, Seifert M, Zubow K, Ay J, Hahn M, Scheerer P, Skerra A, Hohne W (2008) The structure of the anti-c-myc antibody 9E10 Fab fragment/epitope peptide complex reveals a novel binding mode dominated by the heavy chain hypervariable loops. Proteins 73 (3):552-565. doi:10.1002/prot.22080

Laird ME, Desrosiers RC (2007) Infectivity and neutralization of simian immunodeficiency virus with FLAG epitope insertion in gp120 variable loops. Journal of virology 81 (20):10838-10848. doi:10.1128/JVI.00831-07

Lichty JJ, Malecki JL, Agnew HD, Michelson-Horowitz DJ, Tan S (2005) Comparison of affinity tags for protein purification. Protein expression and purification 41 (1):98-105. doi:10.1016/j.pep.2005.01.019

Luo BH, Carman CV, Springer TA (2007) Structural basis of integrin regulation and signaling. Annual review of immunology 25:619-647. doi:10.1146/annurev.immunol.25.022106.141618

Luo BH, Carman CV, Takagi J, Springer TA (2005) Disrupting integrin transmembrane domain heterodimerization increases ligand binding affinity, not valency or clustering. Proceedings of the National Academy of Sciences of the United States of America 102 (10):3679-3684. doi:10.1073/pnas.0409440102

Luo BH, Springer TA, Takagi J (2003) Stabilizing the open conformation of the integrin headpiece with a glycan wedge increases affinity for ligand. Proceedings of the National Academy of Sciences of the United States of America 100 (5):2403-2408. doi:10.1073/pnas.0438060100

Manolaridis I, Kulkarni K, Dodd RB, Ogasawara S, Zhang Z, Bineva G, O'Reilly N, Hanrahan SJ, Thompson AJ, Cronin N, Iwata S, Barford D (2013) Mechanism of farnesylated CAAX protein processing by the intramembrane protease Rce1. Nature 504 (7479):301-305. doi:10.1038/nature12754

McCoy AJ, Grosse-Kunstleve RW, Adams PD, Winn MD, Storoni LC, Read RJ (2007) Phaser crystallographic software. Journal of applied crystallography 40 (Pt 4):658-674. doi:10.1107/S0021889807021206

Morlacchi S, Sciandra F, Bigotti MG, Bozzi M, Hubner W, Galtieri A, Giardina B, Brancaccio A (2012) Insertion of a myc-tag within alpha-dystroglycan domains improves its biochemical and microscopic detection. BMC biochemistry 13:14. doi:10.1186/1471-2091-13-14

Murshudov GN, Vagin AA, Dodson EJ (1997) Refinement of macromolecular structures by the maximum-likelihood method. Acta crystallographica Section D, Biological crystallography 53 (Pt 3):240-255. doi:10.1107/s0907444996012255

Nagae M, Morita-Matsumoto K, Kato M, Kaneko MK, Kato Y, Yamaguchi Y (2014) A Platform of C-type Lectin-like Receptor CLEC-2 for Binding O-Glycosylated Podoplanin and Nonglycosylated Rhodocytin. Structure 22 (12):1711-1721. doi:10.1016/j.str.2014.09.009

Newman PJ, Allen RW, Kahn RA, Kunicki TJ (1985) Quantitation of Membrane Glycoprotein-Iiia on Intact Human-Platelets Using the Monoclonal-Antibody, Ap-3. Blood 65 (1):227-232

Nogi T, Sangawa T, Tabata S, Nagae M, Tamura-Kawakami K, Beppu A, Hattori M, Yasui N, Takagi J (2008) Novel affinity tag system using structurally defined antibody-tag interaction: application to single-step protein purification. Protein science : a publication of the Protein Society 17 (12):2120-2126. doi:10.1110/ps.038299.108

Ogasawara S, Kaneko MK, Price JE, Kato Y (2008) Characterization of anti-podoplanin monoclonal antibodies: critical epitopes for neutralizing the interaction between podoplanin and CLEC-2. Hybridoma 27 (4):259-267.

doi:10.1089/hyb.2008.0017

Ogawa H, Ishiguro K, Gaubatz S, Livingston DM, Nakatani Y (2002) A complex with chromatin modifiers that occupies E2F-and Myc-responsive genes in G(0) cells. Science 296 (5570):1132-1136. doi:Doi 10.1126/Science.1069861

Oshea EK, Lumb KJ, Kim PS (1993) Peptide Velcro - Design of a Heterodimeric Coiled-Coil. Current Biology 3 (10):658-667. doi:Doi 10.1016/0960-9822(93)90063-T

Otwinowski Z, Minor W (1997) Processing of X-ray diffraction data collected in oscillation mode. Macromolecular Crystallography, Pt A 276:307-326. doi:Doi 10.1016/S0076-6879(97)76066-X

Rigaut G, Shevchenko A, Rutz B, Wilm M, Mann M, Seraphin B (1999) A generic protein purification method for protein complex characterization and proteome exploration. Nat Biotechnol 17 (10):1030-1032. doi:10.1038/13732

Rosano C, Rocco M (2010) Solution properties of full-length integrin alpha(IIb)beta3 refined models suggest environment-dependent induction of alternative bent /extended resting states. The FEBS journal 277 (15):3190-3202. doi:10.1111/j.1742-4658.2010.07724.x

Sasaki F, Okuno T, Saeki K, Min L, Onohara N, Kato H, Shimizu T, Yokomizo T (2012) A high-affinity monoclonal antibody against the FLAG tag useful for G-protein-coupled receptor study. Analytical biochemistry 425 (2):157-165. doi:10.1016/j.ab.2012.03.014

Schneider CA, Rasband WS, Eliceiri KW (2012) NIH Image to ImageJ: 25 years of image analysis. Nature Methods 9 (7):671-675. doi:10.1038/nmeth.2089

Smith WC, Dinculescu A, Peterson JJ, McDowell JH (2004) The surface of visual arrestin that binds to rhodopsin. Mol Vis 10:392-398

Springer TA, Dustin ML (2012) Integrin inside-out signaling and the immunological synapse. Current opinion in cell biology 24 (1):107-115. doi:10.1016/j.ceb.2011.10.004

Tabata S, Nampo M, Mihara E, Tamura-Kawakami K, Fujii I, Takagi J (2010) A rapid screening method for cell lines producing singly-tagged recombinant proteins using the "TARGET tag" system. Journal of proteomics 73 (9):1777-1785. doi:10.1016/j.jprot.2010.05.012

Takagi J, DeBottis DP, Erickson HP, Springer TA (2002a) The role of the

specificity-determining loop of the integrin beta subunit I-like domain in autonomous expression, association with the alpha subunit, and ligand binding. Biochemistry 41 (13):4339-4347

Takagi J, Petre BM, Walz T, Springer TA (2002b) Global conformational rearrangements in integrin extracellular domains in outside-in and inside-out signaling. Cell 110 (5):599-511

Taub R, Gould RJ, Garsky VM, Ciccarone TM, Hoxie J, Friedman PA, Shattil SJ (1989) A monoclonal antibody against the platelet fibrinogen receptor contains a sequence that mimics a receptor recognition domain in fibrinogen. The Journal of biological chemistry 264 (1):259-265

Wallace AC, Laskowski RA, Thornton JM (1995) LIGPLOT: a program to generate schematic diagrams of protein-ligand interactions. Protein engineering 8 (2):127-134

Yan B, Smith JW (2001) Mechanism of integrin activation by disulfide bond reduction. Biochemistry 40 (30):8861-8867

Zakrzewska M, Zhen Y, Wiedlocha A, Olsnes S, Wesche J (2009) Size limitation in translocation of fibroblast growth factor 1 fusion proteins across the endosomal membrane. Biochemistry 48 (30):7209-7218. doi:10.1021/bi9007353

Zhu J, Luo BH, Xiao T, Zhang C, Nishida N, Springer TA (2008) Structure of a complete integrin ectodomain in a physiologic resting state and activation and deactivation by applied forces. Molecular cell 32 (6):849-861. doi:10.1016/j.molcel.2008.11.018

List of Publications

Peer-reviewed articles

1. Yuki Fujii, Mika Kaneko, Makiko Neyazaki, Terukazu Nogi, Yukinari Kato, Junichi Takagi「PA tag: a versatile protein tagging system using a super high affinity antibody against a dodecapeptide derived from human podoplanin.」Protein Expession and Purification, 95, 240-247. (2014)

2. Yuki Fujii, Mika Kaneko, Yukinari Kato, Junichi Takagi「"PA tag", a novel affinity tag system that enables protein purification and detection」PSSJ Archives, 7, e075 (2014)

Non peer-reviewed articles

1. Yuki Fujii, Mika Kaneko, Yu Kitago, Yukinari Kato, Junichi Takagi「Structural analysis of NZ-1 Fab complexed with PA peptide」Photon Factory Activity Report, 2013, #31. (2014) B

2. 藤井勇樹, 高木淳一, 金子美華, 加藤幸成「超高親和性を有する新規アフィニティータグシステム "PA タグシステム"」和光純薬時報, 82, 4 (2014)

International meeting abstracts

1. Yuki Fujii, Mika Kaneko, Yukinari Kato, Junichi Takagi「"PA tag", a novel affinity tag system that enables one-step affinity purification of recombinant proteins from dilute sample」International Conference on Structural Genomics 2013 - Structural Life Science, 2013/7/31, (Journal of Structural and Functional Genomics Poster Prize (SILVER))

2. Yuki Fujii, Mika Kaneko, Yu Kitago, Yukinari Kato, Junichi Takagi「"PA tag", a versatile affinity tag system that enables one-step affinity purification and high sensitive detection of recombinant proteins from dilute sample」The 28th Annual Symposium of The Protein Society, 2014/7/28

Domestic meeting abstracts

1. Yuki Fujii, Mika Kaneko, Yukinari Kato, Junichi Takagi「Construction of novel affinity tag system using PA tag」The 13th Annual Meeting of the Protein Science Society of Japan, 2013/6/13, (Young Scientist Award)

2. Yuki Fujii, Kazuo Yamashita, Mika Kaneko, Yu Kitago, Yukinari Kato, Daron M. Standley, Junichi Takagi「Specificity modification of anti-PA tag peptide antibody NZ-1」The 14th Annual Meeting of the Protein Science Society of Japan, 2014/6/25

3. Yuki Fujii, Mika Kaneko, Yu Kitago, Yukinari Kato, Junichi Takagi「Effective usages by the insertion of " PA tag " into the loop regions」The 87th Annual Meeting of the Japanese Biocheminal Society, 2014/10/16

Acknowledgements

The present study was curried out under the direction of Prof. Junichi Takagi, Laboratory of Protein Synthesis and Expression, Institute for Protein Research, Osaka University. I would like to thank Prof. Junichi Takagi for his constant guidance, valuable discussions and encouragement during this study.

I would like to thank Prof. Yukinari Kato, Dr. Mika Kato-Kaneko, and Dr. Satoshi Ogasawara, Regional Innovation Strategy Support Program, Graduate School of Medicine, Tohoku University, for gift of idea for this study, providing an enormous number of NZ-1 antibodies, preparation of IDH1 lysate for Western blotting, and their valuable discussions and encouragement.

I would like to thank Dr. Kenji Iwasaki, Laboratory of Protein Synthesis and Expression, Institute for Protein Research, Osaka University, for his valuable teaching. I would like to thank Dr. Yu Kitago, Laboratory of Protein Synthesis and Expression, Institute for Protein Research, Osaka University, for his valuable and kind advices on the fundamental of protein crystallography including the sample preparation, crystallization and structural determination, determination of NZ-1 structure and his valuable discussion and encouragement. I would like to thank Dr. Terukazu Nogi and Ms, Makiko Neyazaki, Structural Biology Laboratory, Graduate School of Medical Life Science, Yokohama City University, for purification of EGFR and their valuable suggestions on this study.

I would like to thank Dr. Yoshiaki Tomiyama and Dr. Hirokazu Kashiwagi, Department of Hematology and Oncology, Graduate School of Medicine, Osaka University, for teaching the method of activity assay for ligand binding of integrin.

I would like to thank Prof. Tooru Nakano, Department of Pathology, Medical School and Graduate School of Frontier Biosciences, Osaka University, Prof. Seiji Takashima, Department of Biochemistry and Molecular Biology, Medical School and Graduate School of Frontier Biosciences, Osaka University, and Prof. Atsushi Nakagawa, Laboratory of Supramolecular Crystallography, Institute for Protein Research, Osaka University, for their invaluable advices on preparation of this dissertation.

I wish to thank Ms. Emiko Mihara, Keiko Tamura-Kawakami and Ryoko Asaki for their excellent technical supports and Ms. Mie Sakai and Mayumi Nakano for

their clerical supports. I would like to thank all members in Laboratory of Protein Synthesis and Expression (TAKAGI lab); Dr. Kei Suzuki, Dr. Takao Arimori, Dr. Yukiko Matsunaga, Dr. Masataka Umitsu, Dr. Hidenori Hirai, Dr. Shizuka Takagi-Niidome, Ms. Kyoko Matoba, Ms. Mika Hirose, Dr. Masamichi Nagae (RIKEN), Dr. Takeshi Sangawa (Laboratory of Supramolecular Crystallography), Mr. Samuel Thonpson (UCSF), Mr. Zuben Brown and Ms. Shiori Machida for their valuable suggestions on this study and encouragement.

I was supported by JSPS Research Fellowship for Young Scientists (DC2). Finally, I would like to thank my family for their supports during this study.

Yuki Fujii

February 2015